The Role of the Arterial Glycocalyx in Sphingosine-1-Phosphate Induced Cardioprotection in the Isolated Heart of the Wistar Rat

By

Hala Araibi
ARBHAL001

SUBMITTED TO THE UNIVERSITY OF CAPE TOWN
In fulfillment of the requirements for the degree
MSc in Medicine (Physiology)
(HUB 5004W)

Faculty of Health Sciences
UNIVERSITY OF CAPE TOWN

Date of submission: 18 December 2017

Supervisor: Dr. Roisin Kelly-Laubscher*
Co-supervisors: Dr. Asfree Gwanyanya
Dr. Elizabeth van der Merwe
Department of Biological Sciences*
Department of Human Biology.

DECLARATION

I, Hala Araibi, hereby declare that the work on which this dissertation/thesis is based is original work (except where acknowledgments indicate otherwise) and that neither the whole work nor any part of it has been, is being, or is to be submitted for another degree in this or any other university.

I empower the University to reproduce for the purpose of research either the whole or any portion of the contents in any manner whatsoever.

Signed by candidate

Signature: Signature Removed

Date: 18/ 12/ 2017

ABSTRACT

Background: Ischemic heart diseases (IHD) are a leading cause of death among cardiovascular diseases. Unfortunately, the myocardial damage due to ischemia in IHD may be worsened by reperfusion therapy, a phenomenon called ischemic-reperfusion (I/R) injury. Coronary vascular damage is a key feature of I/R injury. Among the coronary vascular structures, the endothelial glycocalyx is a delicate polysaccharide and protein-rich layer that plays an important role in the regulation of vascular permeability, and is easily damaged during I/R. Sphingosine-1-phosphate (S1P) is a membrane phospholipid metabolite that has been shown to protect the heart against I/R. It has also been shown to regulate the synthesis of glycocalyx, but its effects on coronary endothelial glycocalyx damage and possible mechanism during I/R are unknown. Therefore, we hypothesized that S1P-induced cardioprotection is mediated by modulation of the glycocalyx during I/R in the isolated rat heart.

Methods: Isolated male Wistar hearts were perfused on a Langendorff system with Krebs-Henseleit buffer via retrograde perfusion at constant temperature and pressure. The hearts were stabilized and pre-treated with S1P (10 nM for 7 minutes) before inducing 20 minutes of global ischemia, followed by 60 minutes reperfusion. Functional parameters were recorded throughout the protocol, including left ventricular developed pressure (LVDP), left ventricular end diastolic pressure (LVEDP), heart rate (HR) and coronary flow (CF). Ventricular infarct size was measured by using triphenyltetrazolium chloride stain. Coronary net filtration rate (NFR) was calculated as a ratio of the amount of transudate to CF. Cardiac edema was assessed by calculating the heart wet/dry weight ratio and histologically quantifying size of the interstitial compartment. The shedding of the glycocalyx was estimated by measuring the release of the glycocalyx component syndecan-1 in the coronary effluent using enzyme-linked immunosorbent assay (ELISA) and determining relative syndecan-1 staining intensity between groups in immuno-stained wax sections of perfusion-fixed hearts. In addition, the histo-

morphology of the myocardium was assessed using hematoxylin and eosin staining.

Results: The cardiac performance was depressed after I/R, as was reflected by decreased LVDP (P=0.02 vs. control), and an increased LVEDP (P<0.0001 vs. control). I/R also significantly increased infarct size (P=0.04 vs. control). Treatment with S1P before I/R significantly decreased infarct size (P=0.01 vs. I/R), but did not improve the post-ischemic decrease in LVDP or stabilize the LVEDP, and had no effect on CF. I/R significantly increased release of syndecan-1 in the coronary effluent (P=0.0002 vs. control). Immunohistochemically-stained imaging also revealed syndecan-1 staining intensity was significantly decreased or absent in ischemic hearts (P≤0.001 vs. control). Pretreatment with S1P had neither effect on syndecan-1 level in the coronary effluent nor on the intensity of syndecan-1 signal in immuno-stained sections (P=n.s vs. I/R). Histological analysis of cardiac edema revealed an increase in the extracellular area in ischemic hearts compared to the control hearts (P≤0.001 vs. control), and S1P treatment decreased the extracellular area (P≤0.01 I/R+S1P vs. I/R). The NFR, and heart wet/dry ratio were not significantly different post-reperfusion between the groups and S1P had no effect on these parameters.

Conclusion: This study showed that pretreatment with S1P protects the heart against I/R injury, as was indicated by the decreased infarct size, and decreased extracellular cardiac edema. S1P had no effect on hemodynamic performance or the shedding of syndecan-1. These results suggest that S1P-induced cardioprotection is not mediated by protection of the glycocalyx via stabilization of syndecan-1. However, it is possible that S1P may stabilize other minor glycocalyx components which were not measured in this study, such as heparan sulphate and hyaluronic acid. This is the first study that evaluated syndecan-1 in the cardiac effluent of the isolated heart of rats with global ischemia, and the study opens up prospects for further investigation of the role of the glycocalyx in other models of I/R injury, such as the more clinically-relevant regional ischemia disease model.

ACKNOWLEDGEMENTS

I would like to express my deepest gratitude to my supervisor Dr. Roisin Kelly, as well as my co-supervisor Dr. Asfree Gwanyanya, for their continued support during my research, for their patience and for providing me with excellent knowledge. Their guidance and help throughout my research and during the writing up of my thesis is greatly appreciated. I could not have asked for better advisors and without their support and encouragement, I would not have finished this dissertation.

I would like to express my very great appreciation to Dr. Elizabeth van der Merwe for her professional guidance and valuable support in the histology part of my project.

I would like to extend my thanks to Mrs. Morea Petersen, the manager of the histology laboratory (Human Biology department), for her help in my histological experiments. Many thanks to the manager of imaging unit, Mrs Susan Cooper, and Mr Jurgen Geitner, for their help in using the microscope for my project.

I would also like to thank my colleagues, Fatma Alatrag, Mathew Amoni, Viantha Naidoo, for their willingness to assist and for offering the best suggestions. Nazeem. A. Damon, Nuraan Ismail and A-K Samuels thank you for all your assistance and time.

I would like to thank the Libyan Ministry of Higher Education and Libyan Embassy in South Africa for financially supporting my post-graduate research.

Finally, I must express my very profound gratitude to my parents, my husband and my children for providing me with unfailing support and continuous encouragement throughout my years of study and through the process of researching and writing this thesis. This accomplishment would not have been possible without them. Thank you.

LIST OF CONTENTS

LIST OF FIGURES

LIST OF ABBREVIATIONS

ANOVA	Analysis of variance
ATP	Adenosine triphosphate
Akt	Protein kinase B
BSA	Bovine serum albumin
CVD	Cardiovascular diseases
CF	Coronary flow
DAB	3,3-Diaminobenzidine
CS	Chondroitin sulphate
DS	Dermatan sulphate
DMSO	Dimethylsulphoxide
ELISA	Enzyme linked immunosorbent assay
ERK	Extracellular signal regulated kinase
FTY720	Fingolimod (2-amino-2[2-(4-octylphenyl) ethyl] propane-1,3-diolhydrochloride)
GAGs	Glycosaminoglycan chains
HR	Heart rate
H&E	Hematoxylin and Eosin
HRP	Streptavidin-horseradish peroxidase
HDL	High density lipoprotein
HS	Heparan sulphate
HA	Hyaluronic acid
I/R	Ischemia-reperfusion
IPC	Ischemic preconditioning
IPOST	Ischemic post conditioning
IHD	Ischemic heart disease
KS	Keratin sulphate
K-H	Krebs-Henseleit Buffer
LVDP	Left ventricular developed pressure
mPTP	Mitochondrial permeability transition pore
MMP	Metalloproteinase

NFR	Net filtration rate
NO	Nitric oxide
PI3K	phosphoinositide 3-kinase
PBS	Phosphate-buffered saline
PFA	Paraformaldehyde
PKCϵ	Protein kinase C epsilon
RPP	Rate pressure product
RISK	Reperfusion injury salvage kinase
ROS	Reactive oxygen species
RBC	Red blood cell
SAFE	Survivor activating factor enhancement
S1P	Sphingosine-1-phosphate
STAT3	Signal transducer and activation of transcription-3
SSA	sub-Saharan Africa
SEM	Standard error of mean
TTC	Triphenyltetrazolium chloride
TNF-α	Tumor necrosis factor-alpha
TMB	Tetramethylbenzidine
WBC	White blood cell

CHAPTER 1: INTRODUCTION

1.1 Cardiovascular Diseases Major

Cardiovascular diseases (CVD) represent the most common group of non-communicable diseases and is the leading cause of death worldwide (Mathers, Boerma, and Fat 2009). CVD contributed to around 30% of all deaths in USA in 2010 (Santulli 2013). However, in 2015, CVD accounted for around 17.7 million deaths, amounting to 31% of deaths worldwide and more than 75% happen in low- and middle- income countries (WHO 2017). By 2020, CVD is predicted to be the major cause of morbidity and mortality globally (Murray & Lopez 1997). Furthermore, the prevalence of CVD are predicted to continue to rise and remain the leading cause of death, especially in low- and middle-income countries, such as in Africa by 2030 (Holmes et al. 2010).

In sub-Saharan Africa (SSA) there is increasing evidence of a changing disease profile, from infectious diseases and nutritional deficiencies to non-communicable chronic diseases, mainly including CVD (Akinboboye et al. 2003; Mensah 2008b). CVD caused about one million deaths in 2013 which represents 38.3% of non-communicable disease deaths in SSA, and 5.5% of global CVD deaths (Mensah et al. 2015). Furthermore, there was a significant increase in the number of deaths from CVD in SSA, whereas, the number of deaths due to CVD increased by 81% in 2013, in comparison to the deaths that occurred in 1990 (Mensah et al. 2015). In South Africa, non-communicable diseases contribute to premature mortality and cause around 39% of deaths, with 44% of these deaths due to CVD (Nojilana et al. 2016).

This mortality rate may be attributed to the dramatic increase in urbanization and the effects of globalization in recent decades; namely, the changes in lifestyle such as increased high saturated fat and sugar diets, decreased physical activity, high levels of stress and increased tobacco and alcohol consumption (Sampson, Amuyunzu-Nyamongo, and Mensah 2013). In 2010,

the most common leading risk factors of the global burden were hypertension, tobacco consumption and air pollution (Stephen et al. 2012). However, the number of deaths increased by 41% between 1990 and 2013 due to CVD globally, and this was mainly caused by population growth, aging, and epidemiological transition (Roth et al. 2015). Furthermore, It is estimated worldwide, that around eight in one hundred cases of the major non-communicable diseases including CVD and mainly coronary heart disease are due to lack of exercise and physical inactivity (Lee et al 2012). Other known risk factors for CVD such as hypertension and diabetes are also on the rise (Mensah 2008a). Increased blood pressure is the most common risk factor associated with CVD (Santulli et al. 2012). It is therefore important for public health providers to improve people's lifestyles and to manage the most common preventable risk factors of CVD.

The most common CVD representing the leading cause of death in the world is ischemic heart disease (IHD). IHD caused around 12.7% of total global mortality in 2008, with most of these deaths occurring in middle- and low-income countries. The high mortality in these countries may be due to an increase in the prevalence of traditional risk factors for atherosclerotic cardiovascular disease (Finegold, Asaria, and Francis 2013). IHD was previously considered rare in SSA and remains relatively uncommon. However, its incidence and prevalence is increasing and it is expected to increase further in the next twenty years, due to the increase in the occurrence of risk factors, mainly hypertension, diabetes, obesity and other life style changes mentioned above (as reviewed by Onen 2013; Mensah 2008b). Furthermore, age-standardized mortality rates for IHD are estimated to rise by 70% in African men and 74% in African women by 2030 (as reviewed by Onen 2013).

Myocardial ischemia or IHD is caused by interruption of coronary blood flow, due to complete or partial obstruction of the coronary vessels. Prolonged ischemia can lead to infarction and irreversible cell damage. Paradoxically, although reperfusion of ischemic tissue is important to improve the survival of the tissues and prevent irreversible cellular injury, it may lead to more cellular

damage than that caused by ischemia alone (Yamazaki et al. 1986). This type of tissue damage is called ischemia-reperfusion (I/R) injury.

I/R injury is mainly characterized as a myocardial cell disease, but the vasculature also is a major target of the injury (Dignan et al. 1992). Coronary vessels are important in delivering the blood and nutrient to the myocardium. These vessels are lined by endothelial cell which important in maintaining the blood vessel tone, regulating hemostasis, and regulating inflammatory processes. Endothelial cells are also coated with a gel-like layer called endothelial glycocalyx, which is an important structure that acts as a barrier between the vessel wall and circulating blood and maintains the endothelial layer integrity. However, the glycocalyx is very delicate and easily damaged during I/R injury (Mulivor and Lipowsky 2004).

1.2 The Endothelial Glycocalyx

1.2.1 Structure and Function of the Glycocalyx

The glycocalyx is a thin carbohydrate-rich layer that lines the vascular endothelium on the luminal surface. It is an essential structure for vascular homeostasis. In dimension, the glycocalyx is about 0.2 – 0.5 µm thick in small capillaries and increases in thickness with increasing vascular diameter (van den Berg, Vink, and Spaan 2003). The glycocalyx is composed of glycoproteins and proteoglycans which act as an important backbone and a firm connection to the endothelial cell lining (as reviewed by Reitsma et al. 2007). Soluble components also represent another important component of the glycocalyx, and are present within and on top of the proteoglycan and glycoprotein components.

Proteoglycans are the most important backbone molecules of the glycocalyx. These consist of core proteins such as syndecan, glypican, versecan, perlican, mimecan and biglycan, with one or more attached negatively charged sulphated glycosaminoglycan chains (GAGs), such as heparan sulphate (HS), chondroitin sulphate (CS), keratin sulphate (KS), hyaluronic

acid (HA) and dermatan sulphate (DS). GAGs contribute a negative charge to the glycocalyx which allows it to react with the positive charge of albumin to give stability to the glycocalyx. The albumin forms part of the permeability barrier via electrostatic binding between its positive charged arginine chain and the negative charge GAGs of the glycocalyx, and possibly fills the intracellular spaces and makes a network which more efficiently filters and increases the stability of the glycocalyx (Michel 1985; Adamson and Clough 1992). The interaction between individual GAG components is independent of each other. However, enzymatic removal of one GAG chain does not influence other GAGs, and thus will not affect the structural stability of the endothelial glycocalyx (Zeng et al. 2012). HS represents the most common GAG in the glycocalyx. The second most common is CS, and the rest of the glycocalyx is comprised of other GAGs such as KS. Since the proteoglycans are named according to their GAG attachment, HS proteoglycan is the most common and represents about 50-90% of the total proteoglycans. Proteoglycans are sub classified according to their core proteins, with syndecan-1 and glypican-1 being the two major HS proteoglycans (Rapraeger et al. 1985).

Syndecan-1 is a member of the syndecan family. There are four types of syndecans (syndecan 1-4) and each syndecan consists of a transmembrane core protein, with both intracellular and extracellular domains (ectodomain). The cytoplasmic and intracellular domains of the four types of syndecan are similar in their primary sequences and are considered to have 100% homology, but their extracellular domains differ (as reviewed by Zimmermann & David 1999). Furthermore, syndecan-1 structure is identical in rats, mice and humans in the cytoplasmic domain and transmembrane part, but they are different in amino acid sequences of the ectodomain, which exhibits around 70% homology between humans and mice, and 88% homology between rats and mice (as reviewed by Bernfield et al. 1992). Syndecan-1 is expressed in all cell types, mostly in the epithelial cells and maintains epithelial cell morphology and normal growth (Leppä et al. 1992). Further, syndecan-1 has an important role in the regulation of inflammation, cell-cell

and cell extracellular interaction (Li et al. 2002), and it can interact with many biological effector molecules and participate in regulation of many cellular processes, such as cell proliferation, differentiation, migration and cell behaviour (Derksen et al. 2002; Sanderson et al. 1994). HA is the only GAG not linked to the core proteins and is suggested to have an important role in the structure and contribute to the stability of the glycocalyx network (Broekhuizen et al. 2009).

Glycoproteins are also regarded as a backbone component of the glycocalyx which connects the glycocalyx to the endothelial cells. Glycoproteins are composed of proteins with small-branched carbohydrate side chains, which act as adhesion molecules and contribute to the coagulation, fibrinolytic, and hemostatic systems. There are three families of adhesion molecules that are glycoproteins; the selectin family, the integrin family and the immunoglobulin superfamily. The selectin family are responsible for binding of carbohydrate groups on the glycosylated proteins or lipids. The integrin family mediates endothelial adhesion to leukocytes and platelets. Members of the immunoglobulin family are ligands for integrins on leukocytes and platelets and mediate leucocyte homing to the endothelium and subsequent diapedesis (as reviewed by Reitsma et al. 2007). Soluble components are another important part of the glycocalyx. These include soluble proteins derived from blood or endothelium such as albumin and orosomucoid, which are incorporated between and cover the top of the proteoglycan-glycoprotein network and contribute in functional properties of the glycocalyx (Sörensson et al. 1999).

The glycocalyx provides essential functions necessary for vascular homeostasis. It regulates the permeability in peripheral vessels due to its negative charge, which antagonizes positively charged molecules and prevents certain molecules from passing through the endothelial cell membrane (van Haaren et al. 2003; van den Berg et al. 2003). Besides, the glycocalyx thickness in the vessel wall is enough to acts as a physical barrier between the cell adhesion molecules such as P-selectin and blood cells (Patel et al. 1995), thus it prevents adhesion of leukocytes and platelets to

endothelial cells (Mulivor and Lipowsky 2002). Recently, several studies have suggested that the glycocalyx can act as a mechanotransducer. Glycocalyx structures can convert the shear stress force of blood flow into shear-dependent endothelial responses, including vasorelaxation mediated by nitric oxide (NO), which is released from endothelial cells when exposed to shear stress (Gouverneur et al. 2006; Kelly et al. 2006; Tarbell and Pahakis 2006). Furthermore, the glycocalyx is suggested to play a role in the regulation of coagulation pathways, as many mediators which control the coagulation pathways are bound to the glycocalyx (Ho et al 1997). Finally, the glycocalyx can bind to the extracellular superoxide dismutase enzyme which can decrease oxidative stress by quenching oxygen free radicals and increase NO bioavailability (Li et al. 1998).

The function of the glycocalyx is dependent on the structural integrity of the glycocalyx and the health status of blood vessels. The disruption of the glycocalyx leads to failure of its function and the occurrence of pathological events such as increased endothelial permeability, edema formation, increased platelets, leukocyte aggregation and adhesion to the vessel wall, and hypercoagulation. Pathological conditions that can lead to glycocalyx damage include I/R injury (Rubio-Gayosso et al. 2006), diabetes mellitus (Zuurbier et al. 2005), sepsis (Hofmann-kiefer and Kemming 2009), hyperlipidemia (Vink et al. 2000), hypervolemia (Chappell et al. 2014) and severe trauma (Rahbar et al. 2015).

1.3 Ischemia-Reperfusion Injury: Mechanism, Types, and Clinical Relevance.

The mechanisms of I/R injury are still not clear but there are molecular and cellular events that occur during ischemia and reperfusion that are suggested to be responsible for this type of damage (Figure 1).

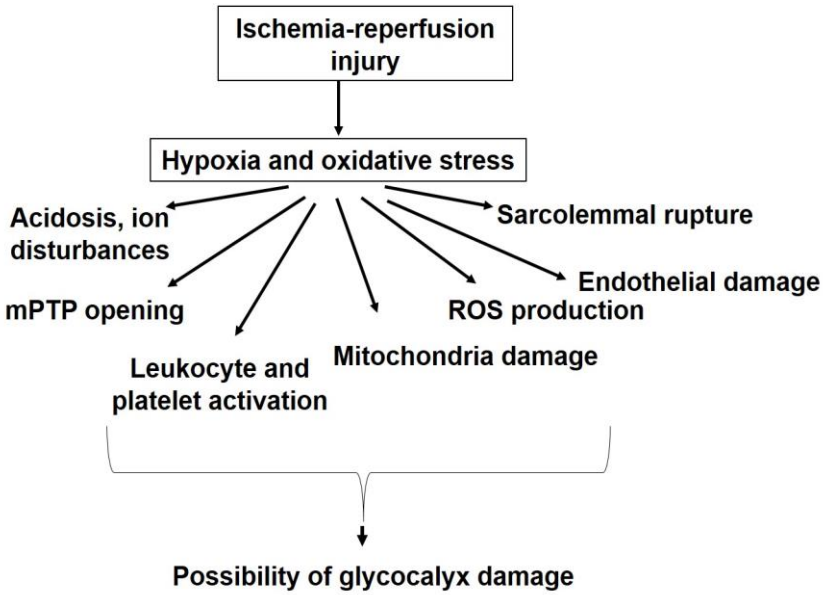

Figure 1: Suggested cascade of events in ischemia-reperfusion injury that may be linked to glycocalyx damage. Mitochondrial permeability transition pore (mPTP), reactive oxygen species (ROS).

Ischemia leads to a shortage of oxygen supply to the cardiac tissue, resulting in hypoxia. Hypoxic cells will undergo oxidative stress which results in cellular metabolic and ultra-structural changes, leading to failure to synthesize energy-rich phosphates, including adenosine-triphosphate (ATP) and phosphocreatine. Anaerobic metabolism and depletion of ATP may result in acidosis and alteration of membrane pump functions, resulting in disturbance of the ionic state across the cell membrane (Van Emous et al. 1998). The most important ionic disturbances are increased entry and accumulation of sodium, and water into the cell and depletion of potassium, which can lead to osmotic swelling and sarcolemmal membrane rupture, leading to necrosis (van Emous et al. 1997). In addition, intracellular calcium increases due to oxidative stress and disturbances in ion transport systems in the sarcolemmal membrane. Accumulation of calcium in cardiac cells leads to hypercontraction of heart cells and damage to mitochondria (Tani and Neely 1989). Further injury and cell death will be caused by the activation of calcium-dependent proteases with ongoing ischemia. Reperfusion of the ischemic tissue will end the ischemic changes, but reperfusion itself leads to

more damage, as sudden introduction of oxygen to the tissues will lead to increased production of toxic free radicals which lead to cellular injury by reaction with proteins, nucleic acid, and lipids (Paradies et al. 1999).

Accumulation of toxic reactive oxygen species (ROS) occurs early during reperfusion of ischemic tissue (Garlick et al. 1987). These molecules are short-lived, unstable, highly reactive, and generated in small amount during mitochondrial respiration, activation of phagocytic cells and xanthine oxidase activity. The normal produced ROS are inactivated by endogenous scavenging systems; however, in I/R injury production of free radicals increases and overwhelming the intracellular free radical scavenger system and results in accumulation of these molecules and cell damage (Zweier 1988). All these metabolic and ionic changes, combined with accumulation of toxic catabolites, result in more osmotic swelling which is sufficient to cause sarcolemmal membrane rupture and cell damage.

The mitochondrial permeability transition pores (mPTP) also play a significant role in the mechanism of reperfusion injury. These pores are situated in the inner mitochondrial membrane, and are impermeable to all metabolites and ions under normal physiological conditions. Accumulation of calcium and ROS during reperfusion leads to prolonged opening of mPTP, resulting in influx of solutes and water to the mitochondrial matrix (Halestrap et al. 1998; Crompton, Costi, and Hayat 1987). Furthermore, mitochondrial swelling and rupture lead to release of pro-apoptotic factors such as cytochrome c, which leads to activation of the caspase cascade and results in mitochondrial dysfunction, which initiates the mitochondrial apoptosis pathway and cell death (Moissac et al. 2000; Barauskaite et al. 2011)

Activation and accumulation of leukocytes in the damaged myocardium occur shortly after reperfusion, and promote the expression of adhesion molecules. Activated neutrophils become adherent to the endothelial cells leading to an increase in the release of cytotoxic and chemotactic substances such as cytokines, proteases, leukotrienes and oxygen free radicals which lead to endothelial damage, increase vascular permeability and thrombosis (Romson

et al. 1983; Baxter 2002). There is also evidence that neutrophils stimulate platelet activation and together exacerbate the post reperfusion cardiac contractile dysfunction (Lefer et al. 1998). Complement system activation also can occur as result of I/R injury, leading to stimulation of inflammatory cells and production of several inflammatory mediators which increase cell permeability, release of histamine, and platelet activating factor resulting in direct cell injury (Weiskopf et al. 2001).

Coronary endothelial dysfunction can occur as a consequence of I/R injury. The endothelium is representing the major source of NO, which leads to vasodilation, decreased platelet aggregation and decreased neutrophil adherence (Jones et al. 1999; Davenpeck et al. 1994), this function will be impaired after reperfusion due to hypoxia and ROS production. Impairment of the endothelial cell function manifests as impaired endothelial-dependent vasodilation and increased response to vasoconstrictors, resulting in decreased blood flow to the tissues (Tsao et al. 1990; Nakanishi et al. 1994). All this inflammatory cell activation and the release of its inflammatory mediators will compromise the integrity of the endothelial barrier, which includes the endothelial glycocalyx (Rubio-gayosso et al. 2006) and can lead to increases in vascular permeability and tissue edema.

The glycocalyx layer is stable under normal physiological conditions, which results from a balance between biosynthesis and shedding of its components (Mulivor and Lipowsky 2004). However, many studies in the isolated heart model have demonstrated that 20 minutes of no-flow ischemia with reperfusion is enough to cause degradation of the glycocalyx layer (Chappell et al. 2009a; Bruegger et al. 2008). Clinical studies have also demonstrated the shedding of glycocalyx components such as syndecan-1 and heparan sulphate in blood samples from patients who undergo vascular surgery with global or regional ischemia, and coronary bypass surgery (Rehm et al. 2007). The mechanisms related to shedding of the glycocalyx in I/R injury are not clear, but production of ROS during I/R has been proposed to play an important role (Rubio-gayosso, Platts, and Duling 2006). Activation of inflammatory cells and macrophages after I/R may also be responsible for

increased shedding, by increasing the production of ROS and other degrading enzymes such as heparanases, and neuraminidase. Tumour necrosis factor-α (TNF-α) is released as a result of inflammatory stimuli, such as ischemia, and has been shown in many studies to disrupt the barrier properties of the glycocalyx layer. TNF-α may cause activation of leukocytes, which then liberate cytokines, proteases and other factors which may disrupt the glycocalyx. TNF-α also has the ability to stimulate the endothelium directly to shed glycocalyx components (Henry and Duling 2000; Chappell et al. 2009b).

Post-ischemic hypoxia can also lead to decreased activity of adenylate cyclase, and intracellular cAMP levels resulting in decreased endothelial barrier function and increased permeability (Ogawa et al. 1992). The degree of endothelial barrier injury is increased in proportion to the duration and the severity of ischemia (Dauber et al. 1990). Myocardial edema after I/R injury is not stable and follows a bimodal pattern. The first one occurs directly after reperfusion, disappears at 24 hrs and then starts to increase progressively to reach maximum levels at day 7 (Fernandez-Jimenez, Sanchez-Gonzalez, et al. 2015). The first wave of edema occurs due to the reperfusion process itself and, the second wave occurs due to the tissue healing process (Fernandez-Jimenez, Garcia-Prieto, et al. 2015).

The severity of the cell damage and death is determined by many factors, including the type of ischemia (whether global or regional) and the duration of ischemia. Global ischemia is caused by complete severing of the blood supply to the entire heart. Regional ischemia is caused by obstruction of coronary arteries and only the part of the myocardium perfused with this artery will become ischemic.

From experimental studies on the effects of both types of ischemia on the myocardium, it is suggested that global ischemia leads to significant depression of cardiac function, and more significant tissue infarction in comparison to regional ischemia (Kim et al. 2012). Moreover, the severity of myocardial injury after I/R is adversely related to the duration of ischemia

itself - either regional or global ischemia. A shorter duration of ischemia (<20 minutes) may not be sufficient to cause irreversible damage to the myocytes, but it can lead to contractile and bio-energetic dysfunction which is markedly depressed with an increased duration of ischemia (>20 minutes), and the affected cells become irreversibly damaged. Bibli et al. (2012) assessed the effect of different durations of both types of ischemia on the functional recovery of the isolated rat heart. They found that a longer duration of ischemia was associated with more tissue damage and post ischemic ventricular dysfunction, which was more prominent after global than regional ischemia. Palmer et al. (2004) have shown the effect of different durations of global ischemia in isolated perfused rat hearts. They stated that the post ischemic dysfunction changed from mild to severe after 20 minutes of global ischemia. However, the left ventricular function was mildly weakened after an ischemic duration of 20 minutes or less, when compared with longer ischemia. Long duration of ischemia >20 minutes leads to an increase in end diastolic pressure, decreased coronary flow, and increases of creatine kinase release which is an indication of the severity of irreversible myocyte injury. In addition, prolonged ischemia can cause a significant edema formation and abnormality in the mitochondrial appearance with markedly swollen of the cristae and decreases in matrix density.

Clinically, regional ischemia is the most common type of myocardial ischemic episode. Regional ischemia occurs during thrombolysis, percutaneous coronary interventions, and coronary bypass. However, global ischemia also occurs in humans during open heart surgery when the aorta is clamped or in cardiac arrest. Revascularization of global or regional ischemic tissue leads to reperfusion injury which is manifested by myocardial stunning (Heyndrickx et al. 1975). This condition is defined as "prolonged post ischemic mechanical dysfunction that persists after reperfusion of previously ischemic tissue, without irreversible damage, and leads to unstable hemodynamic conditions". In addition, repeated episodes of stunning may lead to cardiomyopathy and heart failure (Renkin et al. 1990). Myocardial stunning is caused by calcium overload or generation of oxygen free radicals. Other

manifestations of reperfusion injury are reperfusion arrhythmias which include ventricular tachycardia and ventricular fibrillation which may lead to cardiac arrest and sudden death (Yamazaki et al. 1986). Endothelial dysfunction, myocyte death and necrosis can also occur after reperfusion injury.

1.3.1 Therapeutic Strategies for I/R Injury

The therapeutic strategies that limit I/R injury include ischemic conditioning and pharmacological interventions. Ischemic conditioning is a result of inducing one or more short episodes of ischemia interspersed with periods of reperfusion, either before the prolonged ischemia (a protocol called ischemic preconditioning; IPC) or after prolonged ischemia (a protocol called post conditioning; IPOST). Ischemic conditioning can also protect the heart if short ischemia-reperfusion episodes are applied to another organ distant from the heart before the heart is exposed to prolonged ischemia. This is protocol is called remote ischemic conditioning.

IPC was first described in the dog heart by Murry et al. (1986), and they suggested that IPC can decrease infarct size and improve functional recovery. Moreover, IPC preserves vascular endothelial function (Coulson et al. 1997), reduces apoptosis by inhibiting neutrophil accumulation (Nakamura et al. 2000), preserves cellular structure, and delays the development of structural signs related to ischemic injury (Murry et al. 1990). The mechanism of IPC and IPOST have not been well understood. However, there are many studies suggesting that different triggering substances are involved in mechanisms of ischemic conditioning pathways, which may lead to decreased production of ROS, decreased mitochondrial calcium overload (Wang et al. 2001), improved endothelial function and inhibition of the opening of the mPTP (Javadov et al. 2003; Argaud et al. 2005). Ischemic conditioning also activates prosurvival kinases involved in the reperfusion injury salvage kinase (RISK) pathway (Hausenloy et al. 2005) and the survivor activating factor enhanced (SAFE) pathway (Lacerda et al. 2009; Somers et al. 2012), which include various signaling pathways activated at

the time of reperfusion in both IPC and IPOST mediated cardioprotection. The cardiac protection achieved with IPC provides the same benefits as IPOST (Zhao et al. 2003). The mechanism underlying the remote conditioning are not fully understood and may overlap with those of IPC or IPOST. In addition, mechanisms involving neural or humoral pathways have been proposed in remote ischemic conditioning (Lim, Yellon, and Hausenloy 2010).

Pharmacological conditioning refers to cardiac protection by using pharmacological agents, which have been demonstrated in experimental studies to reduce myocardial infarction. The mechanism of pharmacological agents is to mimic the mechanistic pathway of ischemic conditioning. Some of these agents induced cardioprotection via enhancement of parts of the RISK pathway. These agents include adenosine (Liu et al. 1991), atrial natriuretic peptide (Kitakaze et al. 2007), bradykinin (Wall et al. 1994) atorvastatin (Bell and Yellon 2003) and erythropoietin (Chong et al. 2002). Others are mediated via the SAFE pathway, such as sphingosine-1-phosphate (S1P) (Kelly-Laubscher et al. 2014), and ethanolamine (Kelly et al. 2010). In addition, cyclosporine A induced cardioprotection is mediated by preservation of mitochondrial function during reperfusion (Skyschally, Schulz, and Heusch 2010). Recently, other agents such as antithrombin (Chappell et al. 2009a) and hydrocortisone (Chappell et al. 2007), have been shown to induce cardioprotection mediated by preservation of the endothelial barrier and decreased endothelial glycocalyx damage during I/R.

1.3.2 Pharmacological Protection of the Glycocalyx

Many agents have been shown in animal studies to protect the glycocalyx. These agents, such as glucocorticoids which have anti-inflammatory properties, are suggested to reduce the oxidative stress and glycocalyx damage and can limit the damage caused by inflammation and I/R (Chappell et al. 2007; Chappell et al. 2009b). Antithrombin is a potent anticoagulant and has remarkable anti-inflammatory properties. It has been demonstrated to protect the endothelial glycocalyx in animal models of I/R injury (Chappell et

al. 2009a). Sevoflurane is a volatile anesthetic agent which protects the glycocalyx against I/R and maintains the natural coating of endothelial adhesion molecules and reduces cell adhesion by attenuation of lysosomal cathepsin B release (Annecke et al. 2010; Chappell et al. 2011). Nitric oxide can also protect the heart after I/R injury - it prevents coronary vascular leak and tissue edema post ischemic injury by preserving the glycocalyx layer (Bruegger et al. 2008). Moreover, there are studies in non-ischemic animal models which suggest restoration of the glycocalyx after shedding by infusion of glycocalyx components (Constantinescu, Vink, and Spaan 2003; Henry and Duling 1999). Sphingosine-1-phosphate (S1P) has been known as a potent cardioprotective agent against I/R injury. Recently, S1P has been shown that can protect the glycocalyx against shedding in isolated cells against a non-ischaemic insult (Zeng et al. 2014) and promoting the synthesis of glycocalyx to maintains endothelial permeability (Zeng et al. 2015). However, whether this protection exists in a whole organ, or whether S1P can decrease glycocalyx shedding during I/R, is unknown.

1.4 Sphingosine-1- Phosphate

1.4.1 Structure and Function

S1P is a bioactive sphingolipid metabolite. It is one of the metabolic products of sphingomyelin and other phospholipid precursors by sphingosine kinase stimulation (as reviewed by Pyne & Pyne 2000). It is important in the regulation of many biological processes and cellular responses. S1P is produced and secreted by many cells including red blood cells, platelets, epithelial cells and cardiomyocytes. Platelets are suggested to be the greatest source of extracellular S1P, because they possess a highly active sphingosine kinase and lack the degrading enzyme S1P lyase (Yatorni et al. 1995). However, other studies suggest that red blood cells are the major source of S1P (Bode et al. 2010; Adamson et al. 2014).

S1P concentration in the plasma and serum ranges from 0.3 - 0.5 μM, and about 90% is bound to serum proteins, mainly high density lipoproteins

(HDL), serum albumin and low density lipoproteins (Murata et al. 2000) and these carry it to the endothelial cells to maintain the vascular permeability (Adamson et al. 2014). S1P is lipophilic and has been shown to bind with serum proteins, and these proteins may trap S1P and reduce its binding to its receptors. Therefore, the effective or active concentration of S1P in plasma might be much lower than total amount of the S1P in the plasma (Murata et al. 2000). On the other hand, S1P concentration in the plasma depends on plasma albumin concentration, and any condition that leads to decreased plasma albumin concentration may affect S1P level and compromise endothelial permeability. Moreover, the stability of the glycocalyx structure as part of the endothelial barrier is dependent on the plasma albumin concentration. In particular, removal of plasma proteins leads to decreased S1P delivery to the glycocalyx layer and increased protease dependent shedding of the glycocalyx and increased vascular permeability (Zeng et al 2014). Endothelial cells also represent another source of S1P (Venkataraman et al. 2008), however, experimental studies have concluded that S1P delivered from endothelium is not enough to maintain permeability and experiments on cultured endothelium or isolated vascular segment need a perfusate which saturated with S1P or source of S1P.

S1P has two sites of action: intracellular and extracellular. It acts intracellularly as a second messenger in the regulation of calcium homeostasis, and suppresses apoptosis via inositol trisphosphate-independent mechanisms (Mattie, Brooker, and Spiegel 1994). However, the target of intracellular S1P is still uncertain; it may act directly in the nucleus and influence gene expression. Alternatively, some evidence suggests that S1P can increase the release of calcium from intracellular sources by an inositol trisphosphate-independent pathway (Mattie, Brooker, and Spiegel 1994). Extracellular actions of S1P are mediated through activation of G-protein coupled cell surface receptors called S1P receptors (S1P1-5) (Hla 2001). Cardiomyocytes express S1P1, S1P2 and S1P3 receptors and activation of these receptors affect cardiac contractility and heart rate (Means et al. 2008; Mazurais et al. 2002). S1P1 receptor is the most abundantly

expressed on endothelial cells and contribute to maintain vascular barrier integrity (Zhang et al. 2010). Also, activation of S1P1 receptor by endogenous S1P regulates intracellular calcium levels by maintaining activity of the sarcolemmal Na/H exchanger and its activation is required for the cardioprotective effect of S1P in IPC (Keul et al. 2016).

S1P is found in many systems and is suggested to be involved in the physiological regulation of such systems. In the vascular system, S1P acts as a strong regulator of angiogenesis and may act as a vasoconstrictor or a vasodilator, depending on the expression pattern of S1P receptor sub-type in endothelial cells and vascular smooth muscles (Coussin 2002; Ohmori et al. 2003). In the immune system S1P is expressed in multiple immune cells and regulates their functions, and the S1P analogue FTY720 fingolimod (2-amino-2[2-(4-octylphenyl) ethyl] propane-1,3-diolhydrochloride), is suggested from immunomodulation studies to be an effective drug in the treatment of autoimmune diseases such as multiple sclerosis (Kappos 2006). S1P acts intracellularly as a second messenger to regulate cell growth (Zhang et al. 1991). Further, S1P can regulate functions of other systems such as the nervous and reproductive systems (Hla 2004).

1.4.2 Role of S1P in Cardiovascular Protection

Many studies have demonstrated the role of S1P in cardioprotection. S1P represents as one of the endogenous mediators released from cardiomyocytes during IPC and IPOST and can limit I/R-induced myocardial injury. Evidence for this comes from experiments where the S1P inhibitor, VPC, inhibited protection induced by both types of ischemic conditioning (Vessey et al. 2009). During ischemic conditioning, the released S1P leads to activation of S1P1 and S1P3 receptors and triggers cell-signalling pathways which induce cardioprotection. These signalling pathways include the activation of signal transducer and activator of transcription-3 (STAT3) and TNF-α which are involved in SAFE pathways, as well as the activation of protein kinases Akt and ERK, which are involved in the RISK pathway (Jin, Karliner, and Vessey 2008). IPC and IPOST lead to activation of protein

kinase C epsilon (PKCє) by releasing of mediators, PKCє in turn increases the activity of sphingosine kinase which is an important intracellular mediator leads to increase synthesis of S1P induced cardioprotection after I/R (Jin, Goetzl, and Karliner 2004).

S1P also is known as exogenous cardioprotectant agent which can protect the heart from I/R injury. Karliner et al. (2001) were the first to demonstrate the role of exogenous S1P in cardioprotection. They demonstrated that pretreatment with S1P reduced hypoxic cell death in cultured neonatal rat cardiac myocytes. In this study, the cardioprotective effect of S1P was mediated by protein kinases C and mitochondrial KATP channels. A subsequent study demonstrated that S1P protects cardiomyocytes from I/R injury, via activation of both S1P2 and S1P3 receptors through activation of an Akt-mediated pathway (Means et al. 2007). Furthermore, S1P pretreatment of hearts isolated from PKCє knockout mice and wild-type subjected to I/R injury, induced cardioprotection through a signalling that was independent of PKCє (Jin et al. 2002). Additional evidence for the role of S1P in cardioprotection comes from Theilmeier et al. (2006) who showed that infusion of HDL which is rich in S1P can reduce cardiac damage induced by I/R injury via S1P3 receptor-mediated and NO-dependent pathway. Other mechanisms suggested for the role of S1P-induced cardioprotection against I/R damage are through activation of both SAFE and RISK pathways after pharmacological pre- or post-conditioning of isolated heart with S1P (Kelly-Laubscher et al. 2014; Somers et al. 2012). Also, the S1P can induce cardioprotection via activation of STAT3 as part of SAFE pathways and this protection was mediated by ethanolamine which is a product of S1P metabolism (Kelly-Laubscher et al. 2010).

The cardioprotective effects of synthetic S1P receptor agonists such as S1P1,3 receptor agonist FTY720 and selective S1P1 receptor agonist SEW2871 also have been demonstrated and they are thought to act via Akt activation when applied during reperfusion (Hofmann et al. 2009). Moreover,

FTY720 can prevent arrhythmia induced by I/R injury through PaK1/Akt signalling (Egom et al. 2010). Pretreatment with FTY720 before ischemia

can also reduce post ischemic arrhythmia and decrease leukocyte infiltration with no effect on the infarct size. However, treatment during reperfusion increased mortality due to induction of arrhythmias, and it is suggested that FTY720 is an ideal preconditioning drug but not a post conditioning drug (Hofmann et al. 2010).

S1P has been identified as an important regulator and enhances the endothelial barrier function (Curry, Clark, and Adamson 2012). S1P can inhibit increased vascular permeability induced by inflammatory mediators such as platelet activating factor and bradykinin, which are released mainly during inflammatory conditions and leads to increased endothelial permeability and edema. This protection was mediated by activation of S1P1 receptor (Zhang et al. 2010). In addition, HDL which is the main carrier of S1P in the plasma, promotes endothelial barrier integrity, and these protective effects are suggested to be attributed to its S1P component and S1P1/Akt signalling (Argraves et al. 2008). Other mechanisms by which S1P can enhance the endothelial barrier is by phosphorylation of focal adhesion kinase which is important in actin cytoskeletal rearrangement, as well as increased cell-cell adhesion junctions (Shikata, Birukov, and Garcia 2003). S1P can also maintain endothelial barrier function in normal intact vessels by protecting the endothelial glycocalyx layer via activation of S1P1 receptors (Zhang et al. 2016). Also, S1P has been shown to protect the endothelial glycocalyx against shedding, after removal of plasma albumin in rat fat pad endothelial cells, through suppression of metalloproteinase (MMP) activity via activation of the S1P1 receptor (Zeng et al. 2014). Inhibition of MMPs protected against loss of chondroitin sulphate and syndecan-1 (Zeng et al. 2014). Furthermore, S1P can regulate and induce synthesis of glycocalyx components in rat fat-pad endothelial cells, after their shedding and this was mediated by phosphoinositide 3-kinase (PI3K) pathway (Zeng et al. 2015). However, this ability of S1P to stabilize and replenish the endothelial glycocalyx has not been shown in a whole organ model in the context of I/R injury.

CHAPTER 2: HYPOTHESIS

2.1 Hypothesis

We hypothesize that pretreatment with sphingosine-1-phosphate decreases the cardiac damage induced by I/R injury through stabilization of the glycocalyx.

2.2 Purpose

To assess whether the cardioprotective effect of sphingosine-1-phosphate against ischemic-reperfusion damage in the isolated rat heart model is mediated by stabilizing the glycocalyx.

2.3 Objectives

1. To confirm that I/R injury leads to increased degradation of the endothelial glycocalyx in addition to other molecular- and structural changes in the isolated rat heart model.

2. To assess the effects of sphingosine-1-phosphate on the degradation of the glycocalyx, infarct size, and cardiac edema during ischemia-reperfusion in the isolated rat heart.

CHAPTER 3: MATERIALS AND METHODS

3.1 Animals

Adult male Wistar rats (weight 250 - 300 g) were used in the experiments. All rats were transferred from Stellenbosch University to the Anatomy Building HUB basement at the University of Cape Town, where they were allowed to acclimatize to a new environment for two days before starting the experimental procedures. The rats were kept under controlled conditions (room temperature 21 - 23 ^{o}C and light intensity 150 lux), with free access to standard rat chow (Imbani Nutrition, SA) and water.

All experiments were approved by the Faculty of Health Sciences Animal Ethics Committee, University of Cape Town (Protocol AEC REF NO: 014/012), and performed in compliance with the Guide for the Care and Use of Laboratory Animals published by the US National Institutes of Health (National Research Council, National Press 2011). All the laboratory animal procedures were authorized by the South Africa Veterinary Council (SAVC) (NO: AR15/13426).

3.2 Experimental Design

A total of 117 rats were used in this study. Twelve rats were used in preliminary tests; two were used to train the procedure of perfusion and 10 were used to optimize the I/R protocol. Seventy-three rats were used to collect the data and divided into four groups (N≥16 rats per group), according to the Langendorff perfusion protocols further described below. At the end of reperfusion, each group was divided into three sub groups for; triphenyltetrazolium chloride (TTC) staining to assess infarct size, heart weight wet/dry ratio to assess cardiac edema, and histological investigation to assess syndecan-1 and extracellular edema (Figure 2). An additional group was included to assess the effects of Krebs-Henseleit buffer (K-H) perfusion alone on cardiac edema (N=7). Thirty-two rats were excluded from the study because they either did not comply with the inclusion criteria (see

section 3.3.2) or other reasons such as difficulties in cannulation or the heart not beating on the rig.

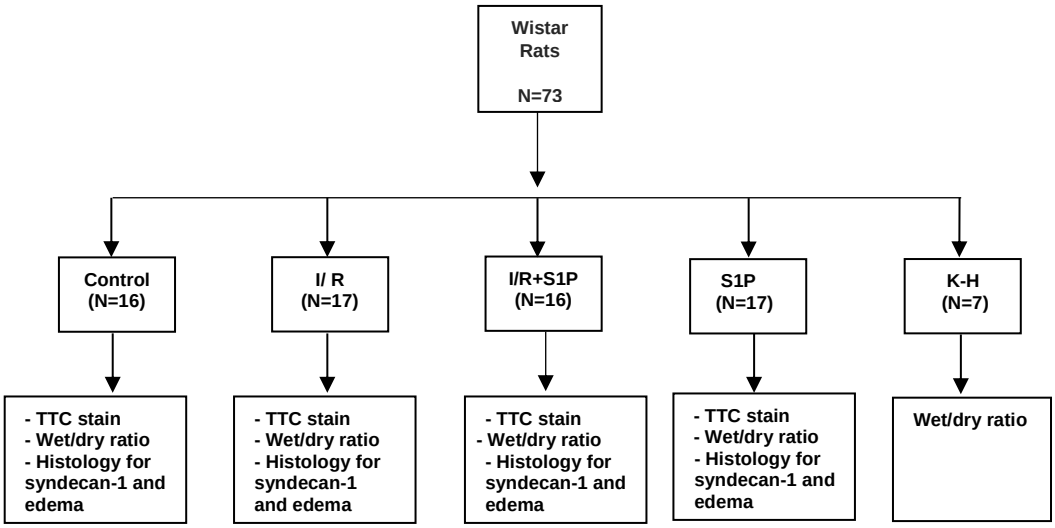

Figure 2: Experimental design. Four groups of rats were used. At the end of the protocol, each group was divided to three sub groups, one for TTC staining to assess infarct size (N≥6 each group), one for measurement of heart weight wet/dry ratio to assess cardiac edema (N=7 each group), and one for histological assessment of syndecan-1 and edema (N=3). A group of K-H perfusion only (N=7) were added to assess cardiac edema.

3.3 Isolated Rat Heart Model

3.3.1 Heart Isolation and Langendorff Perfusion

Male Wistar rats were weighed and anesthetized with sodium pentobarbitone (70 mg/kg, i.p.), with co-administration of heparin (500 IU) to reduce thrombus formation. Once the pedal withdrawal reflex disappeared, the chest cavity was opened through a skin incision performed at the xiphoid–sternum end and continued to lateral anterior axillary lines. The anterior chest wall was deflected upward and the pericardium opened. The heart was excised rapidly, arrested in cold K-H (4 ºC), and mounted on the Langendorff retrograde perfusion system via cannulation of the aorta (Figure 3).

The hearts were perfused with K-H buffer (in mM 118.5 NaCl, 25 $NaHCO_3$, 4.7 KCl, 1.2 KH_2PO_4, 1.8 $CaCl_2$, 1.2 $MgSO_4$, 11 glucose, pH 7.4), bubbled with 95% oxygen and 5% carbon dioxide throughout the protocol (Appendix 1). The perfusion pressure was kept constant at 74 mmHg by placing the K-H reservoir at a height of 1 meter above the tip of the perfusion cannula. The temperature of the perfusate was kept constant throughout the protocol at 37 ^oC, by using water-jacketed reservoirs and a heat exchanger.

A water-filled ventricular balloon was inserted through the left atrium into the left ventricle and was connected to a calibrated pressure transducer (MLT0699, ADInstruments, Australia) by polyethylene tubing. This transducer was connected to a Power Lab 4/30 data acquisition system (ADInstruments, Australia) via a Bridge Amplifier (ML221, ADInstruments, Australia) to measure the hemodynamic parameters. The data were recorded and digitized using Lab chart software version 7.00 (ADInstruments). The left ventricular end diastolic pressure was adjusted between 4 and 12 mmHg at the beginning of protocol. The pulmonary artery was cannulated to allow coronary venous effluent to be collected for measurement of coronary flow rate and syndecan-1.

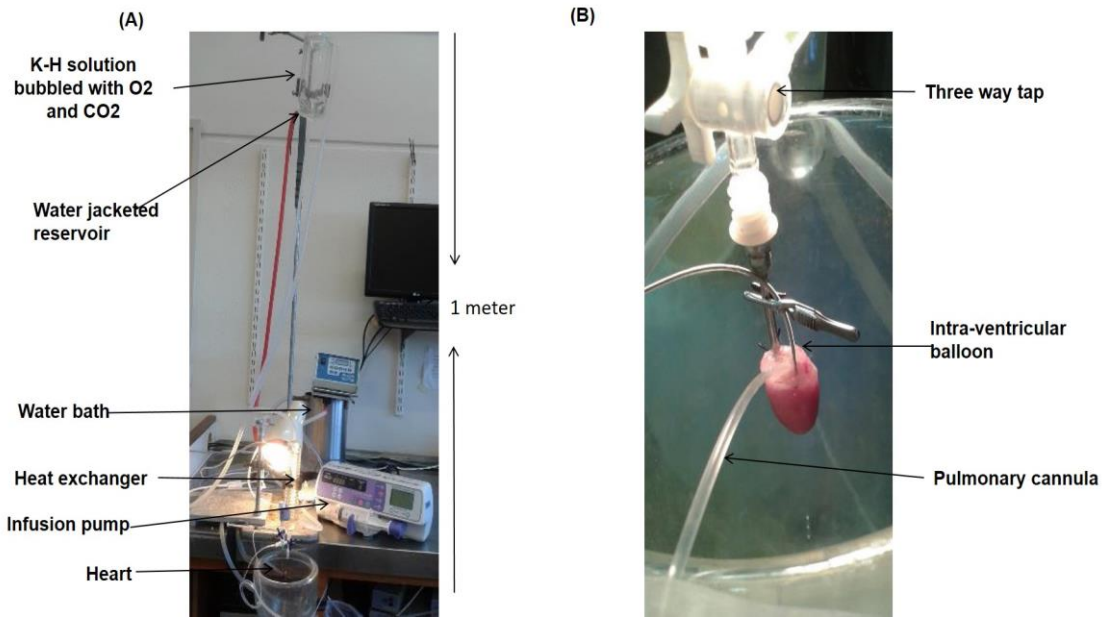

Figure 3: Langendorff retrograde perfusion. (A) Langendorff retrograde perfusion apparatus. (B) Langendorff retrograde heart perfusion technique.

3.3.2 Exclusion Criteria

The rat hearts that did not comply with the following criteria at baseline were removed from the study (N=32 rats):

Criterion	Inclusion Parameter
Heart rate	240-400 beat per minute
Left ventricular developed pressure	70-130 mmHg
Perfusion time due to cannulation problems	>3 min

3.3.3 Langendorff Perfusion Protocol

In preliminary experiments, the duration of global ischemia was optimized with the aim to achieve functional recovery upon reperfusion. Global ischemia was induced by stopping the perfusion flow by closure of a three-way tap above the aortic cannula and reperfusion was induced by restoring the flow. During ischemia, the temperature of the heart was maintained at 37 ^{o}C by immersing it in a warm K-H buffer bubbled with oxygen and carbon dioxide. Three different durations of global ischemia were used: 20, 25 and 30 minutes. We found that only hearts subjected to 20 minutes ischemia recovered during reperfusion, and this duration of ischemia was selected in our ischemia-reperfusion model (Appendix 2 and 3).

During Langendorff perfusions, all hearts were stabilized for 20 minutes and then divided according to treatment and induction of global ischemia (Figure 4) as follows:

Control group: Hearts were infused with the vehicle dimethylsulphoxide (DMSO) (1:10000 diluted in K-H) for 7 minutes, and then perfused with K-H for 90 minutes.

I/R group: Hearts were infused with DMSO for 7 minutes, followed by 10 minutes washout, and then exposed to 20 minutes global ischemia and 1 hour reperfusion.

I/R +S1P group: Hearts were infused with S1P (10 nM) for 7 minutes, followed by 10 minutes washout (Kelly-Laubscher et al. 2014; Lecour et al. 2002), and then exposed to 20 minutes global ischemia and 1 hour reperfusion.

S1P group: Hearts were infused with S1P (10 nM) for 7 minutes and then perfused with K-H for 90 minutes.

An infusion pump (Graseby 2100, Medical Smith, UK) was used to infuse S1P and DMSO to the heart through a 3-way tap connected to both the aortic cannula and K-H reservoir. The infusion speed was adjusted to 1/10 of the CF to minimise alteration of the main perfusion inflow.

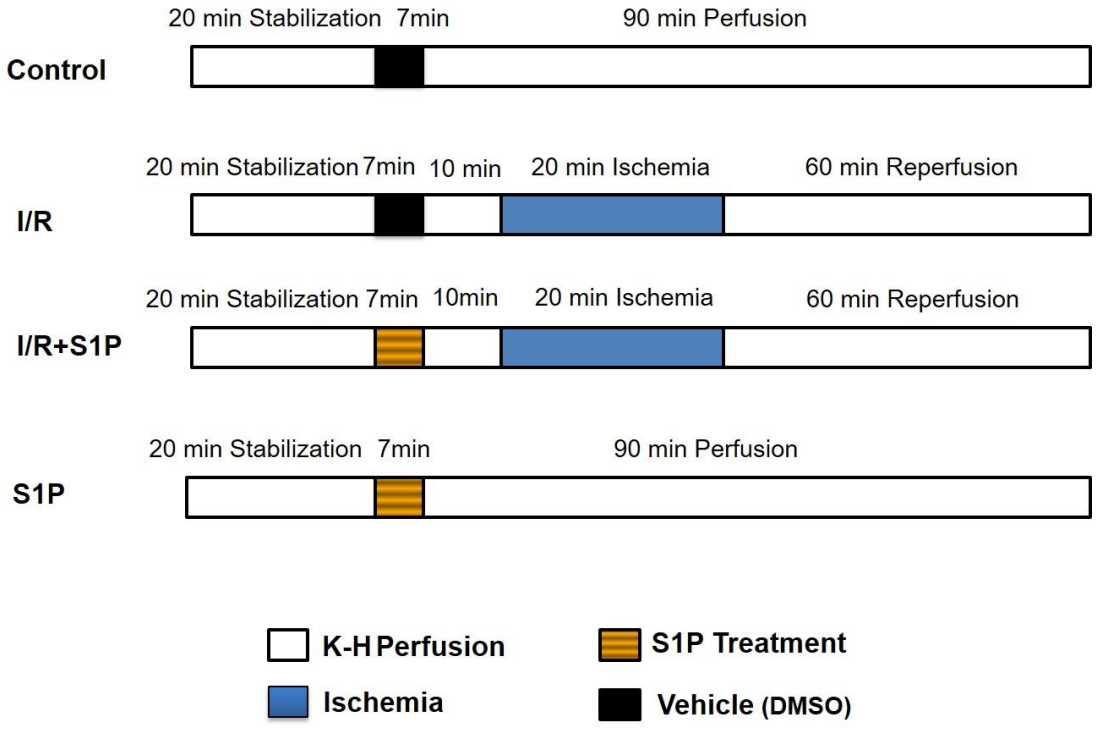

Figure 4: Schematic representation of Langendorff perfusion protocol.

3.4 Hemodynamic Measurements

Various cardiac parameters were measured throughout the experiment, including left ventricular systolic pressure (LVSP), left ventricular end diastolic pressure (LVEDP), heart rate (HR), coronary flow (CF) and left ventricular developed pressure (LVDP: difference between left ventricular systolic and left ventricular end diastolic pressure). Rate pressure product (RPP) was calculated as LVDP × heart rate, and functional recovery was expressed as percentage of baseline. Coronary flow rate was measured by timed collection of coronary effluent through cannulation of the pulmonary artery. The transudate was collected from the apex of the heart and net filtration rate (NFR) was calculated as the ratio between the transudate and effluent flow rate.

3.5 Infarct Size Analysis

Staining with TTC was used to differentiate necrotic cardiac cells from viable cells. At the end of the perfusion protocol, the hearts were decannulated and frozen at -20 ºC. Once frozen they were sectioned to slices of 2 mm thickness, perpendicular to the long axis, and incubated in 1% TTC in phosphate buffer at 37 ºC (pH 7.4) protected from light for 20 minutes. Slices were fixed in 10% formalin solution in a dark cupboard at room temperature, for clearer delineation between the viable (red), and non-viable (pale) tissue. After 24 hours, the heart slices were arranged from apex to base between two transparent plates and digitally scanned on a flat- bed scanner (CanoScan LDE 110, Vietnam). Total tissue area and infarct area were measured using ImageJ software (ImageJ, NIH Image) for the details of measurement (see Appendix 5). Infarct size was expressed as percentage of total ventricular area.

3.6 Assessment of Cardiac Edema

Measurement of cardiac edema was obtained by calculating the wet/dry heart weight ratio. At the end of each protocol, the hearts were decannulated and weighed to obtain wet weight. The hearts were then placed in an oven at 60 ºC for 24 hours and weighed again to obtain dry weight. These values were used to calculate wet/dry heart weight ratio.

In this analysis, another group of rats were added to investigate the effect of DMSO on the cardiac edema. This group was perfused with K-H only for the same duration as other protocols and coronary effluent was collected for analysis of syndecan-1 levels.

Further, histological investigation was added to assess cardiac edema by quantification of the extracellular edema (see sections 3.8, and 3.8.2).

3.7 Determination of the Glycocalyx Components

3.7.1 Sample Collection and Preparation

The samples of coronary effluent were collected from all groups, through the cannulated pulmonary artery over 10 minutes at 0 – 10 minutes after onset of reperfusion (Annecke et al. 2010), then kept at -20 ºC. Once all perfusion experiments were completed, coronary effluent samples were defrosted and centrifuged. Samples of 2 ml each were concentrated to 150 – 200 µL with 10 KDa cut-off ultrafilters centrifugal unit (Millipore, Billerica, MA, USA), using Eppendorf centrifuge (5810/5810 R Swing- bucket rotor centrifuge, Eppendorf, Germany), at 2020 × g at room temperature (20 ºC) for 1 hour. Thereafter, samples were aliquoted and frozen at -80 ºC until used for ELISA (Annecke et al. 2010).

The samples were collected in a series over one year. However, samples were protected from degradation by quick freezing at -20 ºC once collected. Thereafter, samples were aliquoted and kept at -80 ºC once centrifuged for 5 - 8 months until used. Also, freezing thaw of the samples, which may lead to protein denaturation was avoided during the ELISA procedure.

3.7.2 Enzyme-linked Immunosorbent Assay (ELISA)

ELISA is an immunological method. It is used for detection and quantification of proteins, hormones, peptides, and antibodies. Usually 96-well polystyrene plates coated by a special antibody or antigen are used in the assay. There are several types of ELISA-assay (Figure 5):

Direct ELISA, indirect ELISA, and sandwich ELISA

In this study, a Sandwich ELISA was employed. This type of ELISA detects the antigen between two layers of antibodies. The wells of the plate are coated by capture antibody and blocked, before the sample containing antigen is added. An enzyme-linked secondary antibody is added, followed by a substrate which reacts with the enzyme bound to the secondary antibody to give a color or fluorescent signal that can be measured to determine the presence of the antigen.

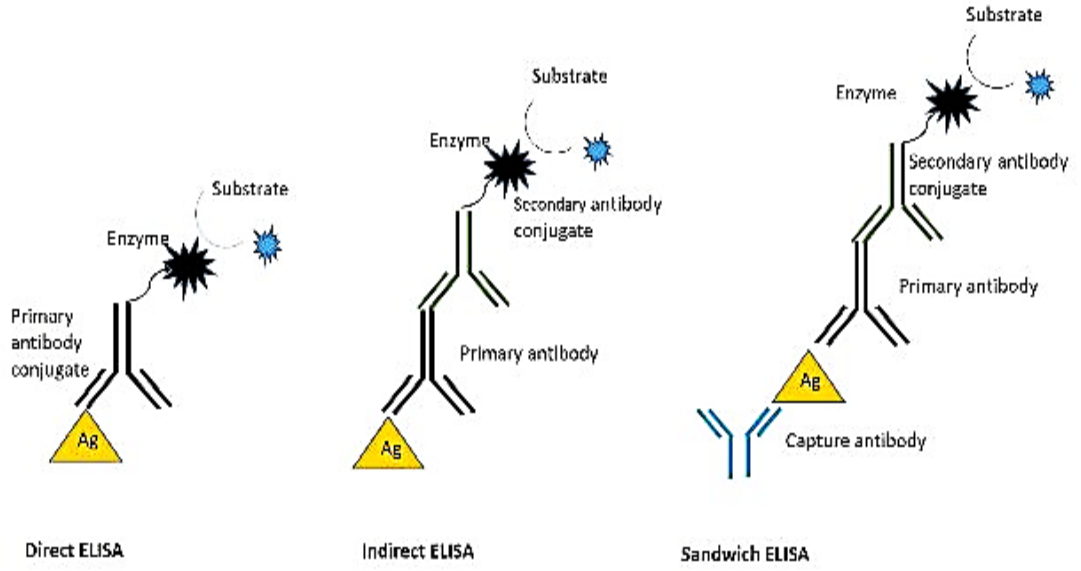

Figure 5: Diagram shows the different types of ELISA (Thermofisher.com).

3.7.2.1 ELISA Procedure

Previous studies in both humans and guineas pigs have used a Human Syndecan-1/CD138 ELISA Kit (Diaclone, France) (Rehm et al. 2007). However, this company also provides a Murine Syndecan-1/CD138 ELISA

Set. When the experiments of the study were designed, it was unclear which of the available ELISA kits would optimally detect syndecan-1 in our model. Therefore, both ELISA kits (Human Syndecan-1/CD138 ELISA Kit, Cat. No. 950.640.192, Diaclone, France) and (Murine Syndecan-1/CD138 ELISA Set, Cat. No. 861.060.005, Diaclone, France) were used and the results compared.

Both ELISA tests done in this study were based on the sandwich principle, using solid-phase monoclonal B-B4 antibody and a biotinylated monoclonal B-D 30 antibody raised against syndecan-1. The detection steps rely on streptavidin-horseradish peroxidase (HRP), and tetramethylbenzidine (TMB) as chromogen. The protein levels were quantified by spectrophotometer (SpectraMax plus 384 Microplate Reader, USA) at 450 nm as the primary wavelength and 620 nm as the reference wavelength. ELISA procedures and assay preparation were carried out in accordance with the supplier's instructions (Diaclone research, Besancon, France). The standard concentration ranges of the human antibody kit were from 8 to 256 ng/ml, the sensitivity was 4.94 ng/ml and the coefficient of variation in 6 replicates was 6.2% intra-assay, and 10.2% inter-assay. However, for the murine antibody the concentration ranges were from 0.5 to 16 ng/ml, the sensitivity was 0.35 ng/ml and the specificity was <3.7% with recombinant human CD138.

3.7.2.2 Murine Syndecan-1/ CD138 ELISA Set

Since the syndecan-1 in the rat and mouse have greater homology (92.3%) than the rat and human (80.5%) (Appendix 7), the murine syndecan-1 antibody was tried first. Microtiter plates of 96-well were used. The plates were coated with 100 µL of diluted capture antibody and incubated overnight at 4 ^{o}C. After incubation, the plate was washed twice with phosphate-buffered saline (PBS) containing 0.05% Tween-20 to remove unwanted materials. A blocking buffer (250 µL), PBS containing 5% bovine serum albumin (BSA) was added to the plate to block non-specific binding sites on the surface. After 2 hours incubation at room temperature (18 to 25 ^{o}C) on the shaker, the plate was again washed three times with PBS. Then 50 µl of each sample, standard and zero or blank (standard diluent) were added to

the plate in duplicate. Diluted biotinylated detection antibody (50 µl) was added to each well and the plate was covered and incubated for 2 hours at room temperature on the shaker. Any unbound antibody was removed by washing the plate twice. The streptavidin-HRP solution (100 µl) was added to every well and after incubation of 30 minutes at room temperature on the shaker, the plate was washed two times. A chromogen substrate TMB (100 µl) was then added to the wells and incubated in the dark by wrapping the plate in aluminium foil for 15 minutes at room temperature. TMB reacts with HRP to produce a blue color. This reaction is stopped by the addition 100 µl of 1 M sulfuric acid, which also turns the color yellow. The amount of color produced, as measured using a spectrophotometer (SpectraMax plus 384 Microplate Reader, USA) was directly proportional to the amount of syndecan-1 in the samples and standards (Appendix 6). A standard curve was created by plotting the absorbance of each standard against the known concentration of each standard (Appendix 6.2.6). This curve was used to quantify the syndecan-1 concentration in the samples. Graph Pad Prism statistical software was used to conduct the analysis (GraphPad Prism, USA).

3.7.2.3 Human Syndecan-1/CD138 Kit

Each sample, standard, control and zero (standard diluent) (50 µL) were added to precoated 96-well microtiter plates in duplicate. The remainder of the procedure was identical to that for the Murine ELISA described above (Appendix 6.2.7 standard curve).

Immunohistochemically investigation also was added to determining relative syndecan-1 staining intensity between groups (see sections 3.8 and 3.8.1).

3.8 Histological Investigation

An additional 12 rats (3 rats per group) were used for histological studies. Hearts were isolated and perfused with K-H buffer in a Langendorff system as described previously in section 3.3.1, and divided into four groups according to the treatment protocol as described in section 3.3.3. At the end of the perfusion protocol the hearts were perfusion-fixed immediately

thereafter with 4% paraformaldehyde (PFA) in PBS (pH 7.4) at room temperature. Fixative was administered using an infusion pump (Graseby 2100, Medical Smith, UK) by switching off three-way tap (stopcock) to stop perfusion of K-H and start infusion of the fixative. Perfusion-fixation were continued for 10 minutes in a fume hood after separating the cannulated heart together with the stopcock and perfusion fixative line from the main rig to avoid contamination of the rig with PFA (Figure 6). The flow rate of fixative was set at the same rate as the coronary flow at the end of reperfusion for each heart and ranged between 0.5 - 2 ml/min. Hearts were decannulated and cut into four pieces similar to that used for TTC assay (see section 3.5), and further immersion-fixed in the above fixative solution overnight at 4 ºC, and processed to wax using an automatic tissue processor (Leica TP1020, Leica Biosystems, Germany). Briefly, tissues were dehydrated in increasing concentrations of ethanol, cleared in xylene, impregnated and embedded in paraffin wax (Appendix 8.1). Sections were cut using a rotary microtome (Leica RM2125RT, Leica Biosystems, Germany) and prepared for immunohistochemistry to assess syndecan-1 levels in blood vessels and for Haematoxylin and Eosin staining (H&E stain) to assess extracellular edema.

Figure 6: Perfusion-fixation of isolated heart. PFA in the syringe was infused at rate ranges between 0.5 - 2 ml/min using an infusion pump connected via tube to the cannulated heart through three-way tap in fume hood.

3.8.1 Immunohistochemistry Protocol

3.8.1.1 Preparation of the Sections

Sections of 6 µm thickness (3 sections/heart) were cut and first floated onto 30% alcohol in water before being transferred to a hot water bath at 43 ºC to flatten the section, and then mounted on coated microscope glass slides (SuperFrost Plus slides, Thermo Scientific, USA). The slides were stored overnight in an oven at 60 ºC. The sections were deparaffinized in xylene, rehydrated and rinsed in running tap water (Appendix 8.2.1 and 8.2.2).

3.8.1.2 Immunostaining Procedure

Optimization for immunofluorescent staining was first attempted using mouse monoclonal antisyndecan-1 (B-A38, ab 34164, Abcam) on sections from a control heart and spleen (PFA-fixed/Paraffin embedded sections) where syndecan-1 was expected to be present. The spleen was used as positive control as recommended by manufacturers. Some sections were subjected to antigen heat retrieval in citrate buffer pH 6 for 5 minutes, followed by the staining protocol for syndecan-1. Briefly, after washing in PBS, the sections were incubated in 50 mM ammonium chloride in PBS for 30 minutes to quench aldehyde-induced auto-fluorescence, and reduce background staining when using fluorescent detection. Non-specific binding was blocked with 3% BSA in PBS/ 0.1% Triton X-100 for 2 hours at room temperature. Thereafter, sections were incubated in increasing dilutions of mouse antisyndecan-1 antibody (1:50, 1:100, 1:250, 1:500) overnight at 4 ºC in a humidity chamber.

After washing in PBS/ 0.1% Tween-20, sections were incubated with anti-mouse CY3 secondary antibody 1:1000 dilution (CY3 anti-mouse, Code. No. 715-166-151, Jackson ImmunoReseatch) for 2 hours in dark humidity chamber at room temperature. Sections were mounted with glycerol and coverslips were applied. Sections were kept in dark cupboard for better viewing on the next day using a fluorescence microscope (Zeiss Axiovert 200 M fluorescent microscope, Carl Zeiss, Germany) using excitation and

emission wavelengths of 546 and 590 nm respectively. However, no fluorescence staining was detected in any sections.

The immunostaining was repeated to increase sensitivity of detection by increasing the time of heat antigen retrieval in citrate buffer pH 6 for 20 minutes, and still no signal was detected.

Furthermore, the immunofluorescent staining was tried on frozen sections which were fixed in 100% methanol to exclude the possibility that the PFA fixation and tissue processing procedure might have affected the signal. Again, no signal was detected.

Chromogenic detection was also tried because it is more sensitive than immunofluorescent. Briefly, sections were treated with heat antigen retrieval in the above buffer or Tris-EDTA pH 9 for 5 minutes. Then endogenous peroxidase was blocked with 3% hydrogen peroxide in distilled water to reduce background staining of non-specific binding. After BSA blocking of non-specific binding sections were incubated with primary antibody (1:50 dilution) overnight at 4 ^{o}C in a humidity chamber. Thereafter, sections were incubated with secondary antibody EnVision+ System- HRP Labelled anti-mouse secondary antibody (K-4000, Dako) for 1 hour at room temperature. After washing in PBS/Tween-20, sections were incubated in 3,3-diaminobenzidine (DAB) (K3467, Dako) and the reaction was observed under the light microscope up to 15 minutes to determine at what time point can stop the reaction. Again, no signal was detected.

Since none of the above approaches yielded success, there was strong possibility that the antibody was defective. Therefore, immunostaining was repeated using a newly purchased rabbit monoclonal [EPR6454] syndecan-1 antibody (ab216458, Abcam).

The above immunofluorescent staining protocol without antigen retrieval was followed using new antibody (rabbit monoclonal antisyndecan-1 antibody). The secondary antibody used for detection was anti-rabbit CY3 secondary antibody (CY3 anti-rabbit, Code. No. 711-166-152, Jackson ImmunoResearch) using a dilution of 1:2000. Sections were mounted and viewed as above (Appendix 8.3.1.1).

Furthermore, chromogenic detection also was tried. Whereas half of sections were treated for heat antigen retrieval using citrate buffer for 5 minutes. The secondary antibody used was goat anti-rabbit HRP- linked (ab6721, Abcam) using a dilution of 1:250 for 1 hour at room temperature. Thereafter sections were incubated with Vector DAB substrate (DAB Peroxidase kit, Cat.No.SK-4100, Vector, Burlingame, CA). The DAB reaction was also optimized by observation of staining reaction under the light microscope, and the reaction was stopped after 5, 6, and 12 minutes by rinsing sections with double distilled. After staining, slides were dehydrated and cleared in xylene. Coverslips were applied to sections and mounted with Dibutyl phthalate-DPX (Sigma). Negative controls were performed by excluding the primary antibody only or excluding both antibodies to determine any non-specific cross reactivity with secondary antibody or endogenous peroxidase respectively.

Based on the findings of the above variations in the protocols, the optimal conditions for detection of syndecan-1 were found to be a 1:500 dilution of primary antibody without antigen retrieval and a 1:250 dilution of HRP-linked secondary antibody. The optimal incubation time of section with DAB substrate was 6 min. Therefore, the immunostaining protocol for syndecan-1 on remaining hearts from different experiments and controls was continued using these conditions (Appendix 8.3.1.2).

Tile scan of the entire sections were captured using the Virtual Slide Microscope System at 40X objective lens magnification (VS120-L100-W, Olympus, Japan). This scan allowed visualizing the entire section and outline the ventricle to assess blood vessels which was not possible to do by fluorescent microscopy (see image analysis for details).

3.8.1.3 Image Analysis

A scoring system was used to evaluate the presence of syndecan-1 in blood vessels based on a previous study (Kliment and Oury 2012) with a modification from their scoring system of 0 - 2 to that of 0 - 3 for this study. The left ventricular area in the section was identified on the tile-scanned images and 20 vessels (arteries and veins excluding small capillary) of the ventricle were visually scored at 40X objective lens magnification. Vessels

were scored as 0 = no staining, 1 = mild staining, 2 = moderate staining, 3 = intense staining according to their staining intensity (Figure 7). Scoring was performed on 3 sections/heart and 3 hearts/group. Scoring data was analysed by Non-parametric one-way ANOVA and data presented as score mean ± SEM (see the statistical analysis section for data analysis details).

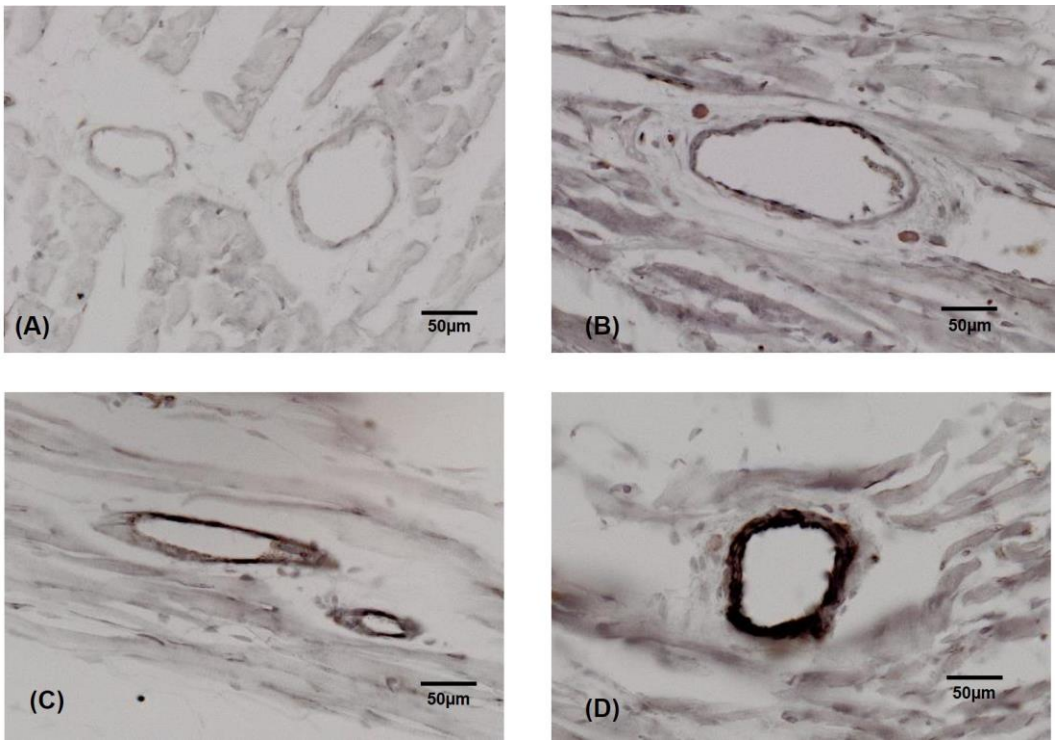

Figure 7: Representative syndecan-1 immunostaining pattern of coronary blood vessels. Scoring categories according to staining intensity of the vessel wall are shown as described in image analysis section; (A) Score 0 = no staining, (B) Score 1 = mild staining, (C) Score 2 = moderate staining, (D) Score 3 = intense staining.

3.8.2 Hematoxylin and Eosin Staining Protocol

3.8.2.1 Preparation and Staining of the Sections

The paraffin-embedded samples of the left ventricle were sectioned to 5 µm thickness (3 section/heart), mounted on non-coated microscopic slide (Frosted microscope slides, Lasec, SA) and prepared for H&E staining for

histological investigation (Appendix 8.3.2). Sections were visualized using an upright light microscope at 20X objective lens magnification (Zeiss Axioskop 2 Mot plus light microscope, Carl Zeiss, Germany) and photographed using CCD camera AxioCamHR controlled by Axiovesion 4.7 software (Carl Zeiss, Germany).

3.8.2.2 Image Analysis

Images of different areas of the left ventricle of each section (3 sections/ heart and 3 images/section) were taken (Figure 8). The extracellular compartment (i.e. any space outside the cardiomyocytes) of the left ventricular field was measured by thresholding this compartment using ImageJ software (ImageJ, NIH Image), and was expressed as percentage of total area of the field of the image (Figure 9) (Appendix 9 for ImageJ analysis).

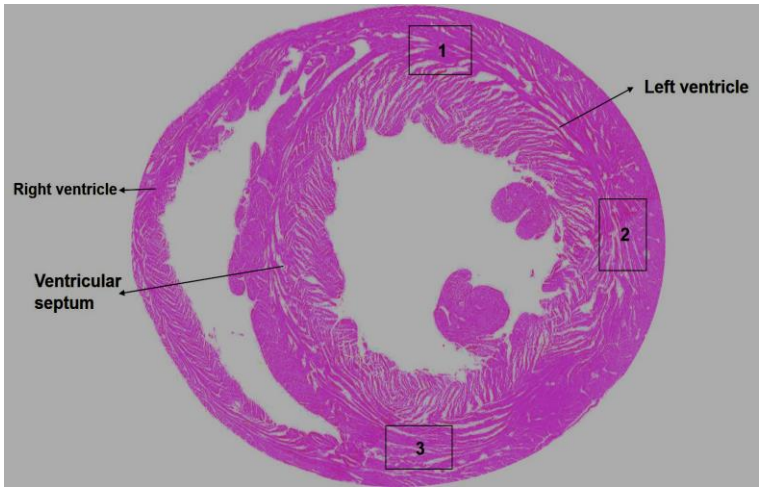

Figure 8: Shown left ventricular section (PFA/Paraffin embedded) stained with Hematoxylin and Eosin stain. Areas 1, 2, 3 represent the site of the images captured by the camera system on the light microscope using a 20X objective lens as described in image analysis section.

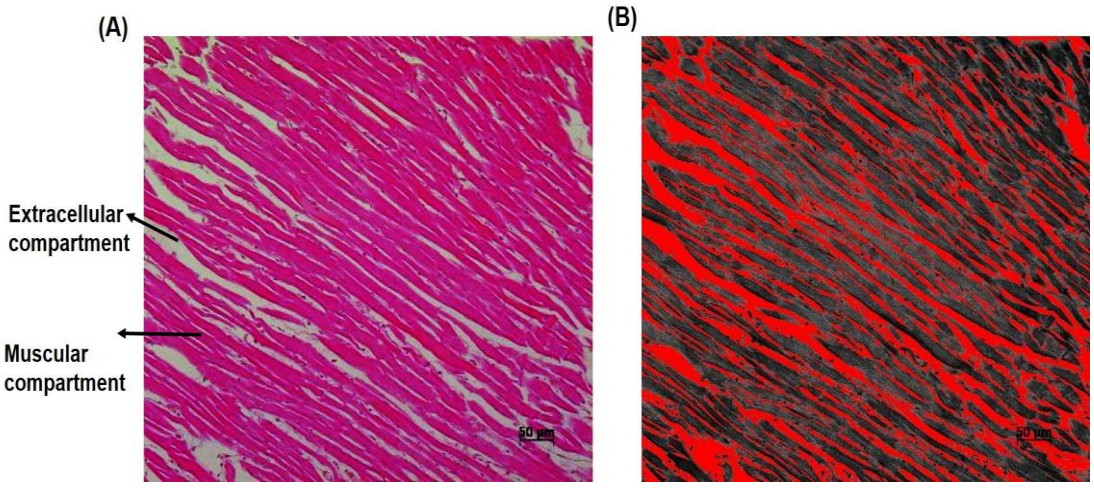

Figure 9: ImageJ analysis to quantify extracellular compartment. (A) H&E stained section of left ventricle using a 20X objective lens. (B) the same image as in (A) after thresholding (red) in ImageJ software.

3.9 Statistical Analysis

In this study, all data were presented as the mean ± SEM. Comparisons between multiple groups were performed using one-way ANOVA, and repeated measures ANOVA were used for measurements in a single group measured more than one time. Non-parametric tests were performed on data that were not normally distributed. Post-hoc tests were performed using Tukey's test. Vasculature syndecan-1 scoring data was analyzed by non-parametric ANOVA, Kruskal-Wallis test with a Dunn's post-test. A value of $P<0.05$ was considered to be statistically significant. GraphPad Prism statistical software version 7 was used to conduct the analysis (GraphPad Prism, USA).

CHAPTER 4: RESULTS

4.1 Effect of S1P on Infarct Size

Isolated rat hearts subjected to 20 minutes global ischemia and 60 minutes reperfusion had an infarct size of 32.34 ± 4.08% of the total ventricular area (Figure 10). By comparison, control hearts had significantly lower infarct sizes of 17.33 ± 1.59% (P= 0.04, control vs. I/R) and S1P perfused hearts had an infarct size of 16.06 ± 4.07 (P=0.02, S1P vs. I/R). Treatment with S1P before ischemia (I/R+S1P) significantly decreased infarct size to 14.17± 4.35% (P= 0.01, I/R+S1P vs. I/R), and there were no significant differences (n.s, P>0.05) between the control and the S1P perfused groups.

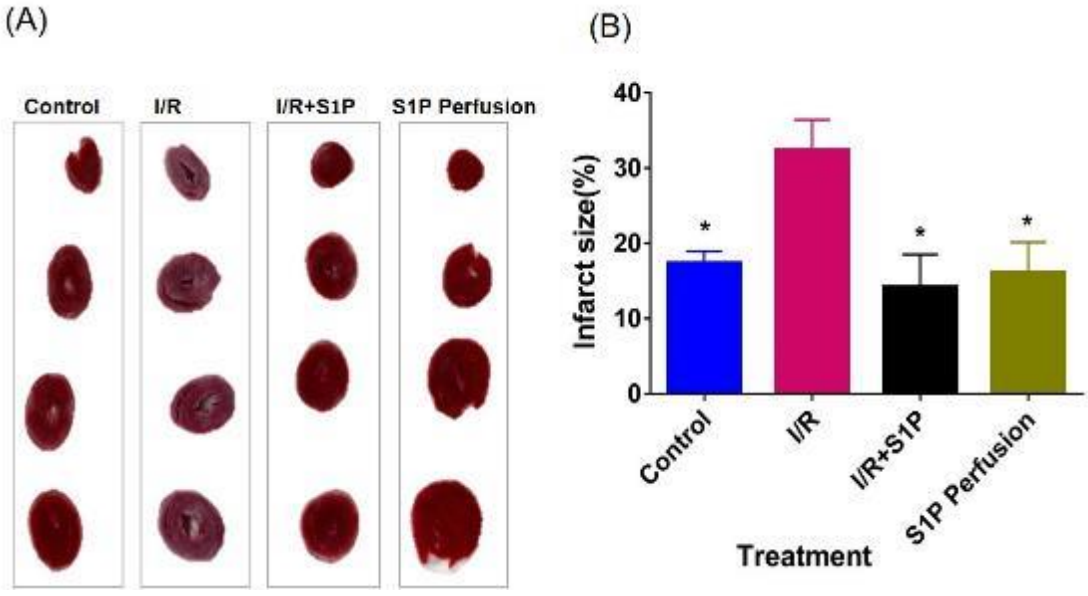

Figure 10: Effect of S1P on infarct size of isolated hearts subjected to 20 minutes ischemia and 1 h reperfusion. (A) Images of ventricular myocardium cross-sections stained with TTC in all four groups. (B) Summary data of infarct size. Infarct size is expressed as a percentage of total ventricular area (*P<0.05 vs. I/R. N≥6/ group).

4.2 Effect of S1P on Hemodynamic Parameters in Isolated Perfused Hearts

The hemodynamic data of the isolated hearts subjected to 20 minutes ischemia and 60 minutes reperfusion, with or without S1P treatment, were recorded at different time points during the protocol for all groups (Figure 11). At the end of the protocol, control hearts had post perfusion LVDP of 40.66 ± 2.02 mmHg and LVEDP of 26.15 ± 3.82 mmHg. I/R caused a significant decrease in LVDP 18.19 ± 4.78 mmHg, ($P=0.02$ vs. control) and an increase LVEDP of 61.37 ± 5.32 mmHg ($P<0.0001$ vs. control). S1P treatment before ischemia did not improve recovery of LVDP (15.51 ± 2.06 mmHg vs. I/R, $P>0.05$ n.s) or LVEDP (69.49 ± 3.62 mmHg vs. I/R, $P>0.05$ n.s). In S1P treated hearts that were not subjected to ischemia, LVDP and LVEDP were not significantly different from the control (LVDP: 39.83 ± 4.24 mmHg $P=0.99$ vs. control; LVEDP: 12.98 ± 1.86 mmHg, $P=0.1$ vs. control). HR, CF, NFR, and RPP were not significantly different between the groups at the end of reperfusion.

The baseline hemodynamic parameters measured at the end of 20 minutes stabilization were not significantly different between the groups. In each single group, there was a significant decrease in LVDP and CF by the end of reperfusion compared to the values measured at the end of stabilization ($P<0.0001$ at the end vs. baseline). All groups except the S1P perfusion group showed a significant increase in LVEDP by the end of reperfusion, compared to the baseline values ($P<0.001$). HR was not significantly different at the end of perfusion in comparison to the baseline values in each group ($P>0.05$). All groups, except the S1P treated group with or without ischemia (I/R+S1P, S1P perfusion) demonstrated a significant increased NFR by the end of reperfusion compared to baseline ($P<0.05$). Also, the ischemic groups (I/R, I/R+S1P) had a significant difference in NFR early after reperfusion, compared to the S1P perfusion group ($P\leq0.002$).

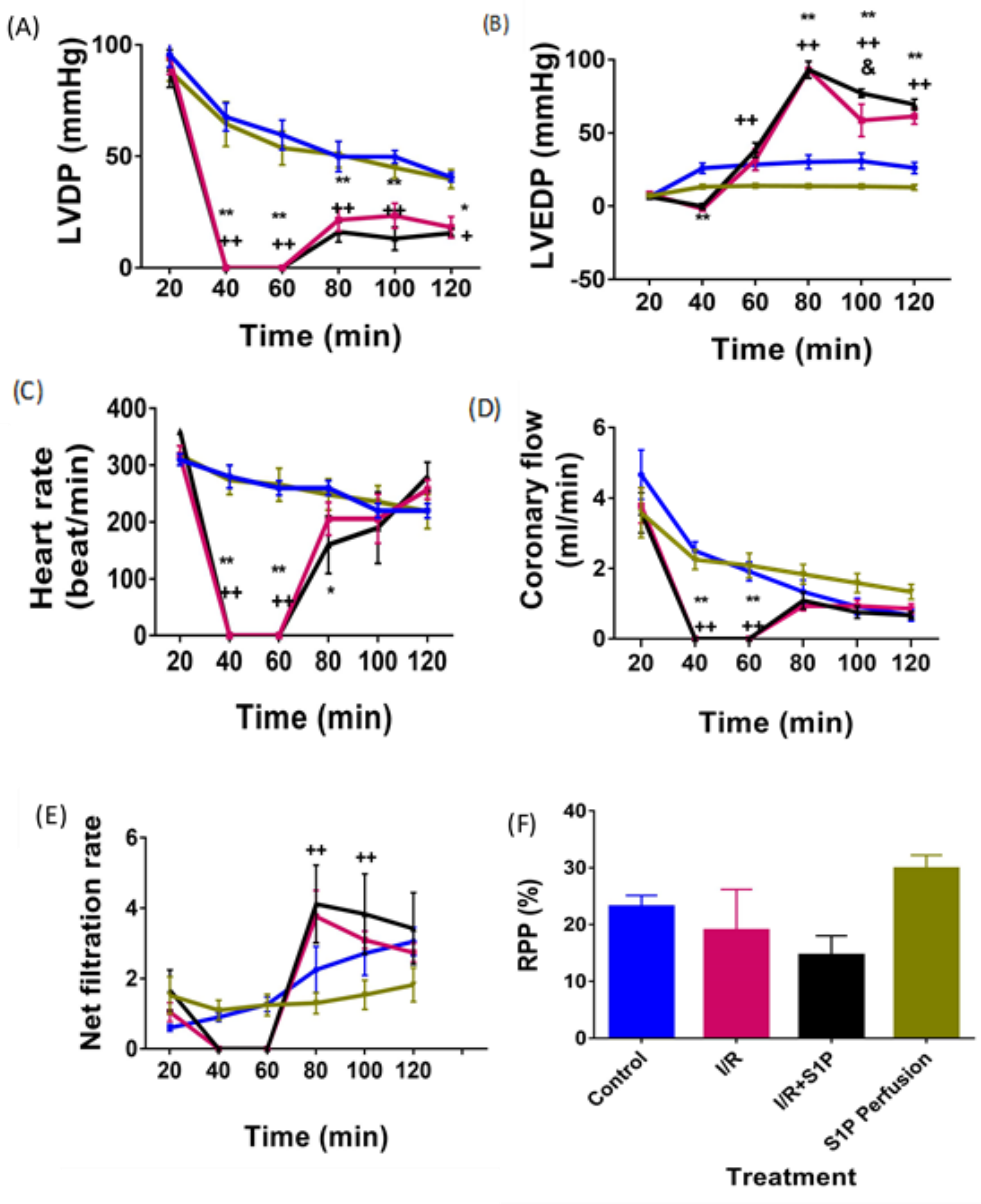

Figure 11: Effect of S1P on hemodynamic parameters of isolated hearts for all groups. Graphs A-E show the changes in: (A) Left ventricular developed pressure (LVDP), (B) Left ventricular end diastoilic pressure (LVEDP), (C) Heart rate (HR), (D) Coronary flow (CF), (E) Net filtration rate (NFR) over time in each group and (F) Shows rate pressure product (RPP) for each group calculated after 60 minutes reperfusion and expressed as percentage of the baseline. Control group (—), Ischemia/reperfusion group(I/R —), Ischemia/reperfusion +S1P (I/R+S1P —), S1P perfusion (—).* P<0.05, **P<0.01 vs. control. $^{+}$P<0.05, $^{++}$P<0.01 vs. S1P perfusion. $^{\&}$P<0.05 I/R vs. I/R+S1P. (N≥6/group).

4.3 Effect of S1P on Cardiac Edema in the Isolated Perfused Heart

Mean wet-to-dry weight ratios of isolated hearts were measured after 20 minutes ischemia (or equivalent perfusion for control groups) and 30 minutes reperfusion with or without S1P treatment (Figure 12). The ratio was not significantly different between the groups (P>0.05). There was also no significant difference between the control and K-H groups which were added to assess the effect of DMSO on cardiac edema.

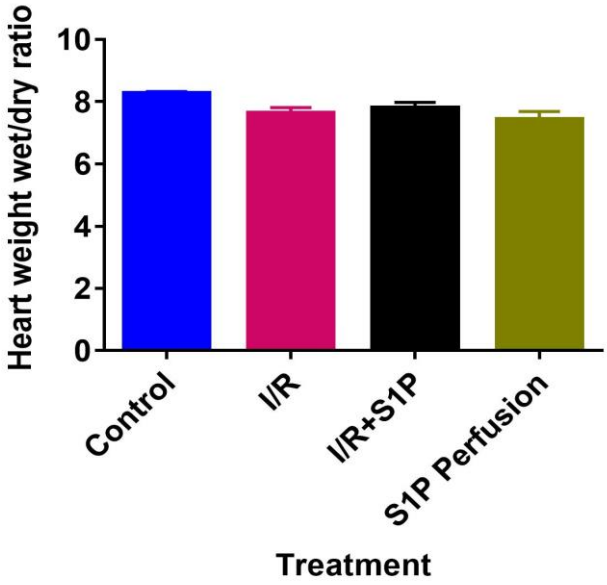

Figure 12: Effect of S1P on heart weight wet/dry ratio of isolated hearts subjected to 20 minutes ischemia 30 minutes reperfusion (P=n.s, N =7/group).

4.4 Effect of S1P Treatment on Syndecan-1 Shedding

Shedding of the glycocalyx was assessed by measuring the level of syndecan-1 in the coronary effluent using ELISA. The results obtained from the murine antibody showed no significant differences in the level of syndecan-1 between the groups (see Appendix 4.2.7).

Using the ELISA with the human antibody, we found that syndecan-1 levels in the coronary effluent of the hearts subjected to 20 minutes global ischemia followed by reperfusion was 10.22 ± 1.39 ng/ml, which was significantly higher than that detected in the control group 3.92 ± 0.76 ng/ml (P=0.0002 vs. control). Pretreatment with S1P before ischemia did not affect the shedding of syndecan-1 which was 8.59 ± 1.14 ng/ml in this group, (P=0.01 vs. control, P=0.7 vs. I/R). The group treated with S1P without ischemia had similar syndecan-1 levels of the control group (3.24 ± 0.47 ng/ml, P=n.s vs. control) and was significantly different from the ischemic groups (P<0.0001 vs. I/R, P=0.0056 vs. I/R+S1P). The level of syndecan-1 in K-H perfusion without ischemia was, 2.44 ± 0.57 ng/ml, and was similar values to the control (P=n.s vs. control, vs. S1P perfusion, P<0.05 vs. I/R, vs. I/R+S1P) (Figure 13).

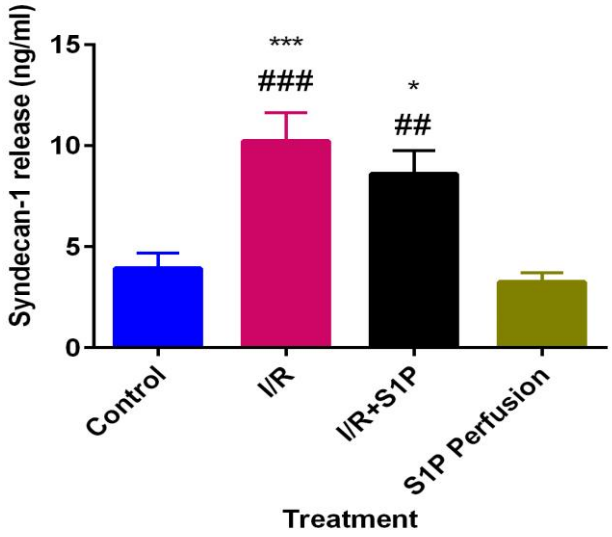

Figure 13: Quantitative measurement of syndecan-1 release in the coronary effluent of isolated hearts. *P< 0.05, ***P<0.001 vs. control, $^{\#\#}$P< 0.01, $^{\#\#\#}$P<0.001 vs. S1P perfusion group.

4.5 Immunohistochemistry Assessment of Syndecan-1

4.5.1 Optimization of Immunostaining

Immunostaining to assess the presence of syndecan-1 in blood vessels using mouse monoclonal antisyndecan-1 (B-A38, ab 34164, Abcam) antibody was unsuccessful for all protocols used as was evidenced by the absence of fluorescence signals. On the other hand, syndecan-1 was detected using rabbit monoclonal anti-syndecan-1 antibody. There was positive immunofluorescent staining detected in both control heart and splenic sections even without antigen retrieval. The negative control where the primary antibody was omitted revealed no signal (Figure 14). The staining was clear and intense with no significant difference noted between the four dilutions of primary antibody used (Figure 15). Therefore, 1:500 dilution of the antibody was used for the rest of the experiment.

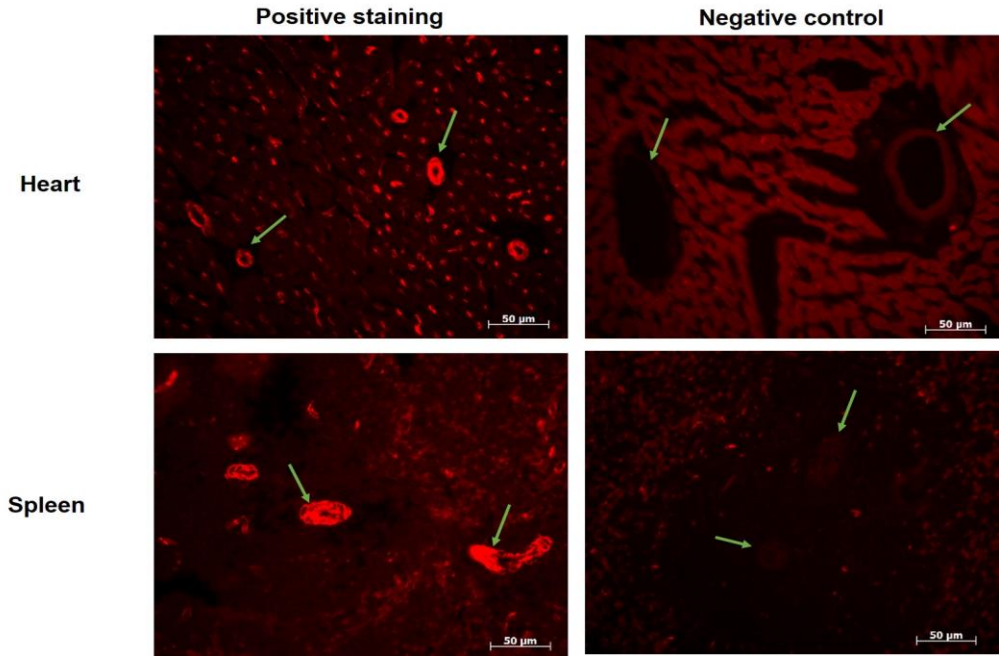

Figure 14: Immunofluorescent staining of the vessel wall of both heart and spleen sections. PFA-fixed/Paraffin-embedded sections were stained for syndecan-1 using rabbit monoclonal antisyndecan-1. Positive immunofluorescent staining was detected in both sections (left side). Syndecan-1 signals were not detected in the negative controls of both sections where the primary antibody was omitted (right side).

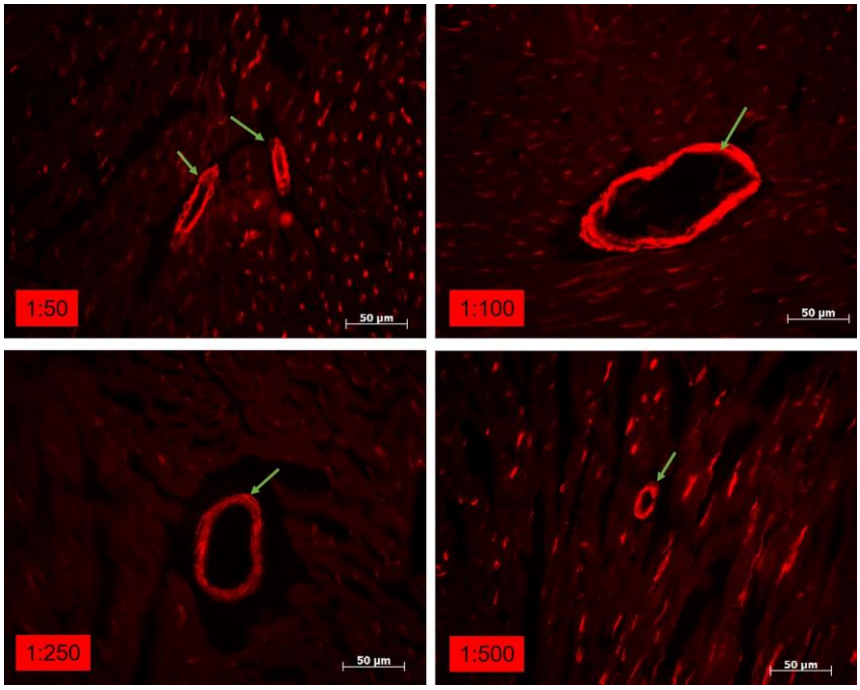

Figure 15: Immunofluorescent staining of coronary vessels (arrow site) of heart tissue (PFA-fixed/Paraffin embedded sections) with four different dilutions of primary antibody of rabbit monoclonal antibody against syndecan-1. There was clear positive staining in all sections with no significant difference in fluorescence intensity between four dilutions.

4.5.2 Assessment of Syndecan-1 by Chromogenic Immunostaining

Chromogenic staining of cardiac sections (PFA-fixed/Paraffin embedded sections) was used for assessment of the presence of syndecan-1 in blood vessels using the antirabbit antisyndecan-1 antibody. This method was preferred as tile-scanned images could be produced which was not possible for fluorescent-stained sections. Generally, the staining intensity of the ventricular sections of non-ischemic groups (control and S1P) was very intense in comparison to that of the ischemic groups (I/R and I/R+S1P), and the staining was more intense in the area close to the epicardial and endocardial regions (Figure 16).

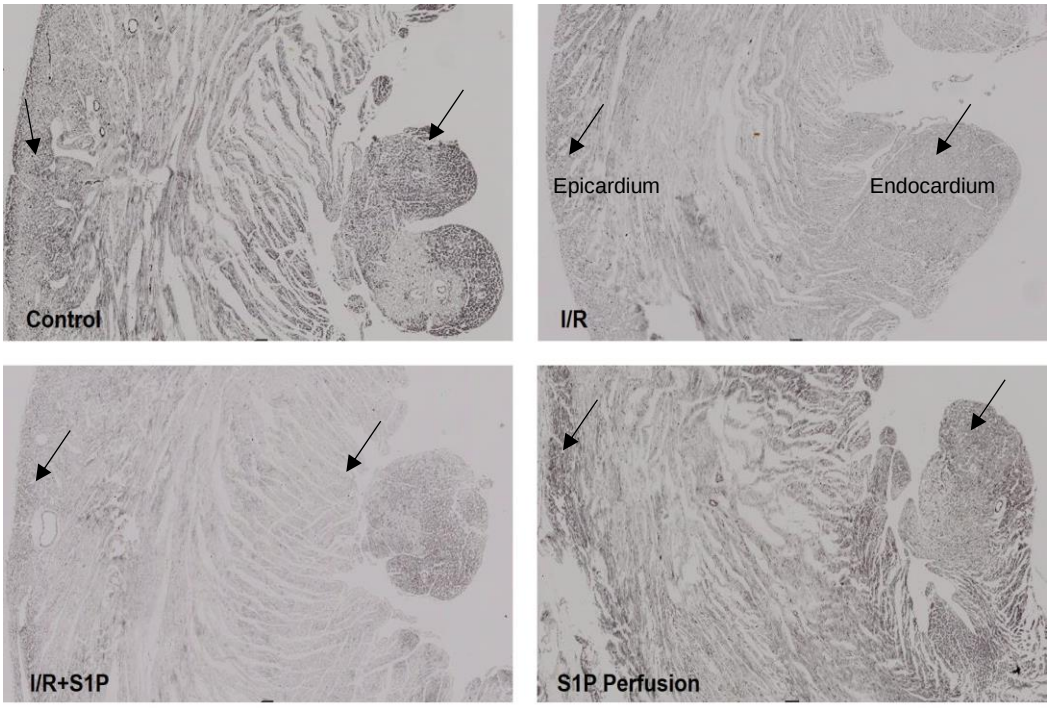

Figure 16: Chromogenic staining of left ventricular sections (PFA-fixed/Paraffin-embedded) stained with rabbit monoclonal antibody against syndecan-1. Staining intensity was more intense in non-ischemic hearts (control and S1P) than in ischemic hearts (I/R and I/R+S1P) and the staining was more intense in the area close to epicardium and endocardium regions (arrow site). Paraformaldehyde (PFA), ischemia/reperfusion (I/R), sphingosine-1-phosphate (S1P).

Syndecan-1 staining level of blood vessels was scored according to the staining intensity. The intensity of syndecan-1 staining was significantly decreased or absent in ischemic group (0.66 ± 0.04) in comparison to the control group (2.56 ± 0.03, P≤ 0.001 I/R vs. control) and the staining reaction was found in both the endothelial lining and medial layer of blood vessels. Treatment with S1P before ischemia (I/R+S1P) had no effect on syndecan-1 intensity compared to the I/R group (0.56 ± 0.03, P=n.s I/R+S1P vs. I/R). Syndecan-1 intensity in hearts treated with S1P without ischemia (S1P) was not significantly different to control hearts but was significantly higher in groups that underwent ischaemia with and without pre S1P treatment (2.38 ± 0.04, P<0.001 vs. I/R, vs. I/R+S1P, P= n.s vs. control) (Figure 17 A, B).

(Appendix 10 a table summarizes the statistical data of syndecan-1 staining intensity scores and the differences between the four groups).

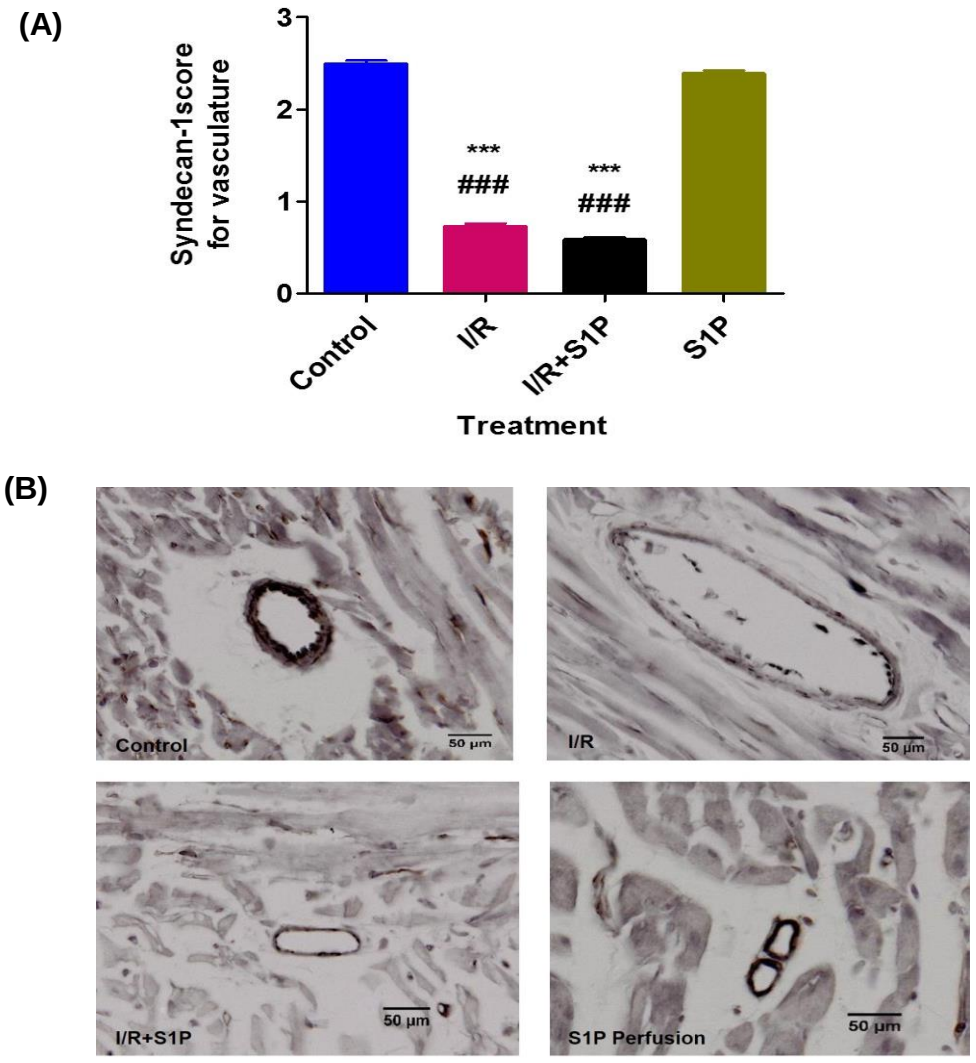

Figure 17: Syndecan-1 immunostaining of the coronary vessels in PFA/ Paraffin-embedded sections of the left ventricle of the isolate rat heart. (A) Histological scoring of syndecan-1 staining of the left ventricular vasculature. Data are reported as mean score ± SEM. ***P<0.001 vs. control, $^{###}$P<0.001 vs. S1P perfusion group. (B) Representative images of syndecan-1 staining. Control and S1P Perfusion hearts show an intense staining of vessel wall, whereas no staining is seen after I/R. Minimal/mild staining can be observed after treatment with S1P before I/R (I/R+S1P).

4.5.2 Cardiac Morphological Features and Quantification of Cardiac Edema

The morphological examination of cardiac cells in H&E-stained left ventricular sections revealed that myocardial fibres of control and S1P treated hearts were regularly arranged with clear striations, intact cell membrane and there were small spaces between the fibres. Hearts that were subjected to I/R displayed some ischemic features such as shortening of muscle fibres, swelling of the cells and ruptured cell membranes with loss of striation and increased separation of the muscle fibres. Hearts that were treated with S1P before ischemia also displayed some ischemic changes (Figure 18. A).

The ratio of interstitial area (i.e. excluding cardiomyocytes) to the total area of the image field was measured to quantify cardiac edema. In the control hearts, interstitial area was 37.06 ± 0.95% and significantly increased in the ischemic group (43.48 ± 1.07%, $P \leq 0.001$ control vs. I/R). Treatment with S1P before ischemia significantly decreased interstitial area to control levels (37.43 ± 0.96%, $P \leq 0.01$ I/R+S1P vs. I/R, $P > 0.05$ I/R+S1P vs. control). S1P treatment without ischemia had no effect on interstitial area (37.96 ± 1.53%, P=n.s S1P vs control and S1P+I/R) (Figure 18. B). (Appendix 11 a table shows a summary of the statistical data and the difference between the four groups).

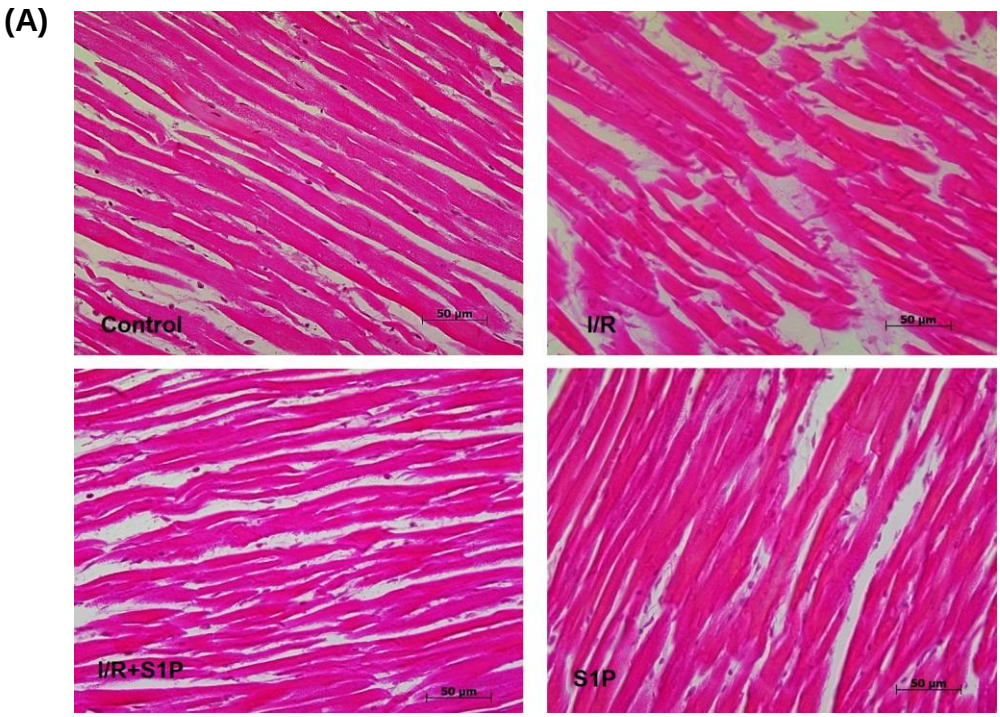

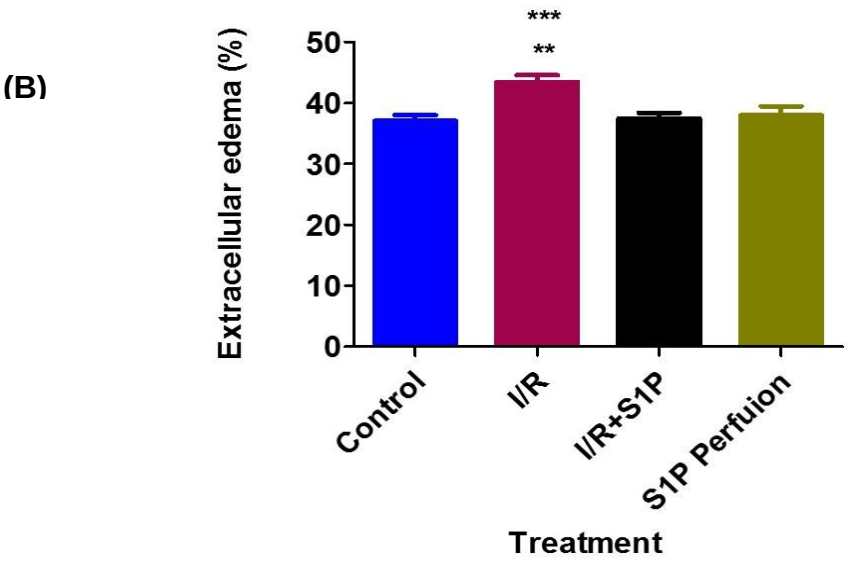

Figure 18: Quantification of cardiac edema in H&E-stained wax sections of the left ventricle. (A) Morphological features of cardiac tissue in four groups. (B) Extracellular area as percentage of total area. $^{***}P \leq 0.001$ vs. control, $^{**}P \leq 0.01$ vs. I/R+S1P vs S1P perfusion group.

CHAPTER 5: DISCUSSION

This study aimed to explore whether the known cardioprotective effect of S1P in isolated rat heart during I/R injury was mediated via the stabilization of the endothelial glycocalyx. The results showed that S1P treatment of the isolated rat heart subjected to I/R injury led to a significant decrease in infarct size, and extracellular edema without an effect on the functional recovery of the heart, NFR and wet/dry heart weight ratio. However, S1P had no effect on the increased level of syndecan-1 in the coronary effluent caused by I/R injury. In addition, histological assessment of syndecan-1 shedding in coronary vessels revealed complete shedding of syndecan-1 as result of I/R damage and pretreatment with S1P had no effect.

In the current study, S1P protected the heart against I/R injury, as was demonstrated by a decrease in infarct size. However, there was no accompanying change in hemodynamic recovery. The effect of S1P on the infarct size in this study was consistent with other studies which used the same dose of S1P (Kelly-Laubscher et al. 2014). Therefore, 10 nM of S1P was effective in reducing the infarction without effect on the hemodynamic function. These results are similar to some other studies that also reported decreases in infarct size without changes in the functional recovery when various drugs were tested (Kelly-Laubscher et al. 2014; Alizadeh et al. 2011). A possible explanation is that although S1P can reduce the infarct size, it may not improve post reperfusion cardiac dysfunction because the myocardium may be reversibly stunned and require more time to improve. Myocardial stunning is defined as post-ischemic ventricular dysfunction and occurs after ischemia and persists even after reperfusion (Takano et al. 2000). Another possibility is that the onset of action of S1P to improve functional parameters is different from the time of the injury occurrence that is suggested to occur within 5 minutes after reperfusion. In addition, one study used a higher dose of S1P (1 and 10 mM) and they found improvement in the LVDP and decreased infarct size (Tsukada et al. 2007). Therefore, although 10 nM S1P has been used in many studies and was determined to decrease

infarct size (Kelly-Laubscher et al. 2014; Lecour et al. 2002; Somers et al. 2012) greater concentrations may be needed to improve cardiac hemodynamics. However, higher concentrations of S1P may lead to side-effects of S1P such as bradycardia, coronary vasoconstriction, and decreased blood pressure (Murakami et al. 2010; Sugiyama et al 2000).

The filtering capacity of the endothelial barrier was determined by measuring the NFR, and heart wet/dry weight ratio. NFR was significantly increased after 5 minutes reperfusion in ischemic groups (I/R, and I/R+S1P) in comparison to the S1P perfusion group (p=0027 vs. S1P), with no significant differences at the end of reperfusion between the groups. The increase in the NFR shortly after reperfusion in the ischemic groups may indicate an increase in endothelial permeability. However, similar differences in NFR were not seen between the ischemic groups and the control group, and may be due to a trend in the S1P-treated hearts to have a lower NFR. This result is similar to a study that tested the effect of S1P on intact vessels which found that S1P maintains normal vascular permeability by maintaining the endothelial barrier in intact microvessels (Zhang et al. 2016). Furthermore, another study by Zeng et al. (2014) found that S1P can stabilize the glycocalyx in cultured rat fat-pad endothelial cells in presence of plasma albumin, and the S1P dose used in this study was higher than used in this study.

There was no significant difference in heart weight wet/dry ratio as an indication of cardiac edema between control and ischemic hearts. Theoretically, this could have been attributed to an effect by the vehicle DMSO on the fluid permeability in the control group. However, this possibility was excluded when an additional group perfused with K-H alone was studied. The level of edema for the K-H group was not significantly different from control hearts which received DMSO. S1P had no effect on heart wet/dry ratio after ischemia, but the S1P perfusion group demonstrated a trend of decreased heart wet/dry ratio, which is consistent with the NFR results.

Histological assessment of cardiac edema was determined by measuring the extracellular area. The extracellular area was increased by ischemia and this, may indicate increased extracellular edema. S1P pretreatment led to decreased extracellular area which may indicate that S1P decreased cardiac edema. These histological results were not consistent with the heart weight wet/dry ratio measurements, which may be surprising as they are both measures of edema. The difference in these results may be related to the method itself. Some studies have suggested that histological assessment is more specific and can distinguish between extracellular and intracellular edema with excluding intravascular water residue which cannot be excluded using heart weight wet/dry ratio (Fehrenbach et al. 2001; Fehrenbach et al. 1999). Moreover, fixation of the tissue sample by an appropriate procedure can give adequate preservation of the fluid accumulation. However, in this study only extracellular edema was measured. The intracellular edema was not clear to measure. There are two possible reasons for this; Firstly, the cells may not have been sufficiently damaged, due to the short ischemic duration used in this study, to cause increased intracellular edema. Secondly, there is a possibility that intracellular edema resolved after reperfusion. This has been indicated by other studies which showed that intracellular edema is an ischemic event and resolved after reperfusion (Askenasy et al. 1995; Askenasy and Navon, 1997; Askenasy and Navon, 2005; Fernandez-Jimenez et al., 2015).

Previously, Straus (2013) indicated from their histological assessment of myocardial edema after I/R, that S1P may act to decrease post-ischemic myocardial edema. Their study obtained a non-significant trend of edema formation in the ischemic group and S1P pretreatment seemed to improve the cardiac edema to levels close to that of the control, but there were no significant differences between the groups, and this supports my results.

The results of this study show that I/R increased the release of syndecan-1 in the coronary effluent, and this may indicate glycocalyx damage. This result was consistent with other studies which also demonstrated that I/R caused damage to the glycocalyx, and leads to release of its components in the

coronary effluent (Rehm et al. 2007; Chappell et al. 2011; Mulivor and Lipowsky 2004). These findings are also consistent with the NFR results described above and may suggest increased endothelial permeability at 5 minutes of reperfusion. In this study, treatment with S1P before ischemia had no effect on syndecan-1 release and suggests that S1P may not protect the heart via stabilization of the glycocalyx. However, this study focused on the most commonly assayed glycocalyx by-product syndecan-1. It is possible that S1P protects via other components of glycocalyx, such as heparan sulphate and hyaluronic acid. Several other studies testing the protective effect of drugs on the glycocalyx have measured two or more components of glycocalyx (Chappell et al. 2009a; Zeng et al. 2014), because some drugs can stabilize one component without any effect on the others. It is also possible that the concentration used in the current study was too low to protect the glycocalyx. Zeng et al. (2014) found the protective level of S1P in cultured rat fat-pad endothelial cells ranged from 0.2 µM to 1 µM even when there is no protein carrier for S1P, which is above the concentration used in this study. In any case, the results of this study indicate that S1P, at a concentration that decreased infarct size, did not significantly decrease the elevated level of syndecan-1 in coronary effluent in ischemic hearts suggesting that this cardioprotective dose of S1P had no effect on the syndecan-1 shedding. To strengthen this argument, a power analysis was conducted and revealed that the number of rats used in ELISA was sufficient to give 80% power to detect differences between means with a significance level of 0.05. In addition, immuno-staining images of syndecan-1 assessment in coronary vessels supported the ELISA results revealing decreased syndecan-1 after I/R, and similar decreases in syndecan-1 staining in ischemic S1P treated hearts.

In the present study, we evaluated the ability of two different antibodies to determine the syndecan-1 level in rat coronary effluent by ELISA. While the murine antibodies failed to detect the syndecan-1 in my sample, which was assumed to work better since the rat and mouse are more homologous than the rat and human (Appendix 7), the human antibody successfully measured syndecan-1 in my samples. While it is possible that the murine ELISA failed

due to experimental error, such as preparation of the coronary samples, this is unlikely since the same samples were used with both antibodies. The murine antibody seems to fail to detect the syndecan-1 in our samples despite its detection of the standard concentration. Therefore, the specificity and the sensitivity of the antibody were most likely the cause of murine antibody failure to detect the syndecan-1.

5.1 Limitations of the Study

Separation of the hearts from the whole animal and Langendorff perfusion technique are synthetic procedures that remove the hormonal and neural effect on the heart and thus may reduce the clinical relevance of our study. The heart is a very delicate and soft tissue and must be handled gently during isolation and instrumentation as the heart is susceptible to contusion injuries. In addition, isolation of the heart from the whole body will prevent the normal humoral and neural regulation of the heart and aortic valve incompetence may occur during cannulation, or due to retrograde perfusion that prevents the perfusate going from the aorta to the coronary vessels. A heart perfused on the Langendorff system may deteriorate in contractile function at approximately 5–10% per hour (Skrzypiec-Spring et al. 2007; Bell, Mocanu, and Yellon 2011). Furthermore, the K-H buffer, a crystalloid buffer used to perfuse the isolated hearts, has restricted capability to give enough oxygenation to the tissue which may be associated with deterioration of the cardiac function. Also, K-H has low oncotic pressure, compared to blood which can cause tissue edema.

Another limitation of the study is the fact that we pretreated hearts with heparin to minimize thrombus formation. There are studies that have shown the effect of heparin on the endothelial permeability and shedding of the glycocalyx. These studies were inconsistent in their findings, with some finding that heparin induced shedding of glycocalyx, and increased endothelial permeability (VanTeeffelen et al. 2007) and others finding that treatment of a canine septic shock model with heparin restored the permeability barrier and protected the glycocalyx against shedding (Yini et al. 2015).

Finally, information from isolated heart studies is difficult to convert into clinical use, because most of the experimental studies on cardioprotection have been done in young healthy animal models, in contrast to the reality that most of the heart disease in humans is accompanied with other systemic disorders and pre-existing disease. In future, further studies using a whole living animal rather than an isolated heart model may be required to investigate the general effects of S1P and allow examining of its long-term effects on the cardiac tissues.

5.2 Future Studies

To clarify the role of the glycocalyx in S1P-induced cardioprotection, further studies should explore the effect of S1P on other components of glycocalyx. We could repeat the experiments using different doses of S1P, measuring more than one component of glycocalyx using ELISA or other procedures such as western blot, immunohistochemistry and electron microscopy.

Many studies have shown the effect of global ischemia on the glycocalyx shedding, so it is important to explore the effect of regional ischemia on shedding of glycocalyx, which is more clinically relevant. This study used isolated rat hearts with global ischemia. Since other studies used guinea pigs, which are known to have large collateral supply to the heart, to investigate the glycocalyx damage our results and protocol may open the possibility to test other drugs to protect the glycocalyx in the rat in regional ischemia.

In order to clarify the effect of the S1P on endothelial barrier integrity and cardiac edema, further work may include repeats of histological analysis accompanied by some modification in the methods, such as adding albumin to K-H perfusate to avoid using crystalloid K-H which has low oncotic pressure. In addition, measuring microvascular permeability by using Evan-blue dyed albumin to quantify colloid protein extravasation could be carried out.

5.3 Conclusion

This study showed that I/R leads to disturbances in cardiac function, increased infarct size, increased release of syndecan-1 in the coronary effluent and histological changes. S1P treatment protects the heart against I/R injury, as was indicated by the decreased infarct size and decreased cardiac edema. However, it had no effect on the shedding of syndecan-1 and hemodynamic performance. These results, while confirming the cardioprotective effect of S1P, may suggest that this protection is not mediated by protection of the glycocalyx via stabilization of syndecan-1. It is possible that S1P may protect the glycocalyx by stabilizing other glycocalyx components that were not measured in the present study. Although this study did not demonstrate a role for the glycocalyx in S1P-induced protection, this is the first study that measured syndecan-1 in the cardiac effluent of the isolated heart of rats with global ischemia. The study opens up prospects of investigating the role of the glycocalyx in other models of I/R injury, including the more clinically relevant regional I/R models.

REFERENCES

Adamson, R. H., J. F. Clark, M. Radeva, A. Kheirolomoom, K. W. Ferrara, and F. E. Curry. 2014. “Albumin Modulates S1P Delivery from Red Blood Cells in Perfused Microvessels: Mechanism of the Protein Effect.” *AJP: Heart and Circulatory Physiology* 306 (7): H1011–17.

Adamson and Clough. 1992. “Plasma Proteins Modify the Endothelial Cell Glycocalyx of Frog Mesenteric Microvessels.” *Journal of Physiology* 3 (445): 473–86.

Akinboboye, O, O Idris, O Akinboboye, and O Akinkugbe. 2003. “Trends in Coronary Artery Disease and Associated Risk Factors in Sub-Saharan Africans CM.” *Journal of Human Hypertention* 17: 381–87.

Akira Murakami, Hiroshi Takasugi, Shinya Ohnuma, Yuuki Koide, Atsuko Sakurai, Satoshi Takeda, Takeshi Hasegawa, et al. 2010. “Sphingosine 1-Phosphate (S1P) Regulates Vascular Contraction via S1P 3 Receptor : Investigation Based on a New S1P 3 Receptor Antagonist.” *Mollecular Pharmacology* 77 (4): 704–13.

Alizadeh, Ali Mohammad, Mahdieh Faghihi, Hamid Reza Sadeghipour, Fahimeh MohammadGhasemi, and Vahid Khori. 2011. “Role of Endogenous Oxytocin in Cardiac Ischemic Preconditioning.” *Regulatory Peptides* 167 (1). Elsevier B.V.: 86–90.

Annecke, T, D Chappell, C Chen, M Jacob, U Welsch, C P Sommerhoff, M Rehm, P F Conzen, and B F Becker. 2010. “Sevoflurane Preserves the Endothelial Glycocalyx against Ischaemia – Reperfusion Injury.” *British Journal of Anaesthesia* 104 (4): 414–21.

Argaud, Laurent, Odile Gateau-Roesch, Olivier Raisky, Joseph Loufouat, Dominique Robert, and Michel Ovize. 2005. “Postconditioning Inhibits Mitochondrial Permeability Transition.” *Circulation* 111 (2): 194–97.

Argraves, Kelley M, Patrick J Gazzolo, M Groh, Brent A Wilkerson, S Bryan, Waleed O Twal, M Samar, et al. 2008. “High Density Lipoprotein-Associated Sphingosine 1-Phosphate Promotes Endothelial Barrier Function.” *Journal of Biological Chemistry* 283 (36): 25074–81.

Askenasy, Nadir, Maria Tassini, Antonio Vivi, and Gil Navon. 1995. “Intracellular Volume Measurement and Detection of Edema: Multinuclear NMR Studies of Intact Rat Hearts during Normothermic Ischemia.” *Magnetic Resonance in Medicine* 33 (4): 515–20.

Askenasy, Nadir, and Gil Navon. 2005. “Measurements of Intracellular Volumes by 59Co and 2H/1H NMR and Their Physiological Applications.” *NMR in Biomedicine* 18 (2): 104–10.

Askenasy, Nadir, and G Navon. 1997. “Continuous Monitoring of Intracellular Volumes in Isolated Rat Hearts during Normothermic Perfusion and Ischemia.” *Journal of Magnetic Resonance (San Diego, Calif. : 1997)* 124

(1): 42–50.

Barauskaite, Jurgita, Regina Grybauskiene, Ramune Morkuniene, Vilmante Borutaite, and Guy C Brown. 2011. “Tetramethylphenylenediamine Protects the Isolated Heart against Ischaemia-Induced Apoptosis and Reperfusion-Induced Necrosis.” *British Journal of Pharmacology* 162 (5): 1136–42.

Baxter, Gary F. 2002. “The Neutrophil as a Mediator of Myocardial Ischemia-Reperfusion Injury: Time to Move on.” *Basic Research in Cardiology* 97 (4): 268–75.

Bell, Robert M., Mihaela M. Mocanu, and Derek M. Yellon. 2011. “Retrograde Heart Perfusion: The Langendorff Technique of Isolated Heart Perfusion.” *Journal of Molecular and Cellular Cardiology* 50 (6). Elsevier Ltd: 940–50.

Bell, Robert M., and Derek M. Yellon. 2003. “Atorvastatin, Administered at the Onset of Reperfusion, and Independent of Lipid Lowering, Protects the Myocardium by up-Regulating a pro-Survival Pathway.” *Journal of the American College of Cardiology* 41 (3): 508–15.

Bernfield, M, R Kokenyesi, M Kato, M T Hinkes, J Spring, R L Gallo, and E J Lose. 1992. “Biology of the Syndecans: A Family of Transmembrane Heparan Sulfate Proteoglycans.” *Annual Review of Cell Biology* 8: 365–93.

Bibli, Sofia-Iris, Eleni V Toli, Agapi D Vilaeti, Varnavas C Varnavas, Giannis G Baltogiannis, Apostolos Papalois, Zenon S Kyriakides, and Theofilos M Kolettis. 2012. “Endothelin-B Receptors and Left Ventricular Dysfunction after Regional versus Global Ischaemia-Reperfusion in Rat Hearts.” *Cardiology Research and Practice* 2012 (January): 1–9.

Bode, Constantin, Sven Christian Sensken, Ulrike Peest, Gernot Beutel, Felicitas Thol, Bodo Levkau, Zaiguo Li, et al. 2010. “Erythrocytes Serve as a Reservoir for Cellular and Extracellular Sphingosine 1-Phosphate.” *Journal of Cellular Biochemistry* 109 (6): 1232–43.

Broekhuizen, Lysette N, Hans L Mooij, John J P Kastelein, Erik S G Stroes, Hans Vink, and Max Nieuwdorp. 2009. “Endothelial Glycocalyx as Potential Diagnostic and Therapeutic Target in Cardiovascular Disease.” *Current Opinion in Lipidology* 20 (1): 57–62.

Bruegger, Dirk, Markus Rehm, Matthias Jacob, Daniel Chappell, Mechthild Stoeckelhuber, Ulrich Welsch, Peter Conzen, and Bernhard F Becker. 2008. “Exogenous Nitric Oxide Requires an Endothelial Glycocalyx to Prevent Postischemic Coronary Vascular Leak in Guinea Pig Hearts.” *Critical Care (London, England)* 12 (3): R73.

Chappell, D., M. Jacob, K. Hofmann-Kiefer, M. Rehm, U. Welsch, P. Conzen, and B. F. Becker. 2009a. “Antithrombin Reduces Shedding of the Endothelial Glycocalyx Following Ischaemia/reperfusion.” *Cardiovascular Research* 83 (2): 388–96.

Chappell, Daniel, Dirk Bruegger, Julia Potzel, Matthias Jacob, Florian Brettner, Michael Vogeser, Peter Conzen, Bernhard F Becker, and

Markus Rehm. 2014. “Hypervolemia Increases Release of Atrial Natriuretic Peptide and Shedding of the Endothelial Glycocalyx.” *Critical Care (London, England)* 18 (5): 538.

Chappell, Daniel, Bernhard Heindl, D Ph, Matthias Jacob, Thorsten Annecke, Congcong Chen, Markus Rehm, Peter Conzen, and Bernhard F Becker. 2011. “Sevoflurane Reduces Leukocyte and Platelet Adhesion after Ischemia-Reperfusion by Protecting the.” *Anesthesiology* 115 (3).

Chappell, Daniel, Klaus Hofmann-kiefer, Ulrich Welsch, and Bernhard F Becker. 2009b. “TNF- a Induced Shedding of the Endothelial Glycocalyx Is Prevented by Hydrocortisone and Antithrombin.” *Basic Research in Cardiology* 104 (1): 78–89.

Chappell, Daniel, Matthias Jacob, Klaus Hofmann-kiefer, Dirk Bruegger, Markus Rehm, Peter Conzen, Ulrich Welsch, D Ph, and Bernhard F Becker. 2007. “Hydrocortisone Preserves the Vascular Barrier by Protecting the Endothelial Glycocalyx.” *The American Society of Anesthesiologists* 107 (5): 776–84.

Chong, Zhao Zhong, Jing Qiong Kang, and Kenneth Maiese. 2002. “Erythropoietin Is a Novel Vascular Protectant through Activation of AKt1 and Mitochondrial Modulation of Cysteine Proteases.” *Circulation* 106 (23): 2973–79.

Constantinescu, Alina a., Hans Vink, and Jos a E Spaan. 2003. “Endothelial Cell Glycocalyx Modulates Immobilization of Leukocytes at the Endothelial Surface.” *Arteriosclerosis, Thrombosis, and Vascular Biology* 23: 1541–47.

Coulson, A S, S Bakhshay, J A Quarnstrom, S Mayer, K Holmes, and M Villarreal. 1997. “Minimally Invasive Direct Coronary Artery Bypass Surgery.” *AORN Journal* 66 (6): 1012–42.

Coussin, F. 2002. “Comparison of Sphingosine 1-Phosphate-Induced Intracellular Signaling Pathways in Vascular Smooth Muscles: Differential Role in Vasoconstriction.” *Circulation Research* 91 (2): 151–57.

Crompton, M, A Costi, and L Hayat. 1987. “Evidence for the Presence of a Reversible Ca2+-Dependent Pore Activated by Oxidative Stress in Heart Mitochondria.” *The Biochemical Journal* 245 (3): 915–18.

Curry, F. E., J. F. Clark, and R. H. Adamson. 2012. “Erythrocyte-Derived Sphingosine-1-Phosphate Stabilizes Basal Hydraulic Conductivity and Solute Permeability in Rat Microvessels.” *AJP: Heart and Circulatory Physiology* 303 (7): H825–34.

Dauber, I M, K M VanBenthuysen, I F McMurtry, G S Wheeler, E J Lesnefsky, L D Horwitz, and J V Weil. 1990. “Functional Coronary Microvascular Injury Evident as Increased Permeability due to Brief Ischemia and Reperfusion.” *Circulation Research* 66 (4): 986–98.

Davenpeck, Kelly L., Theresa W. Gauthier, and Allan M. Lefer. 1994. “Inhibition of Endothelial-Derived Nitric Oxide Promotes P-Selectin Expression and Actions in the Rat Microcirculation.” *Gastroenterology*

107 (4). Elsevier: 1050–58.

Derksen, Patrick W B, Robert M J Keehnen, Ludo M. Evers, Marinus H J Van Oers, Marcel Spaargaren, and Steven T. Pals. 2002. “Cell Surface Proteoglycan Syndecan-1 Mediates Hepatocyte Growth Factor Binding and Promotes Met Signaling in Multiple Myeloma.” *Blood* 99 (4): 1405–10.

Dignan, R J, C M Dyke, A S Abd-Elfattah, H A Lutz, T Yeh Jr., K F Lee, J Parmar, and A S Wechsler. 1992. “Coronary Artery Endothelial Cell and Smooth Muscle Dysfunction after Global Myocardial Ischemia.” *Annals of Thoracic Surgery* 53 (2). The Society of Thoracic Surgeons: 311–17.

Egom, E. Eroume A, Yunbo Ke, Hanny Musa, Tamer M A Mohamed, Tao Wang, Elizabeth Cartwright, R. John Solaro, and Ming Lei. 2010. “FTY720 Prevents Ischemia/reperfusion Injury-Associated Arrhythmias in an Ex Vivo Rat Heart Model via Activation of Pak1/Akt Signaling.” *Journal of Molecular and Cellular Cardiology* 48 (2). Elsevier Ltd: 406–14.

Fehrenbach, Antonia, H. Fehrenbach, T. Wittwer, M. Ochs, T. Wahlers, and J. Richter. 2001. “Evaluation of Pulmonary Edema: Stereological versus Gravimetrical Analysis.” *European Surgical Research* 33 (4): 270–78.

Fehrenbach, H, D Schepelmann, J M Albes, T Bando, F Fischer, A Fehrenbach, N Stolte, T Wahlers, and J Richter. 1999. “Pulmonary Ischemia/reperfusion Injury: A Quantitative Study of Structure and Function in Isolated Heart-Lungs of the Rat.” *The Anatomical Record* 255 (1): 84–89.

Fernandez-Jimenez, Rodrigo, Jaime Garcia-Prieto, Javier Sanchez-Gonzalez, Jaume Aguero, Gonzalo J. Lopez-Martin, Carlos Galan-Arriola, Antonio Molina-Iracheta, Roisin Doohan, Valentin Fuster, and Borja Ibanez. 2015. “Pathophysiology Underlying the Bimodal Edema Phenomenon after Myocardial Ischemia/reperfusion.” *Journal of the American College of Cardiology* 66 (7): 816–28.

Fernandez-Jimenez, Rodrigo, Javier Sanchez-Gonzalez, Jaume Aguero, Jaime Garcia-Prieto, Gonzalo J. Lopez-Martin, Jose M. Garcia-Ruiz, Antonio Molina-Iracheta, et al. 2015. “Myocardial Edema after Ischemia/reperfusion Is Not Stable and Follows a Bimodal Pattern: Imaging and Histological Tissue Characterization.” *Journal of the American College of Cardiology* 65 (4): 315–23.

Finegold, Judith A, Perviz Asaria, and Darrel P Francis. 2013. “Mortality from Ischaemic Heart Disease by Country , Region , and Age : Statistics from World Health Organisation and United Nations.” *International Journal of Cardiology* 168 (2). Elsevier Ireland Ltd: 934–45.

Garlick, P B, M J Davies, D J Hearse, and T F Slater. 1987. “Direct Detection of Free Radicals in the Reperfused Rat Heart Using Electron Spin Resonance Spectroscopy.” *Circulation Research* 61: 757–60.

Gouverneur, M, B Berg, M Nieuwdorp, E Stroes, and H Vink. 2006. “Vasculoprotective Properties of the Endothelial Glycocalyx: Effects of

Fluid Shear Stress." *Journal of Internal Medicine* 259 (4): 393–400.

Halestrap, Andrew P., Paul M. Kerr, Sabzali Javadov, and K. Y. Woodfield. 1998. "Elucidating the Molecular Mechanism of the Permeability Transition Pore and Its Role in Reperfusion Injury of the Heart." *Biochimica et Biophysica Acta - Bioenergetics* 1366 (1–2): 79–94.

Hausenloy, Derek J, a Tsang, Mihaela M Mocanu, and Derek M Yellon. 2005. "Ischemic Preconditioning Protects by Activating Prosurvival Kinases at Reperfusion." *American Journal of Physiology. Heart and Circulatory Physiology* 288 (2): H971–76.

Henry, C B, and B R Duling. 1999. "Permeation of the Luminal Capillary Glycocalyx Is Determined by Hyaluronan." *The American Journal of Physiology* 277 (2): H508–14.

Henry, C B, and B R Duling. 2000. "TNF-Alpha Increases Entry of Macromolecules into Luminal Endothelial Cell Glycocalyx." *American Journal of Physiology. Heart and Circulatory Physiology* 279: H2815–23.

Heyndrickx, G. R., R. W. Millard, R. J. McRitchie, P. R. Maroko, and S. F. Vatner. 1975. "Regional Myocardial Functional and Electrophysiological Alterations after Brief Coronary Artery Occlusion in Conscious Dogs." *Journal of Clinical Investigation* 56 (4): 978–85.

Hla, Timothy. 2001. "Sphingosine 1-Phosphate Receptors." *Prostaglandins & Other Lipid Mediators.* 64: 135–42.

Hla, Timothy. 2004. "Physiological and Pathological Actions of Sphingosine 1-Phosphate." *Seminars in Cell & Developmental Biology* 15 (5): 513–20.

Ho, Guyu, George J Broze, and Alan L Schwartz. 1997. "Role of Heparan Sulfate Proteoglycans in the Uptake and Degradation of Tissue Factor Pathway Inhibitor-Coagulation Factor Xa Complexes" 272 (27): 16838–44.

Hofmann-kiefer, K, and G I Kemming. 2009. "Serum Heparan Sulfate Levels are Elevated in Endotoxemia." *European Journal of Medical Research* 14: 526–31.

Hofmann, U., K. Hu, F. Walter, N. Burkard, G. Ertl, J. Bauersachs, O. Ritter, S. Frantz, and A. Bonz. 2010. "Pharmacological Pre- and Post-Conditioning with the Sphingosine-1-Phosphate Receptor Modulator FTY720 after Myocardial Ischaemia-Reperfusion." *British Journal of Pharmacology* 160 (5): 1243–51.

Hofmann, Ulrich, Natalie Burkard, Carolin Vogt, Annemarie Thoma, Stefan Frantz, Georg Ertl, Oliver Ritter, and Andreas Bonz. 2009. "Protective Effects of Sphingosine-1-Phosphate Receptor Agonist Treatment after Myocardial Ischaemia-Reperfusion." *Cardiovascular Research* 83 (2): 285–93.

Holmes, Michelle D., Shona Dalal, Jimmy Volmink, Clement A. Adebamowo, Marina Njelekela, Wafaie W. Fawzi, Walter C. Willett, and Hans Olov Adami. 2010. "Non-Communicable Diseases in Sub-Saharan Africa: The

Case for Cohort Studies." *PLoS Medicine* 7 (5): 1–8.

Javadov, Sabzali A, Samantha Clarke, Manika Das, Elinor J Griffiths, Kelvin H H Lim, and Andrew P Halestrap. 2003. "Ischaemic Preconditioning Inhibits Opening of Mitochondrial Permeability Transition Pores in the Reperfused Rat Heart." *The Journal of Physiology* 549 (2): 513–24.

Jin, Zhu-Qiu, Edward J Goetzl, and Joel S Karliner. 2004. "Sphingosine Kinase Activation Mediates Ischemic Preconditioning in Murine Heart." *Circulation* 110 (14): 1980–89.

Jin, Zhu-Qiu, Hui-Zhong Zhou, Peili Zhu, Norman Honbo, Daria Mochly-Rosen, Robert O Messing, Edward J Goetzl, Joel S Karliner, and Mary O Gray. 2002. "Cardioprotection Mediated by Sphingosine-1-Phosphate and Ganglioside GM-1 in Wild-Type and PKC Epsilon Knockout Mouse Hearts." *American Journal of Physiology. Heart and Circulatory Physiology* 282 (6): H1970-7.

Jin, Joel S. Karliner, and Donald A. Vessey. 2008. "Ischaemic Postconditioning Protects Isolated Mouse Hearts against Ischaemia/reperfusion Injury via Sphingosine Kinase Isoform-1 Activation." *Cardiovascular Research* 79 (1): 134–40.

Jones, Steven P., Wesley G. Girod, Anthony J. Palazzo, D. Neil Granger, Matthew B. Grisham, David Jourd'Heuil, Paul L. Huang, and David J. Lefer. 1999. "Myocardial Ischemia-Reperfusion Injury Is Exacerbated in Absence of Endothelial Cell Nitric Oxide Synthase." *Am J Physiol Heart Circ Physiol* 276 (5): H1567-1573.

Jordan, J E, Z Q Zhao, and J Vinten-Johansen. 1999. "The Role of Neutrophils in Myocardial Ischemia-Reperfusion Injury." *Cardiovascular Research* 43 (4): 860–78.

Kappos, L. 2006. "Oral Fingolimod (FTY720) for Relapsing Multiple Sclerosis." *N. Engl. J. Med.* 355: 1124–40.

Karliner, J S, N Honbo, K Summers, M O Gray, and E J Goetzl. 2001. "The Lysophospholipids Sphingosine-1-Phosphate and Lysophosphatidic Acid Enhance Survival during Hypoxia in Neonatal Rat Cardiac Myocytes." *Journal of Molecular and Cellular Cardiology* 33 (9): 1713–17.

Kelly-Laubscher, Roisin F., Jonathan C. King, Damian Hacking, Sarin Somers, Samantha Hastie, Tessa Stewart, Aqeela Imamdin, Gerald Maarman, Sarah Pedretti, and Sandrine Lecour. 2014. "Cardiac Preconditioning with Sphingosine-1-Phosphate Requires Activation of Signal Transducer and Activator of Transcription-3 : Cardiovascular Topic." *Cardiovascular Journal Of Africa* 25 (3): 118–23.

Kelly, R, T Ruane-O'Hora, M I Noble, a J Drake-Holland, and H M Snow. 2006. "Differential Inhibition by Hyperglycaemia of Shear Stress- but Not Acetylcholine-Mediated Dilatation in the Iliac Artery of the Anaesthetized Pig." *J Physiol* 573: 133–45.

Kelly, Roisin F, Kim T Lamont, Sarin Somers, Damian Hacking, Lydia Lacerda, Paul Thomas, Lionel H Opie, and Sandrine Lecour. 2010.

"Ethanolamine Is a Novel STAT-3 Dependent Cardioprotective Agent." *Basic Research in Cardiology* 105 (6): 763–70.

Keul, Petra, Marcel M. G. J. van Borren, Alexander Ghanem, Frank Ulrich Müller, Antonius Baartscheer, Arie O. Verkerk, Frank Stümpel, et al. 2016. "Sphingosine- 1- Phosphate Receptor 1 Regulates Cardiac Function by Modulating Ca 2+ Sensitivity and Na + /H + Exchange and Mediates Protection by Ischemic Preconditioning." *Journal of the American Heart Association* 5 (5): e003393.

Kim, Jun Jeong Su June Hong, Jun Jeong Su June Hong Kim, Yong Hyun Park, Kook Jin Chun, Jun Jeong Su June Hong Kim, Young Ho Jang, Mi Young Lee, and Zhelong Xu. 2012. "Cardiodynamics and Infarct Size in Regional and Global Ischemic Isolated Heart Model : Comparison of 1 Hour and 2 Hours Reperfusion." *Korean Circulation Journal* 2012 (42): 600–605.

Kitakaze, Masafumi, Masanori Asakura, Jiyoong Kim, Yasunori Shintani, Hiroshi Asanuma, Toshimitsu Hamasaki, Osamu Seguchi, et al. 2007. "Human Atrial Natriuretic Peptide and Nicorandil as Adjuncts to Reperfusion Treatment for Acute Myocardial Infarction (J-WIND): Two Randomised Trials." *Lancet* 370 (9597): 1483–93.

Kliment and Oury. 2012. "Extracellular Superoxide Dismutase Protects Cardiovascular Syndecan-1 from Oxidative Shedding." *Free Radical Biology & Medicine* 76 (October 2009): 211–20.

Lacerda, Lydia, Sarin Somers, Lionel H Opie, and Sandrine Lecour. 2009. "Ischaemic Postconditioning Protects against Reperfusion Injury via the SAFE Pathway." *Cardiovascular Research* 84: 201–8.

Lecour, Sandrine, Robert M Smith, Brian Woodward, Lionel H Opie, Luc Rochette, and Michael N Sack. 2002. "Identification of a Novel Role for Sphingolipid Signaling in TNF and Ischemic Preconditioning Mediated Cardioprotection." *Journal of Molecular and Cellular Cardiology* 518 (34): 509–18.

Lee, I-min, Eric J Shiroma, Felipe Lobelo, Pekka Puska, Steven N Blair, Peter T Katzmarzyk, Lancet Physical, Activity Series, and Working Group. 2012. "Effect of Physical Inactivity on Major Non-Communicable Diseases Worldwide : An Analysis of Burden of Disease and Life Expectancy." *The Lancet* 380 (9838). Elsevier Ltd: 219–29.

Lefer, a. M., B. Campbell, R. Scalia, and D. J. Lefer. 1998. "Synergism Between Platelets and Neutrophils in Provoking Cardiac Dysfunction After Ischemia and Reperfusion : Role of Selectins." *Circulation* 98 (13): 1322–28.

Leppä, S, M Mali, H M Miettinen, and M Jalkanen. 1992. "Syndecan Expression Regulates Cell Morphology and Growth of Mouse Mammary Epithelial Tumor Cells." *Proceedings of the National Academy of Sciences of the United States of America* 89 (3): 932–36.

Li, Q H, R Bolli, Y M Qiu, X L Tang, S S Murphree, and B A French. 1998.

"Gene Therapy with Extracellular Superoxide Dismutase Attenuates Myocardial Stunning in Conscious Rabbits." *Circulation* 98 (14): 1438–48.

Li, Qinglang, Pyong Woo Park, Carole L. Wilson, and William C. Parks. 2002. "Matrilysin Shedding of Syndecan-1 Regulates Chemokine Mobilization and Transepithelial Efflux of Neutrophils in Acute Lung Injury." *Cell* 111 (5): 635–46.

Lim, Shiang Y., Derek M. Yellon, and Derek J. Hausenloy. 2010. "The Neural and Humoral Pathways in Remote Limb Ischemic Preconditioning." *Basic Research in Cardiology* 105 (5): 651–55.

Liu, G S, J Thornton, D M Van Winkle, a W Stanley, R a Olsson, and J M Downey. 1991. "Protection against Infarction Afforded by Preconditioning Is Mediated by A1 Adenosine Receptors in Rabbit Heart." *Circulation* 84 (1): 350–56.

Mathers, Colin D, Ties Boerma, and Doris Ma Fat. 2009. "Global and Regional Causes of Death." *British Medical Bulletin* 92: 7–32.

Mattie, M, G Brooker, and S Spiegel. 1994. "Sphingosine-1-Phosphate, a Putative Second Messenger, Mobilizes Calcium from Internal Stores via an Inositol Trisphosphate-Independent Pathway." *The Journal of Biological Chemistry* 269 (5): 3181–88.

Mazurais, David, Philippe Robert, Bernard Gout, Isabelle Berrebi Bertrand, and Marie Paule Laville. 2002. "Cell Type-Specific Localization of Human Cardiac S1P Receptors." *The Journal of Histochemistry & Cytochemistry* 50 (5): 661–69.

Means, Christopher Kable, Shigeki Miyamoto, Jerold Chun, and Joan Heller Brown. 2008. "S1P1 Receptor Localization Confers Selectivity for G I-Mediated cAMP and Contractile Responses." *Journal of Biological Chemistry* 283 (18): 11954–63.

Means, Christopher K, Chun-yang Xiao, Zhuangjie Li, Tong Zhang, Jeffrey H Omens, Isao Ishii, Jerold Chun, and Joan Heller Brown. 2007. "Sphingosine 1-Phosphate S1P 2 and S1P 3 Receptor-Mediated Akt Activation Protects against in Vivo Myocardial Ischemia-Reperfusion Injury." *American Journal of Physiology. Heart and Circulatory Physiology* 292: 2944–51.

Mensah, G a. 2008a. "Epidemiology of Stroke and High Blood Pressure in Africa." *Heart (British Cardiac Society)* 94 (6): 697–705.

Mensah, G a. 2008b. "Ischaemic Heart Disease in Africa." *Heart (British Cardiac Society)* 94 (7): 836–43.

Mensah, George A, Gregory A Roth, Uchechukwu K A Sampson, Andrew E Moran, Valery L Feigin, Mohammed H Forouzanfar, Mohsen Naghavi, Christopher J L Murray, and G B D Mortality. 2015. "Cardiovascular Topics Mortality from Cardiovascular Diseases in Sub-Saharan Africa , 1990 – 2013 : A Systematic Analysis of Data from the Global Burden of Disease Study 2013." *Cardiovascular Journal Of Africa* 26 (2): 6–10.

Michel, et al. 1985. “Effects of Native and Modefied Bovien Serum Albumin on the Permeability of Frog Mesenteric Capillaries.” *J. Physiol* 360 (5): 333–46.

Moens, a L, M J Claeys, J P Timmermans, and C J Vrints. 2005. “Myocardial Ischemia/reperfusion-Injury, a Clinical View on a Complex Pathophysiological Process.” *International Journal of Cardiology* 100 (2): 179–90.

Moissac, D, R M Gurevich, H Zheng, P K Singal, and L a Kirshenbaum. 2000. “Caspase Activation and Mitochondrial Cytochrome C Release during Hypoxia-Mediated Apoptosis of Adult Ventricular Myocytes.” *Journal of Molecular and Cellular Cardiology* 32 (1): 53–63.

Mulivor, a W, and H H Lipowsky. 2002. “Role of Glycocalyx in Leukocyte-Endothelial Cell Adhesion.” *American Journal of Physiology. Heart and Circulatory Physiology* 283: H1282–91.

Mulivor, a W, and H H Lipowsky. 2004. “Inflammation- and Ischemia-Induced Shedding of Venular Glycocalyx.” *American Journal of Physiology. Heart and Circulatory Physiology* 286 (5): H1672-80.

Murata, N, K Sato, J Kon, H Tomura, M Yanagita, A Kuwabara, M Ui, and F Okajima. 2000a. “Interaction of Sphingosine 1-Phosphate with Plasma Components, Including Lipoproteins, Regulates the Lipid Receptor-Mediated Actions.” *The Biochemical Journal* 352: 809–15.

Murray, Christopher J L, and Alan D Lopez. 1997. “Alternative Projections of Mortality and Disability by Cause 1990 – 2020 : Global Burden of Disease Study.” *The Lancet* 349: 1498–1504.

Murry, C E, R B Jennings, and K A Reimer. 1986. “Preconditioning with Ischemia: A Delay of Lethal Cell Injury in Ischemic Myocardium.” *Circulation* 74 (5): 1124–36.

Murry, C E, V J Richard, K A Reimer, and R B Jennings. 1990. “Ischemic Preconditioning Slows Energy Metabolism and Delays Ultrastructural Damage during a Sustained Ischemic Episode.” *Circulation Research* 66 (4): 913–31.

Nakamura, Masanori, Ning Ping Wang, Zhi Qing Zhao, Josiah N. Wilcox, Vinod Thourani, Robert A. Guyton, and Jakob Vinten-Johansen. 2000. “Preconditioning Decreases Bax Expression, PMN Accumulation and Apoptosis in Reperfused Rat Heart.” *Cardiovascular Research* 45 (3): 661–70.

Nakanishi, Zhi-Qing Zhao, Jakob Vinten-Johansen, Jon C. Lewis, D.Scott McGee, and John W. Hammon. 1994. “Coronary Artery Endothelial Dysfunction after Global Ischemia, Blood Cardioplegia, and Reperfusion.” *The Annals of Thoracic Surgery* 58 (1): 191–99.

Nojilana, Beatrice, Debbie Bradshaw, Victoria Pillay-van Wyk, William Msemburi, Ria Laubscher, Nontuthuzelo I M Somdyala, Jane D Joubert, Pamela Groenewald, and Rob E Dorrington. 2016. “Emerging Trends in Non-Communicable Disease Mortality in South Africa, 1997 - 2010.”

South African Medical Journal = Suid-Afrikaanse Tydskrif Vir Geneeskunde 106 (5). Health & Medical Publishing Group: 58.

Ogawa, S., S. Koga, K. Kuwabara, J. Brett, B. Morrow, S. A. Morris, J. P. Bilezikian, S. C. Silverstein, and D. Stern. 1992. “Hypoxia-Induced Increased Permeability of Endothelial Monolayers Occurs through Lowering of Cellular cAMP Levels.” *American Journal of Physiology - Cell Physiology* 262 (3).

Ohmori, Tsukasa, Yutaka Yatomi, Makoto Osada, Fuminori Kazama, Toshiro Takafuta, Hitoshi Ikeda, and Yukio Ozaki. 2003. “Sphingosine 1-Phosphate Induces Contraction of Coronary Artery Smooth Muscle Cells via S1P2.” *Cardiovascular Research* 58 (1): 170–77.

Onen, Churchill Lukwiya. 2013. “Review Article Epidemiology of Ischaemic Heart Disease in Sub-Saharan Africa.” *Cardiovascular Journal Of Africa* 24 (2): 34–42.

Palmer, Brian S, Mersiha Hadziahmetovic, Timothy Veci, and Mark G Angelos. 2004. “Global Ischemic Duration and Reperfusion Function in the Isolated Perfused Rat Heart.” *Resuscitation* 62 (1): 97–106.

Paradies, G, G Petrosillo, M Pistolese, N DiVenosa, D Serena, and F M Ruggiero. 1999. “Lipid Peroxidation and Alterations to Oxidative Metabolism in Mitochondria Isolated from Rat Heart Subjected to Ischemia and Reperfusion.” *Free Radical Biol Med* 27 (1–2): 42–50.

Patel, Kamala D., Matthias U. Nollert, and Rodger P. McEver. 1995. “P-Selectin Must Extend a Sufficient Length from the Plasma Membrane to Mediate Rolling of Neutrophils.” *Journal of Cell Biology* 131 (6 II): 1893–1902.

Pyne, Susan, and Nigel J Pyne. 2000. “Sphingosine 1-Phosphate Signalling in Mammalian Cells.” *Biochemical Society* 349: 385–402.

Rahbar, Elaheh, Jessica C Cardenas, Gyulnar Baimukanova, Benjamin Usadi, Roberta Bruhn, Shibani Pati, Sisse R Ostrowski, Pär I Johansson, John B Holcomb, and Charles E Wade. 2015. “Endothelial Glycocalyx Shedding and Vascular Permeability in Severely Injured Trauma Patients.” *Journal of Translational Medicine* 13: 1–7.

Rapraeger, A., M. Jalkanen, E. Endo, J. Koda, and M. Bernfield. 1985. “The Cell Surface Proteoglycan from Mouse Mammary Epithelial Cells Bears Chondroitin Sulfate and Heparan Sulfate Glycosaminoglycans.” *Journal of Biological Chemistry* 260 (20): 11046–52.

Rehm, Markus, Dirk Bruegger, Frank Christ, Peter Conzen, Manfred Thiel, Matthias Jacob, Daniel Chappell, et al. 2007. “Shedding of the Endothelial Glycocalyx in Patients Undergoing Major Vascular Surgery with Global and Regional Ischemia.” *Circulation* 116 (17): 1896–1906.

Reitsma, Sietze, Dick W Slaaf, Hans Vink, Marc a M J van Zandvoort, and Mirjam G a oude Egbrink. 2007. “The Endothelial Glycocalyx: Composition, Functions, and Visualization.” *European Journal of Physiology* 454 (3): 345–59.

Renkin, J, W Wijns, Z Ladha, and J Col. 1990. “Reversal of Segmental Hypokinesis by Coronary Angioplasty in Patients with Unstable Angina, Persistent T Wave Inversion, and Left Anterior Descending Coronary Artery Stenosis. Additional Evidence for Myocardial Stunning in Humans.” *Circulation* 82 (3): 913–21.

Romson, J L, B G Hook, S L Kunkel, G D Abrams, M A Schork, and B R Lucchesi. 1983. “Reduction of the Extent of Ischemic Myocardial Injury by Neutrophil Depletion in the Dog.” *Circulation* 67 (5): 1016–23.

Roth, Gregory A, Mohammad H Forouzanfar, Andrew E Moran, Ryan Barber, Grant Nguyen, Valery L Feigin, Mohsen Naghavi, George A Mensah, and Christopher J L Murray. 2015. “Demographic and Epidemiologic Drivers of Global Cardiovascular Mortality.” *The New England Journal of Medicine* 372 (14): 1333–41.

Rubio-gayosso, Ivan, Steven H Platts, and Brian R Duling. 2006. “Reactive Oxygen Species Mediate Modification of Glycocalyx during Ischemia-Reperfusion Injury.” *American Journal of Physiology. Heart and Circulatory Physiology* 290: 2247–56.

Sampson, Uchechukwu K a, Mary Amuyunzu-Nyamongo, and George a Mensah. 2013. “Health Promotion and Cardiovascular Disease Prevention in Sub-Saharan Africa.” *Progress in Cardiovascular Diseases* 56 (3). Elsevier B.V.: 344–55.

Sanderson, Ralph D., Jeremy E. Turnbull, John T. Gallagher, and Arthur D. Lander. 1994. “Fine Structure of Heparan Sulfate Regulates Syndecan-1 Function and Cell Behavior.” *Journal of Biological Chemistry* 269 (18): 13100–106.

Santulli, Gaetano. 2013. “Epidemiology of Cardiovascular Disease in the 21 St Century : Updated Numbers and Updated Facts.” *Journal of Cardiovascular Disease* 1 (1): 1–2.

Santulli, Gaetano, Canto JG, D’Agostino RB, Petersen JL, Wu E, and Wang TJ. 2012. “Coronary Heart Disease Risk Factors and Mortality.” *Jama* 307 (11): 2120–27.

Shikata, Yasushi, Konstantin G Birukov, and Joe G N Garcia. 2003. “S1P Induces FA Remodeling in Human Pulmonary Endothelial Cells: Role of Rac, GIT1, FAK, and Paxillin.” *Journal of Applied Physiology (Bethesda, Md. : 1985)* 94 (3): 1193–1203.

Skrzypiec-Spring, Monika, Bartosz Grotthus, Adam Szelag, and Richard Schulz. 2007. “Isolated Heart Perfusion according to Langendorff-Still Viable in the New Millennium.” *Journal of Pharmacological and Toxicological Methods* 55 (2): 113–26.

Skyschally, Andreas, Rainer Schulz, and Gerd Heusch. 2010. “Cyclosporine a at Reperfusion Reduces Infarct Size in Pigs.” *Cardiovascular Drugs and Therapy* 24 (1): 85–87.

Somers, Sarin J, Miguel Frias, Lydia Lacerda, Lionel H Opie, and Sandrine Lecour. 2012. “Interplay between SAFE and RISK Pathways in

Sphingosine-1-Phosphate-Induced Cardioprotection." *Cardiovascular Drugs and Therapy / Sponsored by the International Society of Cardiovascular Pharmacotherapy* 26 (3): 227–37.

Sörensson, J, G L Matejka, M Ohlson, and B Haraldsson. 1999. "Human Endothelial Cells Produce Orosomucoid, an Important Component of the Capillary Barrier." *The American Journal of Physiology* 276 (February): H530-4.

Stephen S Lim, Theo Vos, Abraham D Flaxman, Goodarz Danaei, Kenji Shibuya, Kathryn G Andrews* Heather Adair-Rohani, Markus Amann*, H Ross Anderson*, Kalpana Martin Aryee*, Charles Atkinson*, Loraine J Bacchus*, Adil N Bahalim*, Suzanne Barker-Collo Balakrishnan*, John Balmes*, Stephen S. Lim, Theo Vos, Abraham D. Flaxman, et al. 2012. "A Comparative Risk Assessment of Burden of Disease and Injury Attributable to 67 Risk Factors and Risk Factor Clusters in 21 Regions, 1990–2010: A Systematic Analysis for the Global Burden of Disease Study 2010." *The Lancet* 380 (9859): 2224–60.

Straus, David. 2013. "Myocardial Edema Attenuation and Sphingosine- 1-Phosphate." *Cardiovascular Journal* 6 (1): 47–51.

Sugiyama, Atsushi, Nu Nu Aye, Yutaka Yatomi, Yukio Ozaki and Keitaro Hashimoto. 2000. "Effect of Sphingosine-1- Phosphate a Naturally Occuring Bilogically Active Lysophospholibid on the Rat Cardiovascular System." *Jpn. J. Pharmacol.* 82: 338–42.

Takano, H, X Tang, and R Bolli. 2000. "Differential Role of KATP Channels in Late Preconditioning against Myocardial Stunning and Infarction in Rabbits." *American Journal of Physiology* 279 (5 Part 2): H2350–59.

Tani, M, and J R Neely. 1989. "Role of Intracellular Na+ in Ca2+ Overload and Depressed Recovery of Ventricular Function of Reperfused Ischemic Rat Hearts. Possible Involvement of H+-Na+ and Na+-Ca2+ Exchange." *Circulation Research* 65 (4): 1045–56.

Tarbell, J M, and M Y Pahakis. 2006. "Mechanotransduction and the Glycocalyx." *Journal of Internal Medicine* 259 (4): 339–50.

Theilmeier, Gregor, Christoph Schmidt, Jörg Herrmann, Petra Keul, Michael Schäfers, Ilka Herrgott, Jan Mersmann, et al. 2006. "High-Density Lipoproteins and Their Constituent, Sphingosine-1-Phosphate, Directly Protect the Heart against Ischemia/reperfusion Injury in Vivo via the S1P3 Lysophospholipid Receptor." *Circulation* 114 (13): 1403–9.

Tsao, P S, N Aoki, D J Lefer, G Johnson, and a M Lefer. 1990. "Time Course of Endothelial Dysfunction and Myocardial Injury during Myocardial Ischemia and Reperfusion in the Cat." *Circulation* 82 (100001590507): 1402–12.

Tsukada, Yayoi T, M Germana Sanna, Hugh Rosen, and Roberta A Gottlieb. 2007. "S1P1-Selective Agonist SEW2871 Exacerbates Reperfusion Arrhythmias." *Journal of Cardiovascular Pharmacology* 50 (6): 660–69.

van den Berg, Bernard M, Hans Vink, and Jos a E Spaan. 2003. "The

Endothelial Glycocalyx Protects against Myocardial Edema." *Circulation Research* 92 (6): 592–94.

van Emous, J G, M G Nederhoff, T J Ruigrok, and C J van Echteld. 1997. "The Role of the Na+ Channel in the Accumulation of Intracellular Na+ during Myocardial Ischemia: Consequences for Post-Ischemic Recovery." *Journal of Molecular and Cellular Cardiology* 29 (1): 85–96.

Van Emous, J G, J H Schreur, T J Ruigrok, and C J Van Echteld. 1998. "Both Na+-K+ ATPase and Na +-H+ Exchanger Are Immediately Active upon Post-Ischemic Reperfusion in Isolated Rat Hearts." *Journal of Molecular and Cellular Cardiology* 30 (2): 337–48.

van Haaren, Paul M a, Ed VanBavel, Hans Vink, and Jos a E Spaan. 2003. "Localization of the Permeability Barrier to Solutes in Isolated Arteries by Confocal Microscopy." *American Journal of Physiology. Heart and Circulatory Physiology* 285 (6): H2848–56.

VanTeeffelen, Jurgen W G E, Judith Brands, Carin Jansen, Jos A E Spaan, and Hans Vink. 2007. "Heparin Impairs Glycocalyx Barrier Properties and Attenuates Shear Dependent Vasodilation in Mice." *Hypertension* 50 (1): 261–67.

Venkataraman, Krishnan, Yong Moon Lee, Jason Michaud, Shobha Thangada, Youxi Ai, Herbert L. Bonkovsky, Nehal S. Parikh, Cheryl Habrukowich, and Timothy Hla. 2008. "Vascular Endothelium as a Contributor of Plasma Sphingosine 1-Phosphate." *Circulation Research* 102 (6): 669–76.

Vessey, Donald A, Luyi Li, Norman Honbo, and Joel S Karliner. 2009. "Sphingosine 1-Phosphate Is an Important Endogenous Cardioprotectant Released by Ischemic Pre- and Postconditioning." *American Journal of Physiology. Heart and Circulatory Physiology* 297: 1429–35.

Vink, H, a a Constantinescu, and J a E Spaan. 2000. "Oxidised Lipoproteins Degrade the Endothelial Surface Layer." *Circulation* 101: 1500–1502.

Wall, T M, R Sheehy, and J C Hartman. 1994. "Role of Bradykinin in Myocardial Preconditioning." *The Journal of Pharmacology and Experimental Therapeutics* 270 (2): 681–89.

Wang, Lianguo, Gennady Cherednichenko, Lisa Hernandez, Jessica Halow, Albert Camacho, Vincent Figueredo, Saul Schaefer, and S Albert Camacho. 2001. "Preconditioning Limits Mitochondrial Ca 2+ during Ischemia in Rat Hearts : Role of K ATP Channels." *Am J Physiol Heart Circ Physiol* 280: 2321–28.

Weiskopf, Richard B, Charles D Collard, Simon Gelman, and D Ph. 2001. "Prevention of Ischemia – Reperfusion Injury." *American Society of Anesthesiologists* 94 (6): 1133–38.

WHO. 2017. "WHO _ Cardiovascular Diseases (CVDs)." *Cardiovascular Diseases (CVDs)*.

Yamazaki, S, Y Fujibayashi, R E Rajagopalan, S Meerbaum, and E Corday.

1986. “Effects of Staged versus Sudden Reperfusion after Acute Coronary Occlusion in the Dog.” *Journal of the American College of Cardiology* 7 (3). American College of Cardiology Foundation: 564–72.

Yatorni, By Yutaka, Fuqiang Ruan, and Sen-itiroh Hakomori. 1995. “Platelet-Activating Sphingolipid Released From Agonist-Stimulated Human Platelets.” *The American Society of Hematology* 86 (1): 193–202.

Yini, S., Z. Heng, A. Xin, and M. Xiaochun. 2015. “Effect of Unfractionated Heparin on Endothelial Glycocalyx in a Septic Shock Model.” *Acta Anaesthesiologica Scandinavica* 59 (2): 160–69.

Zeng, Ye, Roger H Adamson, Fitz-Roy E Curry, and John M Tarbell. 2014. “Sphingosine-1-Phosphate Protects Endothelial Glycocalyx by Inhibiting Syndecan-1 Shedding.” *American Journal of Physiology. Heart and Circulatory Physiology* 306 (3): H363-72.

Zeng, Ye, Eno E Ebong, Bingmei M Fu, and John M Tarbell. 2012. “The Structural Stability of the Endothelial Glycocalyx after Enzymatic Removal of Glycosaminoglycans.” *PloS One* 7 (8): 1–14.

Zeng, Ye, Xiao-heng Liu, John Tarbell, and Bingmei Fu. 2015. “Sphingosine 1-Phosphate Induced Synthesis of Glycocalyx on Endothelial Cells.” *Experimental Cell Research* 339 (1). Elsevier: 90–95.

Zhang, Gengqian, Sulei Xu, Yan Qian, and Pingnian He. 2010. “Sphingosine-1-Phosphate Prevents Permeability Increases via Activation of Endothelial Sphingosine-1-Phosphate Receptor 1 in Rat Venules.” *AJP: Heart and Circulatory Physiology* 299 (5). American Physiological Society: H1494-504.

Zhang, Hong. 1991. “Sphingosine-1- Phosphate, a Novel Lipid, Involved in Cellular Proliferation.” *The Journal of Cell Biology* 114 (1): 155–67.

Zhang, Lin, Min Zeng, Jie Fan, John M. Tarbell, Fitz-Roy E. Curry, and Bingmei M. Fu. 2016. “Sphingosine-1-Phosphate Maintains Normal Vascular Permeability by Preserving Endothelial Surface Glycocalyx in Intact Microvessels.” *Microcirculation* 23 (4): 301-310.

Zhao, Zhi-Qing, Joel S Corvera, Michael E Halkos, Faraz Kerendi, Ning-Ping Wang, Robert a Guyton, and Jakob Vinten-Johansen. 2003. “Inhibition of Myocardial Injury by Ischemic Postconditioning During Reperfusion: Comparison with Ischemic Preconditioning.” *American Journal of Physiology* 285 (2): H579–88.

Zimmermann, Pascale, and Guido David. 1999. “The Syndecans, Tuners of Transmembrane Signaling.” *The FASEB Journal* 13 Suppl (9001): S91–100.

Zuurbier, Coert J, Cihan Demirci, Anneke Koeman, Hans Vink, and Can Ince. 2005. “Short-Term Hyperglycemia Increases Endothelial Glycocalyx Permeability and Acutely Decreases Lineal Density of Capillaries with Flowing Red Blood Cells.” *Journal of Applied Physiology (Bethesda, Md. : 1985)* 99 (July 2005): 1471–76.

Zweier, J. L. 1988. “Measurement of Superoxide-Derived Free Radicals in the Reperfused Heart. Evidence for a Free Radical Mechanism of Reperfusion Injury.” *Journal of Biological Chemistry* 263 (3): 1353–57.

APPENDICES

1. Krebs-Henseleit Buffer for Langendorff Perfusion (3 L)

NaCl	118.5 mM	20.775 g
KCl	4.7 mM	1.051 g
$NaHCO_3$	25 mM	6.301 g
KH_2PO_4	1.2 mM	0.490 g
Glucose	11 mM	5.945 g
$MgSO_4$	1.2 mM	0.433 g
$CaCl_2$	1.8 mM	0.599 g

Bubble with carbogen (pH7.4) before adding $CaCl_2$

2. Preliminary Data: Testing Duration of Ischemia

For optimization of ischemia duration some preliminary experiments were done to demonstrate the perfusion protocol conditions and duration. Whereas, hearts subjected to 20, 25, and 30 minutes ischemia followed by reperfusion (N=10).

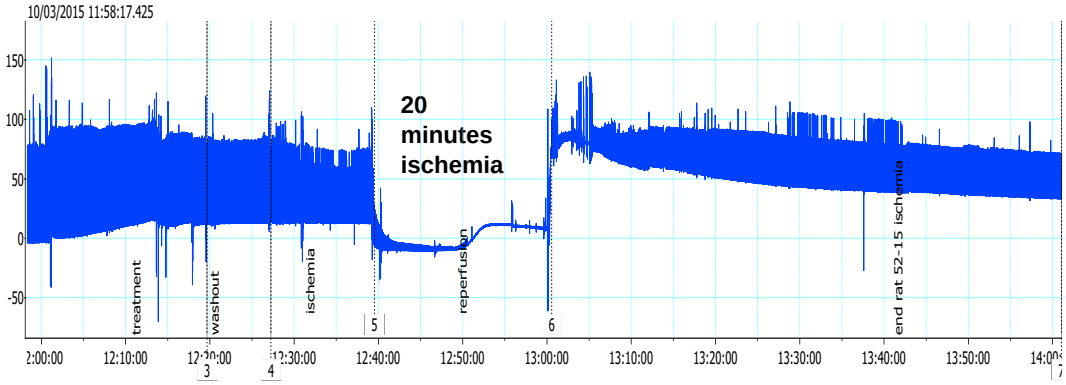

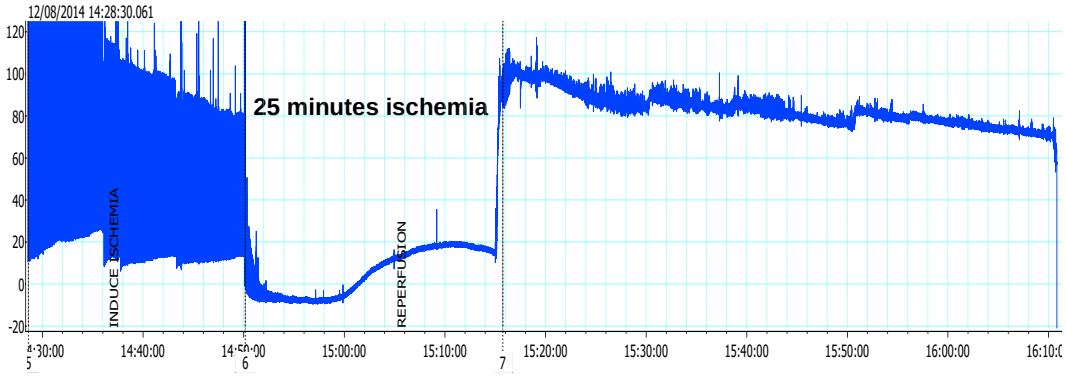

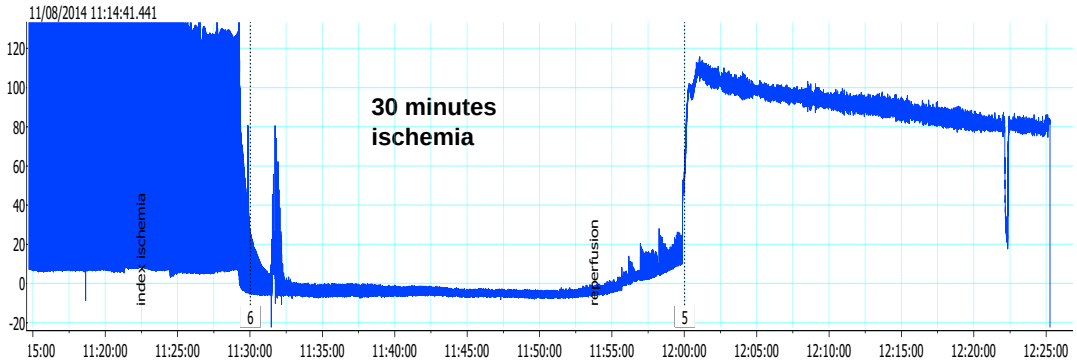

3. Preliminary data: Comparing Values at the Baseline to the Values at the End of Reperfusion of the Three-Different Ischemia Duration.

Duration of ischemia	20 min	25 min	30 min
Number of hearts	4	3	1
Recovery after ischemia	Yes	No	No
LVDP (mmHg)			
Baseline	70.51 ± 8.97	74.63 ± 2.38	116.96 ± 0.0
End of reperfusion	2.27 ± 1.08	0.00 ± 0.0	0.00 ± 0.0
LVEDP (mmHg)			
Baseline	8.65 ± 2.2.42	11.89±1.36	7.29 ± 0.0
End of reperfusion	66.73 ± 8.12	0.00 ± 0.0	0.00 ± 0.0
Heart rate (bpm)			
Baseline	285.00 ± 15.00	320 ± 20.00	300 ± 0.0
End of reperfusion	225 ± 15.00	0.00 ± 0.0	0.00 ± 0.0
Coronary flow (CF)			
Baseline	6.25 ± 1.34	12.83± 3.09	30 ± 0.00
End of reperfusion	4.00 ± 0.41	0.33 ± 0.33	0.00 ± 0.0

4. Hemodynamic Parameters Measured at the End of Stabilization Compared to the Measurements at the End of Reperfusion: *P<0.05, vs. control, vs. S1P perfusion. ****P<0.0001, vs. control, vs. S1P perfusion.

Parameters	Baseline	Reperfusion at 60 min
LVDP (mmHg)		
Control	95.9 ± 5.6	40.6 ± 2.0
I/R	93.9 ± 7.2	18.1 ± 4.7 *
I/R+S1P	89.3± 8.4	15.5 ± 2.1 *
S1P Perfusion	88.4 ± 4.7	39.8 ± 4.2
LVEDP (mmHg)		
Control	6.4 ± 0.6	26.1± 3.8
I/R	8.4 ± 0.9	61.4 ± 5.3 ****
I/R+S1P	6.5 ± 0.9	69.5 ± 3.6 ****
S1P Perfusion	7.0 ± 0.8	13.1 ± 1.9
Heart rate (bpm)		
Control	310 ± 15	220 ± 12
I/R	317 ± 17	257 ± 17
I/R+S1P	360 ± 0	280 ± 25
S1P Perfusion	317 ± 17	218 ± 30
Coronary flow (ml/min)		
Control	4.6 ± 0.7	0.6 ± 0.1
I/R	3.7 ± 0.4	0.9 ± 0.1
I/R+S1P	3.5 ± 0.5	0.7 ± 0.1
S1P Perfusion	3.2 ± 0.7	1.3 ± 0.2
Net filtration rate		
Control	0.6 ± 0.1	3.1 ± 0.4
I/R	1.0 ± 0.3	2.7 ± 0.3
I/R+S1P	1.7 ± 0.6	3.4 ± 1.0
S1P Perfusion	1.5 ± 0.5	1.8 ± 0.5

5. TTC Stain from Defrosted Heart Sections

1. Recipe for TTC buffer solution A

Monobasic sodium (acidic phosphate) 15.6 g

Distilled water 1000 ml

2. Recipe for TTC buffer solution B

100 µM Dibasic sodium (alkaline phosphate) 14.2 g

Distilled water 1000 ml

3. Recipe for 1% TTC solution

Mix 4 parts solution B with 1 part solution A and titrate to pH 7.4, add 250 mg TTC in 25 ml buffer solution.

TTC stain was conducted using the standard protocol

Infarct size quantification with ImageJ

File ⟶ Open ⟶ View one side of the heart at a time⟶ Zoom to accurate viewing⟶ Select polygonal icon⟶ Hold shift and click on the outline of heart slide then release shift ⟶ Select analysis icon ⟶ Measure (this will measure the entire area of all the slices) ⟶ Edit ⟶ Clear outside ⟶ Image ⟶ colure ⟶ Split channel ⟶ Close the other windows use only the green one ⟶ Image⟶ Adjust ⟶ Threshold.

The gray area represents the infarct area, with image J this cannot be measured so there is a need to measure the red area and minus it from the total in an excel worksheet, then the infarct area presented as percentage to the total area.

6. ELISA Preparation and Method

6.1 Preparation of ELISA Solutions

1. *1×Phosphate Buffered Saline (PBS Buffer) Recipe*

a- Dissolve the following in 800 ml distilled water H_2O.

- 8 g of NaCl
- 0.2 g of KCl
- 1.44 g of Na_2HPO_4
- 0.24 g of KH_2PO_4

b- Adjust pH to 7.4 with HCl.

c- Adjust volume to 1 L with additional distilled water.

d- Sterilize by autoclaving.

2. *Blocking buffer (1×PBS, 5% BSA)*

Add 2.5 g bovine serum albumin (BSA) to 50 ml of PBS.

3. *Wash buffer (1×PBS, 0.05% Tween 20)*

Add 45 µL of Tween 20 to 100 ml PBS

4. *Standard and secondary antibody dilution buffer (1×PBS, 1% BSA)*

Add 0.15 g BSA to 15 ml PBS.

5. *Coating buffer (1×PBS, pH 7.2-7.4)*

6. *HRP diluent buffer (1×PBS, 1% BSA, 0.1% Tween 20)*

Add 0.25 g BSA to 25 ml PBS to 22.5 µL Tween 20.

7. *Reconstitution buffer (1×PBS, 0.09% Azide)*

Add 0.09 g Azide to 100 ml PBS

8. Stop reagent (1 M sulfuric acid)

Add 2.78 ml sulfuric acid into 50 ml distilled water.

6.2 ELISA Assay Preparation

6.2.1 Assay Design

This figure represents the design of organization of samples which are required for analysis plus standard, control and zero or blank. All tested in duplicate.

	Standards /Controls		Sample wells									
	1	2	3	4	5	6	7	8	9	10	11	12
A	256	256										
B	128	128										
C	64	64										
D	32	32										
E	16	16										
F	8	8										
G	zero	zero										
H	Ctrl	Ctrl										

6.2.2 Preparation of Standard

Standard vials reconstituted with volume of standard diluent (0.76 ml) this gives stock solution of 256 ng/ml of CD138. Serial dilution of the standard is made directly in the assay to provide the concentration range from 256 to 8 ng/ml. A fresh standard curve is produced for every new assay.

6.2.3 Preparation of Biotinylated Antibody (Anti-CD138)

This antibody is prepared immediately before use. 96-wells plate need to dilute 240 µl of biotinylated antibody into 6.36 ml of biotinylated antibody diluent.

6.2.4 Preparation of Streptavidin-HRP

Dilute the 5 µl vial of streptavidin-HRP with 0.5 ml of HRP diluent immediately before use. Then further dilution required according to the number of wells, for 96-wells need to dilute 150 µl into 10 ml streptavidin-HRP.

6.2.5 Summary of the Method

Add 50 µl of sample and diluted standard /control and 50 µl biotinylated anti CD138

↓

Incubate 1 hour at room temperature

↓

Wash three times

↓

Add 100 µl of streptavidin-HRP

↓

Incubate for 30 min

↓

Wash three times

↓

Add 100 µl of ready to use TMB

↓

Protect from light and incubate for 12-15 min

↓

Add 100 µl sulfuric acid

↓

Read absorbance at 450 nm

6.2.6 (A) Syndecan-1 Standard Curve, (B) Syndecan-1 levels using Murine Antibody Kit.

(A)

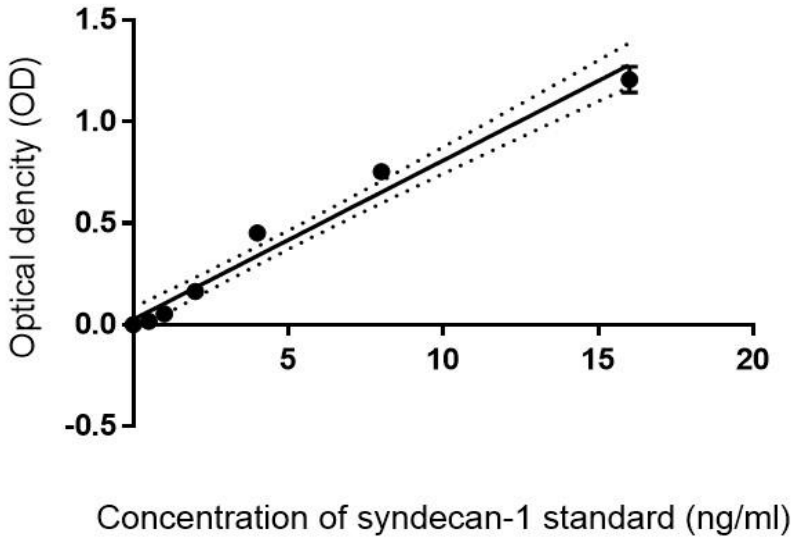

(B)

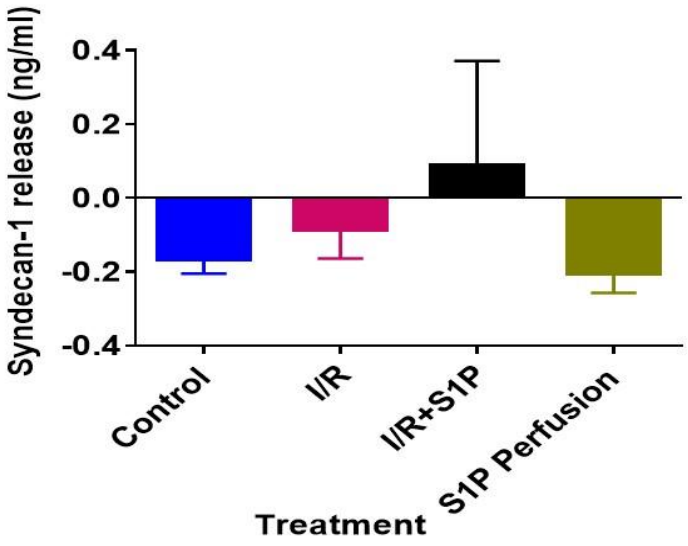

6.2.7 Syndecan-1 Standard Curve of Human Kit

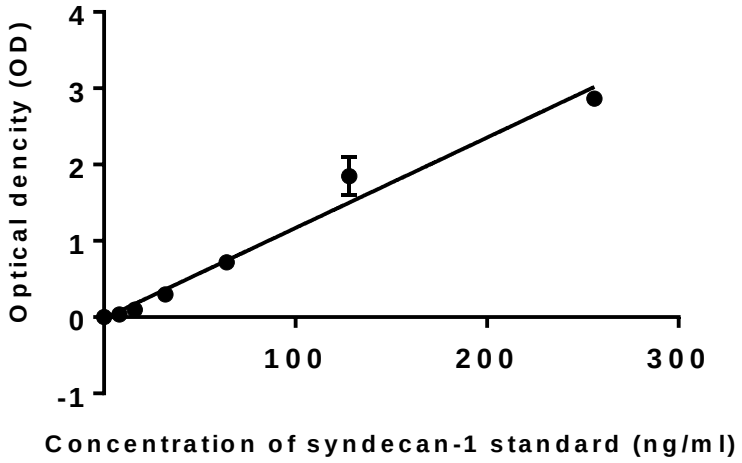

7. Syndecan-1 Homology across the Mouse, Rat, Human

Comparison between the amino acid sequences of syndecan-1 across the species (human, rat, mouse) using Pair Wise Sequences Alignment> Emboss Needle program

7.1 Syndecan-1 Homology Between Human vs. Rat

```
########################################
# Program: needle
# Rundate: Mon 30 Jan 2017 11:46:29
# Commandline: needle
#    -auto
#    -stdout
#    -asequence emboss_needle-I20170130-114628-0077-20079328-
es.asequence
#    -bsequence emboss_needle-I20170130-114628-0077-20079328-
es.bsequence
#    -datafile EBLOSUM62
#    -gapopen 10.0
#    -gapextend 0.5
#    -endopen 10.0
#    -endextend 0.5
#    -aformat3 pair
#    -sprotein1
#    -sprotein2
# Align_format: pair
# Report_file: stdout
########################################

#=======================================
#
# Aligned_sequences: 2
# 1: AAH08765.1
# 2: AAH61834.1
# Matrix: EBLOSUM62
# Gap_penalty: 10.0
# Extend_penalty: 0.5
#
# Length: 313
# Identity:     240/313 (76.7%)
# Similarity:   252/313 (80.5%)
# Gaps:           3/313 ( 1.0%)
# Score: 1213.5
#
#
#=======================================
```

```
AAH08765.1        1
MRRAALWLWLCALALSLQPALPQIVATNLPPEDQDGSGDDSDNFSGSG
AG     50
                  ||||||||||||||.|||||||||..|:||||||||||||||||||.|
AAH61834.1        1
MRRAALWLWLCALALRLQPALPQIVTANVPPEDQDGSGDDSDNFSGSG
TG     50

AAH08765.1        51
ALQDITLSQQTPSTWKDTQLLTAIPTSPEPTGLEATAASTSTLPAGEGPK
100
                  ||.|:|||:||||||||..||||.||:||||..:..|..||.|||||.|:
AAH61834.1        51
ALPDMTLSRQTPSTWKDVWLLTATPTAPEPTSRDTEATLTSILPAGEKPE
100

AAH08765.1       101 EGEAVVLPEVEPGLTAR--
EQEATPRPRETTQLPTTHQASTTT-ATTAQE    147
                  |||.|...|.||..|||  |:|||.|||||||||.|.|||||.. |||||.
AAH61834.1       101
EGEPVAHVEAEPDFTARDKEKEATTRPRETTQLPVTQQASTAARATTAQ
A    150

AAH08765.1       148
PATSHPHRDMQPGHHETSTPAGPSQADLHTPHTEDGGPSATERAAEDG
AS    197
                  ..|||||.|:|||.|||..|..|.|.|...|..||||.|..:...||..:
AAH61834.1       151
SVTSHPHGDVQPGLHETLAPTAPGQPDHQPPSVEDGGTSVIKEVVEDET
T    200

AAH08765.1       198
SQLPAAEGSGEQDFTFETSGENTAVVAVEPDRRNQSPVDQGATGASQG
LL    247
                  :||||.||||||||||||||||..||||.|||||||:||||||||||
AAH61834.1       201
NQLPAGEGSGEQDFTFETSGENTAVAGVEPDLRNQSPVDEGATGASQG
LL    250

AAH08765.1       248
DRKEVLGGVIAVGLVGLIFAVCLVGFMLYRMKKKDEGSYSLEEPKQANG
G    297
                  ||||||||||.||||||||||.||||||||||||||||||||||||
AAH61834.1       251
DRKEVLGGVIAGGLVGLIFAVCLVAFMLYRMKKKDEGSYSLEEPKQANG
G    300

AAH08765.1       298 AYQKPTKQEEFYA    310
                  ||||||||||||
```

AAH61834.1 301 AYQKPTKQEEFYA 313

#---------------------------------------
#---------------------------------------

7.2 Syndecan-1 Homology Between Human vs. Mouse

Human vs. mouse##
Program: needle
Rundate: Mon 30 Jan 2017 12:01:22
Commandline: needle
-auto
-stdout
-asequence emboss_needle-I20170130-120121-0691-66201215-oy.asequence
-bsequence emboss_needle-I20170130-120121-0691-66201215-oy.bsequence
-datafile EBLOSUM62
-gapopen 10.0
-gapextend 0.5
-endopen 10.0
-endextend 0.5
-aformat3 pair
-sprotein1
-sprotein2
Align_format: pair
Report_file: stdout
##

#=======================================
#
Aligned_sequences: 2
1: AAH08765.1
2: CAA80254.1
Matrix: EBLOSUM62
Gap_penalty: 10.0
Extend_penalty: 0.5
#
Length: 312
Identity: 237/312 (76.0%)
Similarity: 248/312 (79.5%)
Gaps: 3/312 (1.0%)
Score: 1195.5
#
#
#=======================================

AAH08765.1 1 MRRAALWLWLCALALSLQPALPQIVATNLPPEDQDGSGDDSDNFSGSG AG 50

```
                ||||||||||||||||.||||||||||.|:||||||||||||||||||.|
CAA80254.1         1
MRRAALWLWLCALALRLQPALPQIVAVNVPPEDQDGSGDDSDNFSGSG
TG     50

AAH08765.1        51
ALQDITLSQQTPSTWKDTQLLTAIPTSPEPTGLEATAASTSTLPAGEGPK
100
                ||.| |||:||||||||..||||.||:||||......|.||.|||||.|:
CAA80254.1        51 ALPD-
TLSRQTPSTWKDVWLLTATPTAPEPTSSNTETAFTSVLPAGEKPE     99

AAH08765.1       101 EGEAVVLPEVEPGLTAR--
EQEATPRPRETTQLPTTHQASTTTATTAQEP    148
                |||.|:..|.|||.|||  |:|.|.|||||.|||.|.:|||...||||..
CAA80254.1       100
EGEPVLHVEAEPGFTARDKEKEVTTRPRETVQLPITQRASTVRVTTAQAA
149

AAH08765.1       149
ATSHPHRDMQPGHHETSTPAGPSQADLHTPHTEDGGPSATERAAEDGA
SS    198
                .|||||..||||.||||.|..|.|.|...|..|.||.|..:...|||.::
CAA80254.1       150
VTSHPHGGMQPGLHETSAPTAPGQPDHQPPRVEGGGTSVIKEVVEDGT
AN    199

AAH08765.1       199
QLPAAEGSGEQDFTFETSGENTAVVAVEPDRRNQSPVDQGATGASQGL
LD    248
                ||||.|||||||||||||||.||||..|||.|||:|||||||.|||
CAA80254.1       200
QLPAGEGSGEQDFTFETSGENTAVAAVEPGLRNQPPVDEGATGASQSL
LD    249

AAH08765.1       249
RKEVLGGVIAVGLVGLIFAVCLVGFMLYRMKKKDEGSYSLEEPKQANGG
A    298
                ||||||||||.||||||||||.||||||||||||||||||||||||
CAA80254.1       250
RKEVLGGVIAGGLVGLIFAVCLVAFMLYRMKKKDEGSYSLEEPKQANGG
A    299

AAH08765.1       299 YQKPTKQEEFYA    310
                ||||||||||||
CAA80254.1       300 YQKPTKQEEFYA    311

#---------------------------------------
#---------------------------------------
```

7.3 Syndecan-1 Homology Between Rat vs. Mouse

```
########################################
# Program: needle
# Rundate: Mon 30 Jan 2017 12:03:50
# Commandline: needle
#    -auto
#    -stdout
#    -asequence emboss_needle-I20170130-120349-0345-83427194-
es.asequence
#    -bsequence emboss_needle-I20170130-120349-0345-83427194-
es.bsequence
#    -datafile EBLOSUM62
#    -gapopen 10.0
#    -gapextend 0.5
#    -endopen 10.0
#    -endextend 0.5
#    -aformat3 pair
#    -sprotein1
#    -sprotein2
# Align_format: pair
# Report_file: stdout
########################################

#=======================================
#
# Aligned_sequences: 2
# 1: AAH61834.1
# 2: CAA80254.1
# Matrix: EBLOSUM62
# Gap_penalty: 10.0
# Extend_penalty: 0.5
#
# Length: 313
# Identity:     283/313 (90.4%)
# Similarity:   289/313 (92.3%)
# Gaps:           2/313 ( 0.6%)
# Score: 1466.0
#
#
#=======================================

AAH61834.1        1
MRRAALWLWLCALALRLQPALPQIVTANVPPEDQDGSGDDSDNFSGSG
TG     50
                 ||||||||||||||||||||||..||||||||||||||||||||
CAA80254.1        1
MRRAALWLWLCALALRLQPALPQIVAVNVPPEDQDGSGDDSDNFSGSG
TG     50
```

```
AAH61834.1      51
ALPDMTLSRQTPSTWKDVWLLTATPTAPEPTSRDTEATLTSILPAGEKPE
100
                |||| |||||||||||||||||||||||||.:||...||:||||||||
CAA80254.1      51 ALPD-
TLSRQTPSTWKDVWLLTATPTAPEPTSSNTETAFTSVLPAGEKPE    99

AAH61834.1      101
EGEPVAHVEAEPDFTARDKEKEATTRPRETTQLPVTQQASTAARATTAQ
A   150
                |||||.||||||.|||||||||.|||||||.|||:||:||| .|.|||||
CAA80254.1      100
EGEPVLHVEAEPGFTARDKEKEVTTRPRETVQLPITQRAST-VRVTTAQA
148

AAH61834.1      151
SVTSHPHGDVQPGLHETLAPTAPGQPDHQPPSVEDGGTSVIKEVVEDET
T   200
                :|||||||.:|||||||.||||||||||||||.||.||||||||||||.|.
CAA80254.1      149
AVTSHPHGGMQPGLHETSAPTAPGQPDHQPPRVEGGGTSVIKEVVEDG
TA   198

AAH61834.1      201
NQLPAGEGSGEQDFTFETSGENTAVAGVEPDLRNQSPVDEGATGASQG
LL   250
                |||||||||||||||||||||||||.|||.||||.||||||||||.||
CAA80254.1      199
NQLPAGEGSGEQDFTFETSGENTAVAAVEPGLRNQPPVDEGATGASQS
LL   248

AAH61834.1      251
DRKEVLGGVIAGGLVGLIFAVCLVAFMLYRMKKKDEGSYSLEEPKQANG
G   300
                ||||||||||||||||||||||||||||||||||||||||||||||||||||||||||||
CAA80254.1      249
DRKEVLGGVIAGGLVGLIFAVCLVAFMLYRMKKKDEGSYSLEEPKQANG
G   298

AAH61834.1      301 AYQKPTKQEEFYA   313
                ||||||||||||
CAA80254.1      299 AYQKPTKQEEFYA   311


#---------------------------------------
#---------------------------------------
```

8. Histological Protocols

8.1 Tissue Preparation

8.1.1 Fixation of the Tissues

Tissue were perfused-fix with 4% PFA in PBS and cut into four pieces, before immersion-fix over night at 4 ºC in the same buffer.

-Preparation of 1 L of 4% PFA solution in PBS used for tissue fixation.

- For 1 L PFA solution, add 800 ml of 1 X PBS (pH 7.4) to a glass beaker on a stir plate in fume hood.

- Add 40 g of PFA powder to the PBS. Heat gradually until 60 ºC while stirring without letting the solution to boil.

-The PFA powder will gradually dissolve into the solution until the solution clears.

- Let the solution to cool once the PFA dissolved then filtered.

- Adjust the pH to 7.4.

- Adjust the volume of the solution to 1 L with PBS and stored at 4 ºC.

8.1.2 Tissue Processing

Once tissues fixed, tissues were processed using a gentle agitation on standard tissue processing system (Leica TP1020, Germany) as follow:

1- Dehydration stage in which the tissues were dehydrated in increasing concentration of alcohol:

- 70% alcohol 2 x 1 hour
- 96% alcohol 2 x 1 hour
- 100% alcohol 2 x 1 hour

2- Clearing stage: tissues were cleared in xylene:

- Xylene 2 x 1 hour

3- Paraffin wax impregnation:

- Melted paraffin (58 ºC) 2 X 1 hour

8.1.3 Tissues Embedding in Paraffin Block

After tissue processing, the tissue slices were embedded in wax block. This involved placement of the tissues in a metal moulding block. Melted wax was poured into the block using wax melting system (WD-4, Germany), and the block was cooled on a cold plate (CPL-4, Axel Johnson Lab system, Germany). Afterward, the moulding block was removed from the wax block which contains the tissue slice and ready for sectioning.

8.2 Preparation of the Tissue Sections

8.2.1 Tissue Sectioning

The wax block which containing the tissue was sectioned using rotary microtome (Leica RM2125RT, Germany) into 6 µm thickness for IHC or 5 µm for H&E staining, and gently with untoothed forceps the sections were transferred into a dish containing 30% alcohol in distilled water. Then the sections transferred to a hot distilled water bath 43 ºC (Leica H1210, Germany) using a glass slide to flatten the section. Then, sections were mounted on glass slide and stored at 60 ºC in the oven overnight.

8.2.2 Deparaffinization and Hydration of the Section

Tissue sections were deparaffinized in xylene. whereas the sections transferred quickly from oven to xylene to facilitate de-waxing of the section. Then, sections were rehydrated into decreasing concentration of alcohol and rinsed in running tape water as follow:

- xylene: 3 x 5 min
- 100% alcohol: 2 x 3 min
- 96% alcohol: 2 x 2 min
- 70% alcohol: 1 x 1 min
- Rinse in running tape water: 1 min

8.3 Staining Protocol

8.3.1 Immunohistochemistry Staining Protocol

8. 3.1.1 Immunofluorescent Protocol

- After hydration, the sections were washed with PBS for 5 min.
- antigen retrieval: after wash in PBS the sections were treated with heat antigen retrieval using citrate buffer or Tris-EDTA.

A. Preparation of Antigen Retrieval Buffer

1) Preparation of citrate buffer (10 mM citric acid, 0.05% Tween 20, pH 6.0) used for antigen retrieval

Citric acid (anhydrous)	1.92 g
Distilled water	1 L

Mix on stirrer until dissolve. Adjust pH to 6.0 then add 0.5 ml of tween 20 and mix well. Store at 4ºC.

2) Preparation of Tris-EDTA (10 mM tris base, 1 mM EDTA solution, 0.05% Tween 20, pH 9).

Tris base	1.21 g
EDTA	0.37 g
Distilled water	1 L

Mix well and adjust pH to 9 then add 0.5 ml of Tween 20 and store at 4 ºC.

B. Heat induced antigen retrieval using pressure cooker

1. The cooker was filed with distilled water to appropriate level and the antigen retrieval buffer (citrate buffer or Tris-EDTA) were poured into plastic coplin jar and placed into the cooker.
2. The cooker was placed together with buffer on a hot plat and the lid was loosely then the plat turned on.

3. The cooker was left to boil then the slides were transferred into container which containing the buffer and the lid was secured as manufacture's instruction. As soon as the cooker reach maximum pressure the time was set for 5 or 20 min depend on the protocol.
4. When the time have relapsed, hot plat was turned off and the cooker was transferred into sink containing water, the pressure release valve was activated and tap water ran over the cooker. Then the lid was opened and the slid container were transferred out of the cooker and left to cool at room temperature for 10 min.

- Sections were washed with PBS/Tween-20 (3 times jet washes then wash for 5 min on the stirrer).
- Sections were incubated into 50 mM ammonium chloride for 30 min to quench aldehyde induced auto-fluorescent to reduce back ground staining.
- Sections were washed with PBS/ 0.1 % Tween-20 for 5 min.
- Non-specific binding was blocked with 3% BSA in PBS/ 0.1% Triton X-100 for 2 hours at room temperature in humidity chamber.
- Slides were drained without rinse it and wiped around the section with tissue paper.
- Sections were incubated with primary antibody overnight at 4 ^{o}C in humidity chamber.
- Slides were drained and washed with PBS/Tween-20 for 15 min on stirrer.
- Sections were incubated with secondary antibody CY3 either anti-mouse CY3 1:1000 dilution in 1 % BSA in PBS or antirabbit CY3 1:2000 dilution in 1% BSA in PBS in humidity chamber for 2 hours in dark at room temperature.
- Sections were washed with PBS for 30 min in dark on stirrer.
- Slides were drained and wiped around the section then were mounted with glycerol and coverslip.
- Sections were kept in the dark until viewed with fluorescent microscope.

8.3.1.2 Chromogenic Staining Protocol (final protocol)

- After de-waxing and hydration of the sections.
- Sections were rinsed in running water for 1 min.
- Sections were washed with PBS for 5 min on stirrer.
- Endogenous peroxidase was blocked by incubation of the sections in 3% hydrogen peroxide in distilled water for 15 min on stirrer bar
- Wash with PBS/Tween-20 jet wash 3 times then wash for 5 min on stirrer.
- Section were incubated with 3% BSA in PBS/0.1% Triton X-100 to block non-specific binding for 1 hour at room temperature.
- Slide were drained without rinse it and wiped around the section with tissue paper.
- Sections were incubated with primary antibody; antirabbit anti-syndecan-1 (1:500 dilution) diluted in 3% BSA in PBS with 0.1% Triton X-100 in humidity chamber overnight at 4 ^{o}C.
- Sections were washed in PBS/Tween-20 for 5 min on stirrer.
- Section were incubated with goat antirabbit secondary antibody 1:250 were diluted in PBS with 1% BSA in humidity chamber at room temperature for 1 hour.
- Wash again with PBS/Tween- 20 for 15 min on stirrer.
- Sections were incubated with DAB substrate for 6 min then rinsed with double distilled water to stop the reaction.
- Slide were drained and dehydrated in increasing concentration of alcohol 70%, 95% x 2, 100% x 2. Then cleared in two changes of xylene.
- Mount with DPX and coverslips.
- Sections were viewed under light microscopes.

8.3.2 Hematoxylin and Eosin (H&E) Staining Protocol.

- Sections were de-waxed and hydrated in the same way were described for immunostaining.
- Sections were rinsed in running tap water for 1 min.
- Sections were stained with hematoxylin for 5 min.
- Sections were rinsed in running tap water for 1 min.
- Sections were blued in Scott's water for 1 min.
- Sections were rinsed in running tap water for 1 min.
- Sections were countered stain with eosin for 15 second.
- Sections were rinsed briefly in running water for <10 sec.
- Section then were dehydrated in increasing concentration of alcohol (brief immersion with gentle agitation) as follow:
    - 70% alcohol x 2
    - 96% alcohol x 2
    - 100% alcohol x 2
    - Clearing in xylene x 2
- The sections were stayed in the last xylol until ready to coverslip.
- Section were mounted with Dibutyl phthalate-DPX (Sigma) and coverslip and leave to dry at room temperature before viewing under microscope.

9. Quantification of the Extracellular Cellular Area Using Image J.

Open the picture in ImageJ.

Image → type 8-bit

Image → brightness/ contrast → apply

Image → threshold → analysis → set measurement → limit to threshold (limit to the extracellular area)

Analysis → measure (this will measure the extracellular compartment).

10. A summary of the Statistical Data of Syndecan-1 Staining Intensity Scores and Difference Between Groups: control, ischemia followed by reperfusion (I/R), S1P treatment before ischemia (I/R+S1P) and S1P treatment without ischemia (S1P perfusion).

Kruskal-Wallis test				
P value	P<0.0001			
P value summary	***			
	Control	**I/R**	**I/R+S1P**	**S1P**
Number of values	360	360	360	360
Mean	2.558	0.6556	0.5611	2.381
Std. Deviation	0.7328	0.7672	0.6564	0.7591
Std. Error	0.03862	0.04043	0.03459	0.04001
Dunn's Multiple Comparison Te	Significant? P < 0.05?	Summary		
Control vs I/R	Yes	***		
Control vs I/R+S1P	Yes	***		
Control vs S1P	No	ns		
I/R vs I/R+S1P	No	ns		
I/R vs S1P	Yes	***		
I/R+S1P vs S1P	Yes	***		

11. A summary of Statistical Data of Quantification of Cardiac Edema and Difference Between Groups: control, ischemia followed by reperfusion (I/R), S1P treatment before ischemia (I/R+S1P) and S1P treatment without ischemia (S1P perfusion).

One-way analysis of variance				
P value	0.0002			
P value summary	***			
Number of groups	4			
Tukey's Multiple Comparison Test	Significant?	Summary		
Control vs I/R	Yes	***		
Control vs I/R+S1P	No	ns		
Control vs S1P Perfuion	No	ns		
I/R vs I/R+S1P	Yes	**		
I/R vs S1P Perfuion	Yes	**		
I/R+S1P vs S1P Perfuion	No	ns		
	Control	**I/R**	**I/R+S1P**	**S1P Perfuion**
Number of values	54	54	54	54
Mean	37.06	43.48	37.43	37.96
Std. Deviation	7.027	7.849	7.081	11.24
Std. Error	0.9562	1.068	0.9636	1.529

12. Ethics Committee Certificate Approved the Study

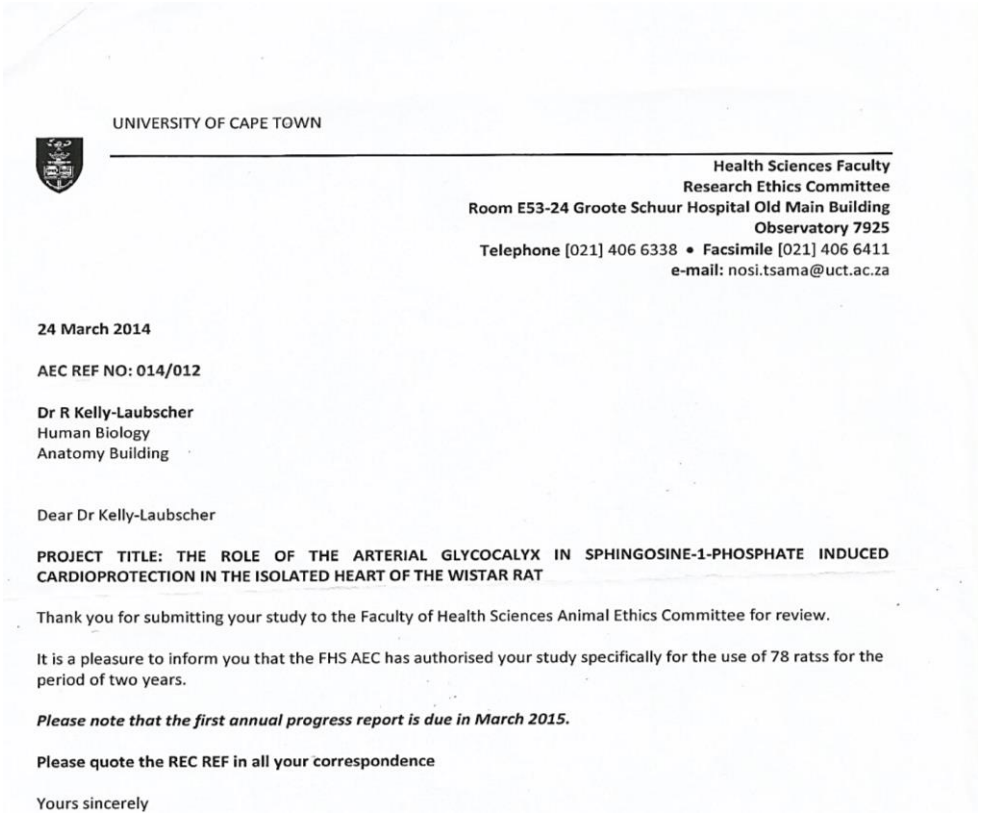

UNIVERSITY OF CAPE TOWN

Health Sciences Faculty
Research Ethics Committee
Room E53-24 Groote Schuur Hospital Old Main Building
Observatory 7925
Telephone [021] 406 6338 • **Facsimile** [021] 406 6411
e-mail: nosi.tsama@uct.ac.za

24 March 2014

AEC REF NO: 014/012

Dr R Kelly-Laubscher
Human Biology
Anatomy Building

Dear Dr Kelly-Laubscher

PROJECT TITLE: THE ROLE OF THE ARTERIAL GLYCOCALYX IN SPHINGOSINE-1-PHOSPHATE INDUCED CARDIOPROTECTION IN THE ISOLATED HEART OF THE WISTAR RAT

Thank you for submitting your study to the Faculty of Health Sciences Animal Ethics Committee for review.

It is a pleasure to inform you that the FHS AEC has authorised your study specifically for the use of 78 ratss for the period of two years.

Please note that the first annual progress report is due in March 2015.

Please quote the REC REF in all your correspondence

Yours sincerely